CNIC-01170
CNDC-0020
INDC(CPR)-042 / L

中国核科技报告

CHINA NUCLEAR SCIENCE AND TECHNOLOGY REPORT

COMMUNICATION OF NUCLEAR DATA PROGRESS

No.17 (1997)

China Nuclear Data Center

中国核情报中心
原子能出版社

China Nuclear Information Centre
Atomic Energy Press

CNIC-01170
CNDC-0020
INDC(CPR)-042 / L

COMMUNICATION OF NUCLEAR DATA PROGRESS

No.17 (1997)

China Nuclear Data Center

China Nuclear Information Centre

Atomic Energy Press

Beijing, June, 1997

EDITORIAL NOTE

This is the 17th issue of *Communication of Nuclear Data Progress* (CNDP), in which the nuclear data achievements and progress in China during the last year are carried, including measurements of angular distributions at 6.0 and 7.0 MeV for $^{58}Ni(n,\alpha)^{55}Fe$ and $^{54}Fe(n,\alpha)^{51}Cr$ reactions, and activation cross sections for $^{182,184}W(n,p)$, $^{182,186}W(n,2n)$, $^{182}W(n,n'\alpha)$, $^{186}W(n,\alpha)$ reactions around 14 MeV and $^{180}Hf(n,\gamma)$ reaction at 0.52~1.60 MeV; SUNF Code for fast neutron data calculation, adjustment of the parameters in the calculations of the γ-production data, calculations of $d+^{6,7}Li$, ^{7}Be, ^{51}V, ^{52}Cr, $^{56,57}Fe$, $p+^{56,57}Fe$ and $n+^{169}Tm$ reactions; evaluations of $^{46,47}Ti$, ^{59}Co, $^{60}Ni(n,p)$, $^{58,60,61,62,64,Nat}Ni$, ^{169}Tm, $^{181}Ta(n,2n)$, $^{169}Tm(n,3n)$, (n,γ), (n,x) reactions; a new method to correct ^{238}U fission rate measured using uranium foils, the integral test of the reactor dosimetry data; systematics calculation for cross section of (p,n) reaction on 16 targets up to 100 MeV; energy balance for natural elements, progress on Chinese Evaluated Nuclear Parameter Library; activities and cooperations on nuclear data in China in 1996.

We hope that our readers and colleagues will not spare their comments, in order to improve this publication.

Please write to Drs.Liu Tingjin and Zhuang Youxiang
Mailing Address: China Nuclear Data Center
China Institute of Atomic Energy
P.O.Box 275 (41), Beijing 102413
People's Republic of China
Telephone: 86-10-69357729 or 69357830
Telex: 222373 IAE CN
Facsimile: 86-10-6935 7008
E-mail: CNDC @ MIPSA.CIAE.AC.CN

EDITORIAL BOARD

CONTENTS

I EXPERIMENTAL MEASUREMENT

Measurement of Angular Distribution at 6.0 MeV and 7.0 MeV for $^{58}Ni(n,\alpha)^{55}Fe$ and $^{54}Fe(n,\alpha)^{51}Cr$

Tang Guoyou Fan Jihong Chen Jinxiang Zhang Guohui Shi Zhaomin
(Institute of Heavy Ion Physics, Peking University, Beijing 100871)

Yu.M.Gledevor G.Khuukhenkhuu
(Joint Institute for Nuclear Research, Dubna 141980, Russia)

Chen Zemin Chen Yintang
(Tsinghua University, Beijing 10084)

Abstract

α particle angular distributions of $^{58}Ni(n,\alpha)^{55}Fe$ and $^{54}Fe(n,\alpha)^{51}Cr$ reactions have been measured at incident neutron energies 6.0 and 7.0 MeV by using a gridded-ionization chamber. The neutron fluence is determined by a fission chamber with ^{238}U. Preliminary results of total cross section and angular distribution have been obtained.

Introduction

Nickel and Iron are important component elements of the alloys those are widely used as fusion reactor materials. It is important to measure the cross section and the angular distribution of $^{58}Ni(n,\alpha)^{55}Fe$ and $^{54}Fe(n,\alpha)^{51}Cr$ reactions for determining radiation resistant ability of alloys. On the other hand, the information from the measurement is also useful to develop model of theoretical calculation. The angular distribution of ^{58}Ni reaction has been measured recently by using a gridded-ionization chamber (GIC) at incident neutron energies 6.0 and 7.0 MeV. (The metal ^{58}Ni target of $1mg/cm^2$ in thickness was used for obtaining angular distribution data.

One of 0.5mg/cm^2 in thickness was used to view α particle energy spectrum.) And so has ^{54}Fe(n,α) reaction at incident neutron energy 7.0 MeV.

1 Experimental Setup

1.1 Gridded-ionization Chamber(GIC) and Target

The structure of GIC is the same as that described in Ref.[1]. The experimental condition can see Table 1.

Table 1

Item	condition(1)	condition(2)
Counting gas	97.5% Kr+2.5% CO_2	98% Kr+2% CO_2
Pressure of mixture gas	1.4 atm	2.0 atm
Distance between the grid and the cathode	5.0 cm	3.6 cm
Target diameter	4.0 cm	6.0 cm
Thickness of ^{58}Ni target	1.04 mg/cm^2	0.5 mg/cm^2
Thickness of ^{54}Fe	1.0 mg/cm^2	

Note: condition(1) were to measuring angular distribution.

condition(2) were to view α spectrum.

1.2 Fission Chamber of ^{238}U

The neutron fluency was determined by fission chamber with ^{238}U. Information of this fission chamber can be found in Ref.[1] also. During the experiment, the solid angle subtend for the neutron source by target of ^{58}Ni, ^{54}Fe and sample ^{238}U remained unchanged, it is about 8 degree.

2 Results and Their Errors

2.1 Angular Distribution

The angular distribution was derived from the method as that in Ref.[2]. Figs.1 and 2 showing the anode spectrum with sample and without sample, it is obvious that the background at E_n = 7.0 MeV is more than the one at E_n = 6.0 MeV(The average ratio of event to background at E_n = 6.0 MeV was about 10 for both forward and backward. But the average of ratio at E_n = 7.0 MeV was about 2 for forward and 1.3 for backward). Therefore the error caused by uncertain deduction background at E_n = 7.0 MeV is also more than the one at E_n = 6.0 MeV. The uncertainty of

absolute $\bar{X}_b$ data is also error source for the angular distribution. Our presently used Pu-source to calibrate energy was thicker, so that scattering of α particles in the source is obvious. Though the energy resolution of anode spectra is small than 100 KeV, the boundary line at 0 degree and 90 degree of cathode spectra is not sharp. The error for each angle, which include uncertainty of absolute $\bar{X}_b$ data else, was about 10% at E_n = 6.0 MeV, about 15% at E_n = 7.0 MeV. Figs.3 and 4 show the measured results of angular distribution.

2.2 Total Cross Section

Based on cross section of ENDF/B6 for ^{238}U and information from fission chamber with ^{238}U, see Ref.[2], we got the absolute neutron fluence that throw in sample. Because the fission cross sections of ^{238}U in E_n = 6.0 ~ 8.0 MeV region change sharply, the error of absolute neutron fluence at E_n = 7.0 MeV is very larger in comparison with uncertainty of neutron energy, it includes the uncertainty of absolute high voltage of accelerator(about 100 keV) and the uncertain of energy lose of deuteron in D-Ti target (about 200 keV), and the uncertainty due to deduct back-ground from measured spectrum with sample at E_n = 7.0 MeV is also more than the one at E_n = 6.0 MeV. Therefor the error of total cross section at incident neutron E_n = 7.0 MeV is more than the one at E_n = 6.0 MeV.

Preliminary results of total cross section are given as follows:

For ^{58}Ni(n,α)^{55}Fe: 75±7.5 mb at E_n = 6.0 MeV
For ^{58}Ni(n,α)^{55}Fe: 71±14 mb at E_n = 7.0 MeV
For ^{54}Fe(n,α)^{51}Cr: 8.8±2.6 mb at E_n = 7.0 MeV

2.3 Double-differential Spectrum

Using 0.5 mg/cm^2 in thick of ^{58}Ni as target, for E_n = 7.0 MeV measurement, it is obvious that double-differential spectrum resolve itself into peak of ground level and excited levels for residual nucleus. Typical double-differential spectrum of $\cos\theta$ = ±0.9, ±0.8 is shown in Figs.5 and 6. Resolving those spectrum by Gas-Fit method the ratio of intensity of the ground level to the excited levels may be estimated. The ratios on different emissive angles of α particle are roughly shown in Table 2.

3 Some Consideration for Future Measurement

3.1 Suppression of Background

a. The background above 6.0 MeV for α particle spectrum of ^{58}Ni(n,α) or ^{56}Fe(n,α) reaction are mainly from ^{86}Kr(n,α),^{82}Kr(n,α) reaction. To reduce this background, we should use collimator between neutron source and GIC. But during fission chamber is used to determine neutron fluence when old GIC is used, it may be difficult. New small GIC, which can work at (7~12)×10^{5}P$_a$, has been supplied by JINR/Dubna of Russian. And we have replaced the old GIC by the new one.

b. If using collimator, the background may descend about several times or even more. For the background of output particle spectrum in the region 4.0 MeV to 6.0 MeV mainly from α peak of ^{16}O reaction, for present moderating gas the peak from CO_2 gas is very violent to yield of events. But the losing energy of proton from (n,p) reaction in counting gas is lower than those at 3.0 MeV during GIC used to detect α particles. Thus the gas CO_2 should be replaced by CH_4 as the moderating gas.

3.2 In order to reduce error of cross section at E_n = 7.0 MeV, it is also necessary that (n,f) reaction should be replaced by other reaction as absolute determination of neutron fluency.

3.3 The Solid Angle Subtend for Neutron Source

The solid angle subtend for neutron source is restricted by the angular resolution and the fluctuation of counts.

The angular resolution of the GIC detector can be estimated by the following equations.

$$P_a = E\left[1-\left(\bar{X}_b/d\right)\cdot\cos\ \theta\right] \quad (1)$$

$$P_c = E\left[1-\left(\bar{X}_b/d\right)\cdot\cos\ \theta\right] \quad (2)$$

$$\Delta\cos\ \theta = (d/\bar{X}_b - \cos\ \theta)\cdot\sqrt{(\Delta P_a/P_a)^2+(\Delta P_c/P_c)^2} \quad (3)$$

where ΔP_a and ΔP_c are the resolution of the anode and cathode spectra respectively and assumed to be independent each other. In this measurement, $\Delta\cos\theta$ is estimated to be 0.05 ~ 0.08 since $\bar{X}_b/d$ is 0.357 and ΔP_a and ΔP_c are about 100 keV.

Based on those considerations, we adopted angle subtend for the neutron source by target, 8 degree.

Table 2

cos θ	S_n	S_0	S_n/S_0	cos θ	S_n	S_0	S_n/S_0
0.95	118	40.6	2.9	-0.45	145	14	10.4
0.85	151	47	3.2	-0.55	149	14	10.9
0.75	170	44	3.9	-0.65	153	16	9.6
0.65	168	44	3.8	-0.75	160	18	8.8
0.55	171	26	6.6	-0.85	137	28	4.9
0.45	149	28	5.3	-0.95	120	17	7.2

Note: S_0 is relative value of peak-area for ground level of residual nucleus.

S_n is the sum of relative peak-area for excited levels of residual nucleus.

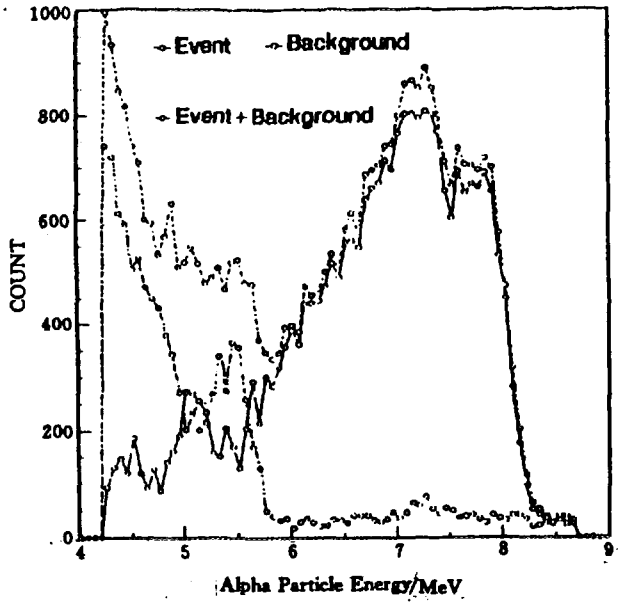

Fig1-1: Anode spectrum of out particle for ^{58}Ni(n,α) reaction (Forward) E_n = 6.0 MeV

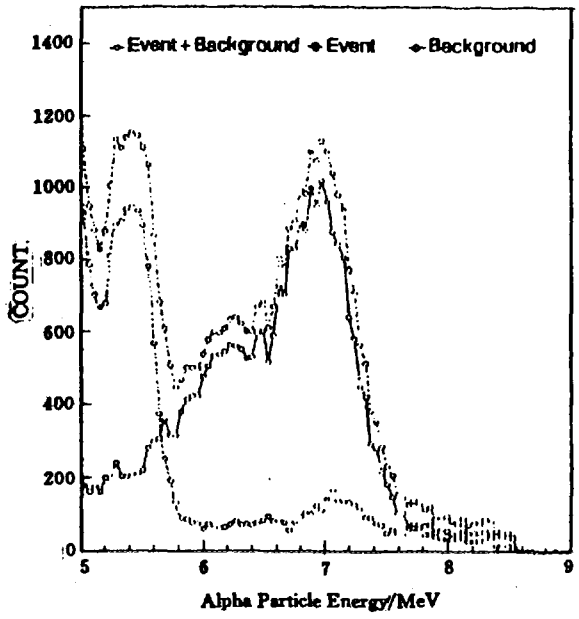

Fig1-2: Anode spectrum of out particle for ^{58}Ni(n,α) reaction (Backward) E_n = 6.0 MeV

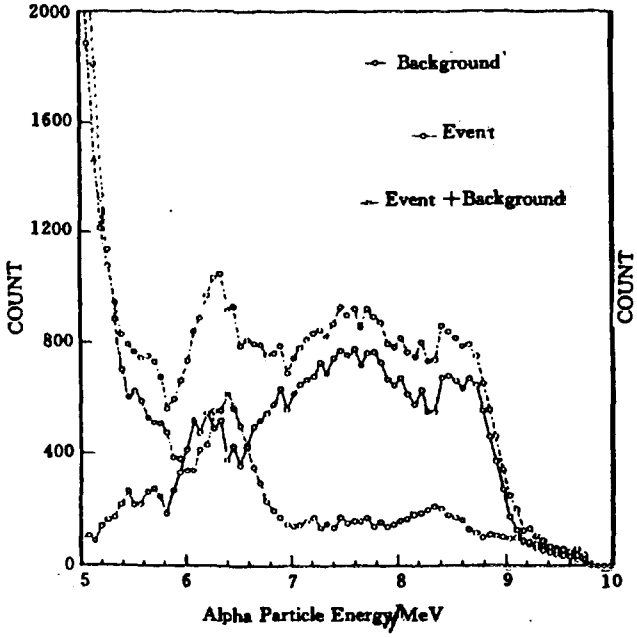

Fig2-1: Anode spectrum of out particle for ^{58}Ni(n,α) reaction (Forward) E_n = 7.0 MeV

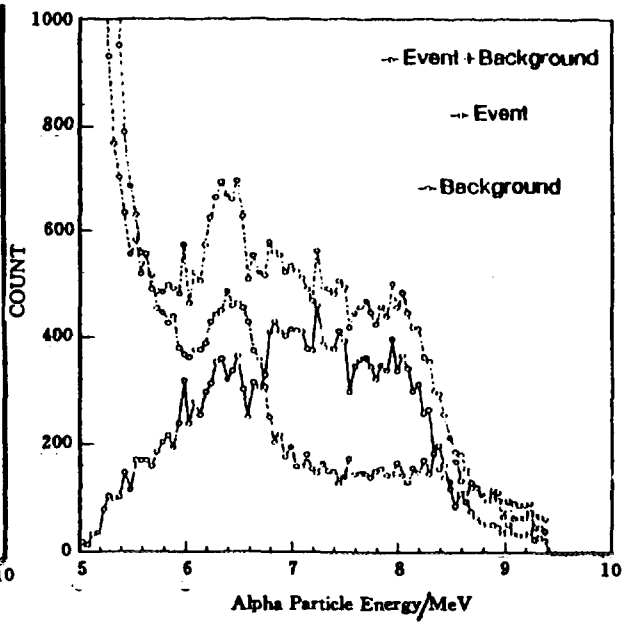

Fig2-2: Anode spectrum of out particle for ^{58}Ni(n,α) reaction (Backward) E_n = 7.0 MeV

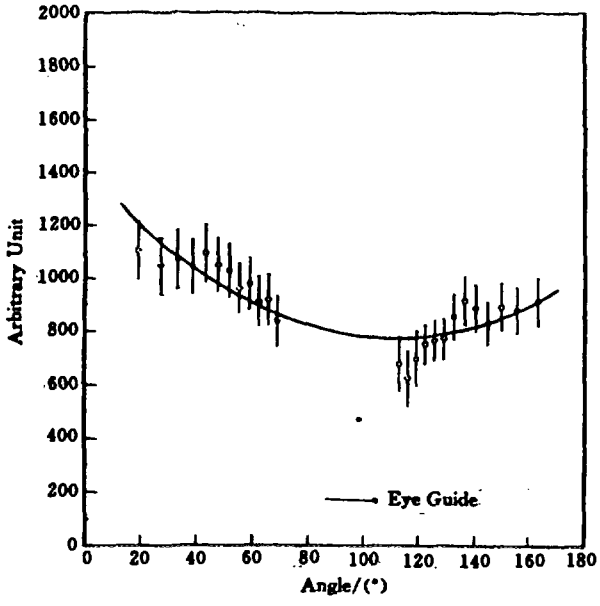

Fig3-1: Angular Distribution $^{58}Ni(n,\alpha)^{55}Fe$ at E_n = 6.0 MeV (C-M Frame)

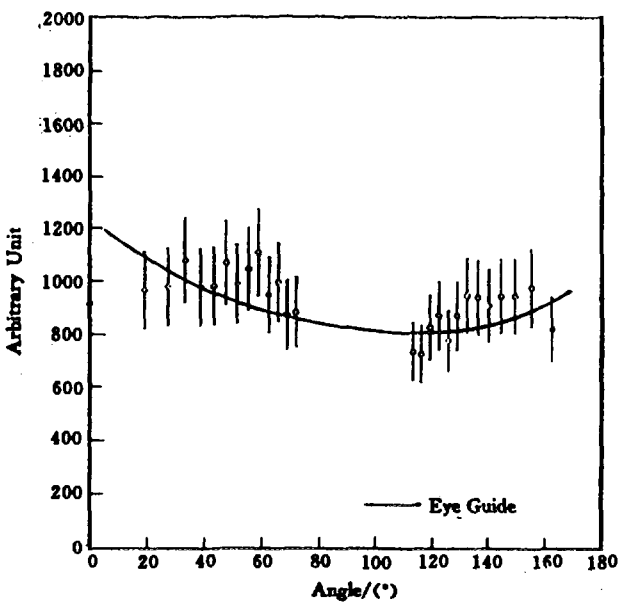

Fig3-2: Angular Distribution $^{58}Ni(n,\alpha)^{55}Fe$ at E_n = 7.0 MeV (C-M Frame)

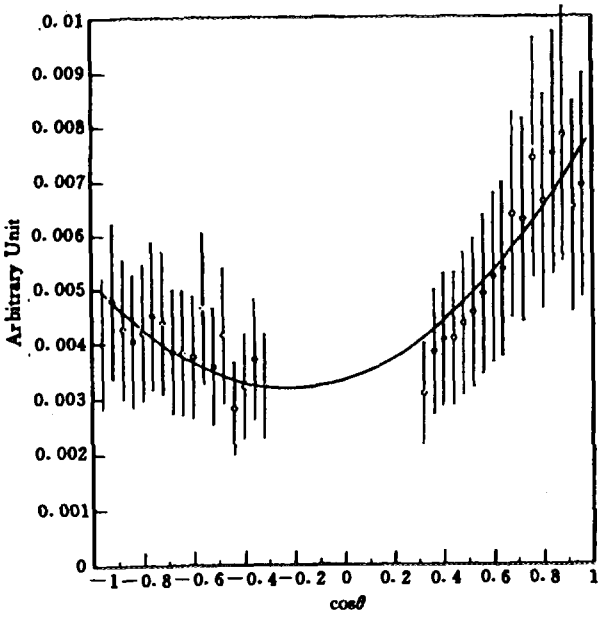

Fig4-1: Angular Distribution $^{58}Ni(n,\alpha)^{55}Fe$ at E_n = 7.0 MeV (C-M Frame)

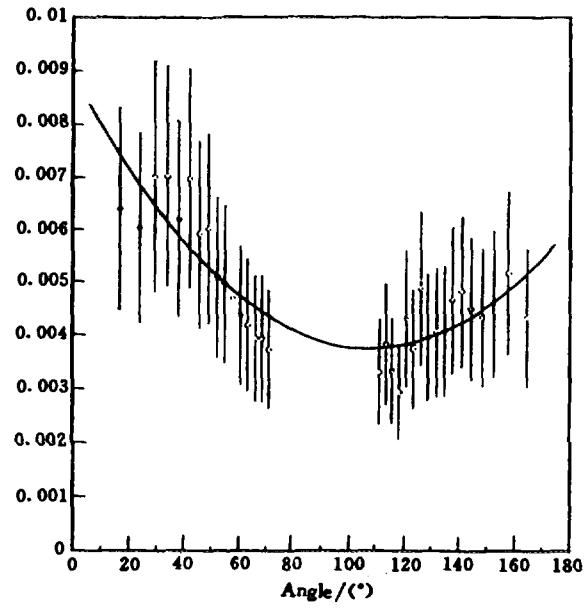

Fig4-2: Angular Distribution $^{58}Ni(n,\alpha)^{55}Fe$ at E_n = 7.0 MeV (C-M Frame)

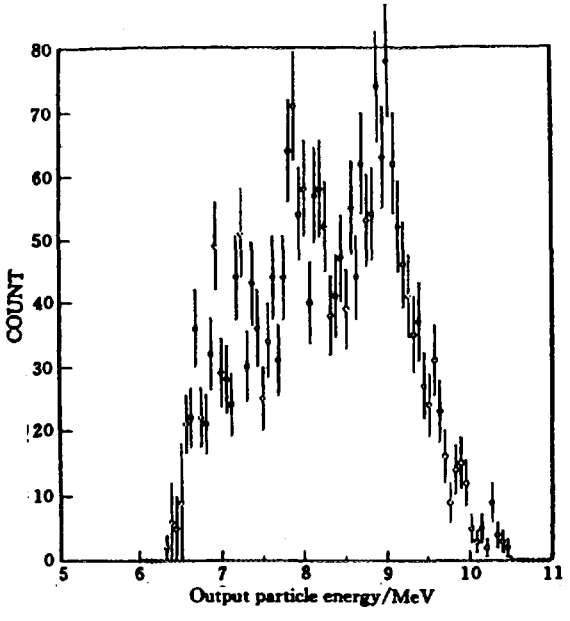

Fig5-1: Output α particle spectrum at E_n = 7 MeV (cos θ = 0.8)

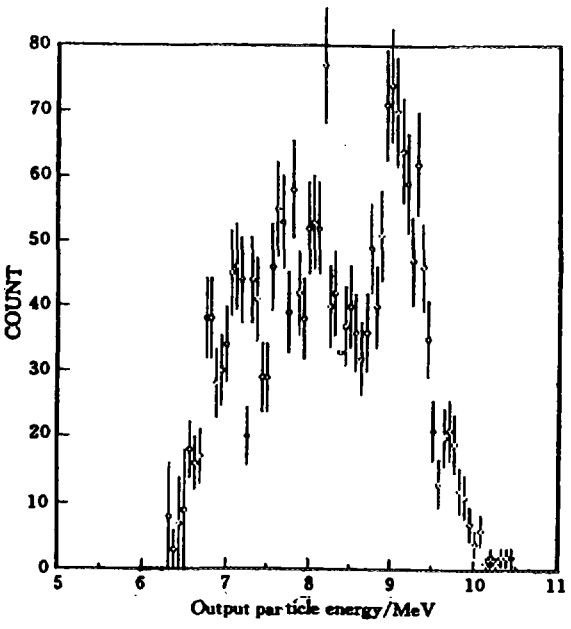

Fig5-2: Output α particle spectrum at E_n = 7 MeV (cos θ = 0.9)

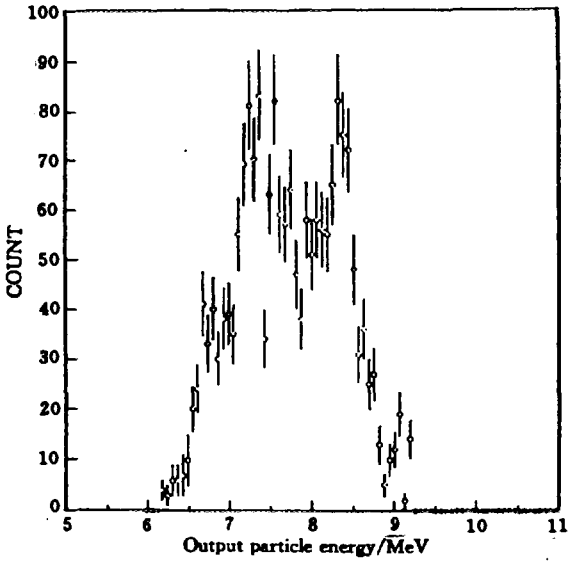

Fig6-1: Output α particle spectrum at E_n = 7 MeV (cos θ = -0.8)

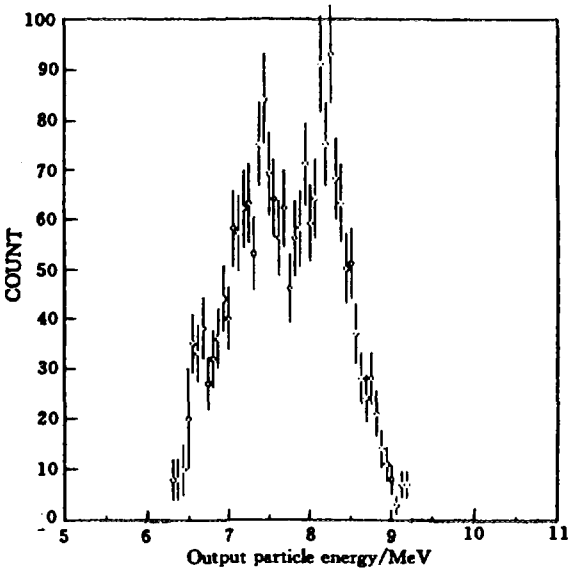

Fig6-2: Output α particle spectrum at E_n = 7 MeV (cos θ = -0.9)

References

[1] Tang Guoyou et al., Chin.J. of Nucl.Phys.,16(3):1994

[2] Tang Guoyou et al., Nuclear Technique(In Chinese),17(3):129,1994

Cross Sections of 14 MeV Neutron Induced Reactions on Wolfram Isotopes

Kong Xiangzhong Hu Shangbin Yang Jingkang

(Department of Modern Physics, Lanzhou University, Lanzhou, 730001)

Introduction

The importance of nuclear data for fusion power reactor design has been acknowledged, in particular for safety, environment reasons and economics. The 14 MeV neutron activation cross sections are the key nuclear data for environmental impact, material recycling, waste handling. Due to the large number of materials and traces of alloy elements and contamination, there are requirements for a complete database covering large number of nuclides. Problems still exist for some reactions, for example, for $^{182}W(n,n'\alpha)^{178m2}Hf$ reaction only one measurement was published[1], so we have measured cross sections for $^{182}W(n,p)^{182}Ta$, $^{184}W(n,p)^{184}Ta$, $^{186}W(n,\alpha)^{183}Hf$, $^{182}W(n,2n)^{181}W$, $^{186}W(n,2n)^{185}W$ and $^{182}W(n,n'\alpha)^{178m2}Hf$ reactions by using the activation method at the Lanzhou University Intense Neutron Generator.

1 Experimental Procedure

The irradiation of samples was carried out at the ZF-300-II Intense Neutron Generator at Lanzhou University with the neutron yield about $(1\sim3)\times10^{12}s^{-1}$. Neutrons were produced by $T(d,n)^4He$ reaction with an effective deuteron beam energy of 125 keV and a beam current of 20 mA. The thickness of T-Ti target used in the generator was 0.9 mg/cm^2. The neutron flux was monitored by a uranium fission chamber so that corrections could be made for variance of neutron yields during the irradiation. The samples were placed at the angles 0 ~ 140° relative to the beam direction and were irradiated for 5.1 ~ 100.48 h. The cross sections of the reactions were determined relatively to the cross sections of $^{54}Fe(n,p)^{54}Mn$ or $^{93}Nb(n,2n)^{92m}Nb$ reactions, which were used as monitors. In this experiment, the samples of W, Fe and Nb with 20 mm in diameter and 2 mm, 0.5 mm and 0.2 mm in thickness and 99.9%, 99.95% and 99.9% in chemical purity, respectively were made of natural metal foil. The W sample in each group was sandwiched between two Fe or Nb foils. Groups of samples were placed at 1 ~ 25 cm away from the neutron

source. The neutron energies at where the samples were placed were determined by the method of cross section ratios for the reactions $^{90}Zr(n,2n)^{89m+g}Zr$ and $^{93}Nb(n,2n)^{92m}Nb$[2].

After irradiation the activities of the samples were measured by gamma-ray spectrometer consisting of a CH8403 coaxial HPGe detector made in China and a EG & G ORTEC 7450 Multichannel Analyzer. The energy resolution of the detector is 2.7 keV for 1.33 MeV gamma-rays. The efficiency of the detector was calibrated by using the standard gamma-ray source. Standard Reference Material 4275 was from the National Institute of Standard and Technology. The relative photopeak detection efficiency of the detector was known within an error of ±2%[3]. The decay data used in this study are taken from Ref.[4] and listed in Table 1.

Table 1. Reactions and decay data of products

Abundance of target isotope	Reaction	Product half-life	E_γ / keV	I_γ
0.058	$^{54}Fe(n,p)^{54}Mn$	312.20d	834.826	0.99975
1.0	$^{93}Nb(n,2n)^{92m}Nb$	10.15d	934.53	0.99
0.263	$^{182}W(n,p)^{182}Ta$	115.0d	1121.302	0.347
0.3067	$^{184}W(n,p)^{184}Ta$	8.7h	414.04	0.739
0.286	$^{186}W(n,\alpha)^{183}Hf$	1.067h	783.753	0.65
0.263	$^{182}W(n,2n)^{181}W$	121.2d	152.214	0.00084
0.286	$^{186}W(n,2n)^{185}W$	75.1d	125.354	0.00019
0.263	$^{182}W(n,n'\alpha)^{178m2}Hf$	31y	574.18	0.837

In the measurement of gamma-ray activities, the corrections were made for the effects of neutron intensity fluctuation, gamma-ray self-absorption in the sample, the sum peak effects in the investigated nuclide and the counting geometry, etc.

2 Results and Discussion

The cross sections were calculated by the following formula:

$$\sigma_x = \frac{\left[S\varepsilon I_\gamma NKMD\right]_0\left[\lambda AFC\right]_x}{\left[S\varepsilon I_\gamma NKMD\right]_x\left[\lambda AFC\right]_0}\sigma_0$$

where

σ_x ,σ_0 are the measured and standard cross section, respectively,

ε is full-energy peak efficiency of the measured characteristic gamma-rays,

I_γ is gamma-ray intensity,

N is abundance of the target nuclide,

M is mass of sample,

D is e counting collection factor,

t_1, t_2 is time intervals from the end of the irradiation to the start and finish of counting, respectively,

A is atomic weight,

C is measured full-energy peak area,

F is total correction factor of the activity,

F is $f_s \times f_c \times f_g$.

where f_s, f_c and f_g are correction factors for the self-absorption of the sample at a given gamma energy and the coincidence sum effect of cascade gamma rays in the investigated nuclide and in the counting geometry, respectively.

K is neutron fluctuation factor,

$$K = \left[\sum_{1}^{L} \phi_i \left(1 - e^{-\lambda \Delta t_i}\right) e^{-\lambda T_i} \right] / \phi S$$

where

L is number of time intervals into which the irradiation time is divided,

Δt_i is duration of the i' th time interval,

λ is decay constant,

T_i is time interval from the end of the i' th interval to the end of irradiation,

ϕ_i is neutron flux averaged over the sample in Δt_i,

ϕ is neutron flux averaged over the sample in the total irradiation time T,

S is $1 - e^{-\lambda T}$ growth factor of the product nuclide.

The measured results of the cross sections are listed in Table 2.

Table 2. Cross sections of the 14 MeV neutrons induced reactions on wolfram isotopes in mb

Reaction	Neutron Energies in MeV				
	13.5±0.2	13.7 ± 0.2	14.2 ± 0.2	14.5 ± 0.2	14.7 ± 0.2
$^{182}W(n,p)^{182}Ta$	2.25 ± 0.11	2.62 ± 0.12	3.09 ± 0.15	4.08 ± 0.20	4.47 ± 0.22
$^{184}W(n,p)^{184}Ta$	1.65 ± 0.08	1.92 ± 0.09	2.25 ± 0.11	2.97 ± 0.14	3.25 ± 0.16
$^{186}W(n,\alpha)^{183}Hf$	0.30 ± 0.06	0.34 ± 0.08	0.45 ± 0.09	0.57 ± 0.10	0.62 ± 0.11
$^{182}W(n,2n)^{181}W$	2050 ± 70	2065 ± 73	2115 ± 75	2110 ± 75	2097 ± 73
$^{186}W(n,2n)^{185}W$	1955 ± 89	1960 ± 89	1995 ± 90	1985 ± 90	1975 ± 90
$^{182}W(n,n'\alpha)^{178m2}Hf$					0.018 ± 0.005

The errors reported in our work are from counting statistics, standard cross sections, detector efficiency, weighting of samples, self-absorption of γ, coincidence sum effect of cascade γ-rays.

Acknowledgements

We would like to thank the group of the Intense Neutron Generator at Lanzhou University with the irradiation work and Prof. Lu Hanlin for helpful comments and discussions.

References

[1] Lu Hanlin, Zhao Wenrong and Yu Weixiang, Chin. J. Nucl. Phys., 16, 267(1994).

[2] V. E. Lewis and K. J. Zieba, Nucl. Instrum. Method, 174, 141(1980).

[3] Wang Yongchang, Ren Zhongliang, Yuan Junqian et al., High Energy Phys.& Nucl. Phys., 14, 923 (1990).

[4] E. Browne and R. B. Fireatone, Table of Radioactive Isotopes, 1986.

CN9702234

Activation Cross Section Measurement for the $^{180}Hf(n,\gamma)$ ^{181}Hf Reaction

Chen Jinxiang Shi Zhaomin Tang Guoyou Zhang Guohui
(Institute of Heavy Ion Physics, Peking University, Beijing 100871)

Lu Hanlin Han Xiaogang Huang Xiaolong
(China Institute of Atomic Energy, P. O. Box 275(3), Beijing 102413)

Introduction

D. L. Smith and E. T. Cheng have reviewed the contemporary nuclear data needs and status for fusion-reactor technology. Activation cross sections were found to be unsatisfactory in 83 of 153 reaction reviewed[1]. $^{180}Hf(n,\gamma)^{181}Hf$ cross sections are also desired for the fusion-reactor technology. Some experimental data for this reaction from 3 keV to 4 MeV are reported in the literatures[2-6]. This reaction is considered as inadequate for the present in this review. To evaluate these experimental data, it is necessary to re-measure the cross sections for this reaction.

The cross sections for the $^{180}Hf(n,\gamma)^{181}Hf$ reaction have been measured relative to the $^{197}Au(n,\gamma)^{198}Au$ reaction at neutron energies of 0.52, 1.10 and 1.60 MeV using the activation method in combination with high resolution HPGe detector gamma-ray spectroscope. The errors of the measured results were 5% ~ 6%. Cross sections are calculated with the code UNF. Our recommended data for the reaction are also given. Our results have a good agreement with those by other authors.

1 Experimental Measurement

The experiments were carried out at the 4.5 MV Van de Graaff accelerator of the Institute of Heavy Ion Physics, Peking University. The monoenergetic neutrons with energies 0.52, 1.10 and 1.60 MeV were produced via the $T(p,n)^3He$ reaction on a solid T-Ti target of 1.48 mg/cm^2 in thickness. The energies of the proton beam were 1.45, 2.0, 2.5 MeV respectively.

The samples were made of natural metallic hafnium powder, which was pressed into disks of 10 mm in diameter and about 1.5 mm in thickness. The gold disks each of 10 mm in diameter and 0.1 mm in thickness were used as neutron fluence monitors. The purities were 88.398% for Hf and 99.9% for Au. Each sample was sandwiched between two gold disks. The sample groups were wrapped with

cadmium foils of 0.5 mm in thickness.

The samples were placed in the 0° direction relative to the incident proton beam at a distance of about 1.4 cm from the target. The proton beam currents were generally 9 ~ 12 μA and the duration of irradiation was 21 to 24 h at each energy. The fluctuation of neutrons fluence rate was monitored with a BF_3 long counter at 0° at a distance of 315 cm from the neutron source. In order to record the neutron fluence rate as a function of time during the irradiation, the integral count rate of the long counter per 10 minutes was recorded continuously by microcomputer multi-scaler and stored on magnetic disk for calculating the correction to nonuniform irradiation history.

After irradiation, the activities from residual nuclei were measured with HPGe γ-detector (105 cm^3). The detector was calibrated with standard gamma sources in the energy range of 0.1 ~ 1.5 MeV and the efficiency curve was fitted with the least-square method. The peak area of measured γ-rays was analysed using the program H developed for an IBM compatible computer.

From the measured γ-spectrum, counting rates under the concerned full-energy peaks were obtained. The relevant decay data of ^{181}Hf and ^{198}Au are listed in Table 1. After the corrections for the detector efficiency, cascade effect, γ-intensity, fluctuation of neutron fluence rate and γ-ray self-absorption in the samples, the cross sections of $^{180}Hf(n,\gamma)^{181}Hf$ were calculated by using well-known activation equation. The measured cross sections for the $^{180}Hf(n,\gamma)^{181}Hf$ reaction and the $^{197}Au(n,\gamma)^{198}Au$ reaction recommended by ENDF/B-6 are listed in Table 2. The principal contributions of errors are given in Table 3.

Table 1. Decay data[7] of radioactive products

Resid. nucl.	$T_{1/2}$ / h	E_γ / keV	I_γ / %
^{181}Hf	1017.36 ± 0.14	482	80.5 ± 0.4
^{198}Au	64.684 ± 0.005	411.8	95.58 ± 0.12

Table 2. Measured results of cross sections/mb

E_n / MeV	$^{180}Hf(n,\gamma)^{181}Hf$	$^{197}Au(n,\gamma)^{198}Au$
0.52 ± 0.03	36.3 ± 1.8	127.0 ± 4.4
1.10 ± 0.03	45.3 ± 2.7	77.2 ± 3.4
1.60 ± 0.04	39.8 ± 2.4	66.5 ± 2.9

Table 3. Principal sources of errors/ %

Decay data	relative errors/%
Reference cross section	3.5 ~ 4.5
γ-counting statistics for ^{181}Hf	0.7 ~ 1.0
γ-counting statistics for ^{198}Au	0.5 ~ 0.8
γ-detection efficiency for ^{181}Hf	1.5
γ-detection efficiency for ^{198}Au	1.5
correction of self absorption for ^{181}Hf	1.0
correction of cascade effect for ^{181}Hf	1.5
^{180}Hf sample weight	0.2
^{197}Au foil weight	0.1

2 Theoretical Calculation

In order to compare the measured data given in Table 2 with theoretical results, we made a theoretical calculation with UNF code[8]. The code consists of the spherical optical model, the semi-classical theory of multi-step nuclear reaction processes. The pre-equilibrium nuclear reaction processes are described with the J-dependent exciton model, while the equilibrium processes are described by the Hauser-Feshbach theory with width fluctuation correction. In UNF code there are two parts for the radiation capture processes. The statistical radiation capture includes pre-equilibrium and equilibrium radiation capture. Direct gamma radiation capture is also calculated in UNF code.

A set of optimum neutron optical potential parameters for Hf are taken from Ref.[9]. It is selected as follows:

$$V = 51.4429+0.1546E-0.0246E^2-24.00(N-Z)/A$$

$$W_S = \max\{0.0, 9.1002-0.3507E-12.00\,(N-Z)/A\}$$

$$W_V = \max\{0.0, -1.2155+0.1940E+0.016E^2\}$$

$$U_{SO} = 6.2$$

$$\gamma_R = 1.1906, \quad \gamma_S = 1.3202, \quad \gamma_V = 1.5881, \quad \gamma_{SO} = 1.1906$$

$$\alpha_R = 0.5789, \quad \alpha_S = 0.6687, \quad \alpha_V = 0.3615, \quad \alpha_{SO} = 0.5789$$

$$\gamma_C = 1.25$$

Where V, W, U and E in MeV; γ and α in fm.

Using the relevant level density and giant dipole resonance parameters and this set of neutron optical potential parameters, the neutron radiation capture cross sections of ^{180}Hf were calculated using UNF code. The exciton model parameter K is taken as 800 MeV^3. The calculated results are given in Fig.1.

3 Discussion

Our experimental data together with the literature values[3-6] are plotted as a

function of neutron energy in Fig.1. In Fig.1, the long-dashed line is our calculated results and the dash-two-dotted line is the ENDF/B-6 data. From Fig.1, we can find our results are in agreement with the other experimental data within error ranges. Our experimental results are also generally in agreement with those of the calculation. So we consider that the experimental data including our data are adequate. We fit these experimental data to get the recommended data. The recommended data in energy region 0.3 ~ 3.0 MeV are given in Table 4. In Fig.1, the solid line is our recommended data.

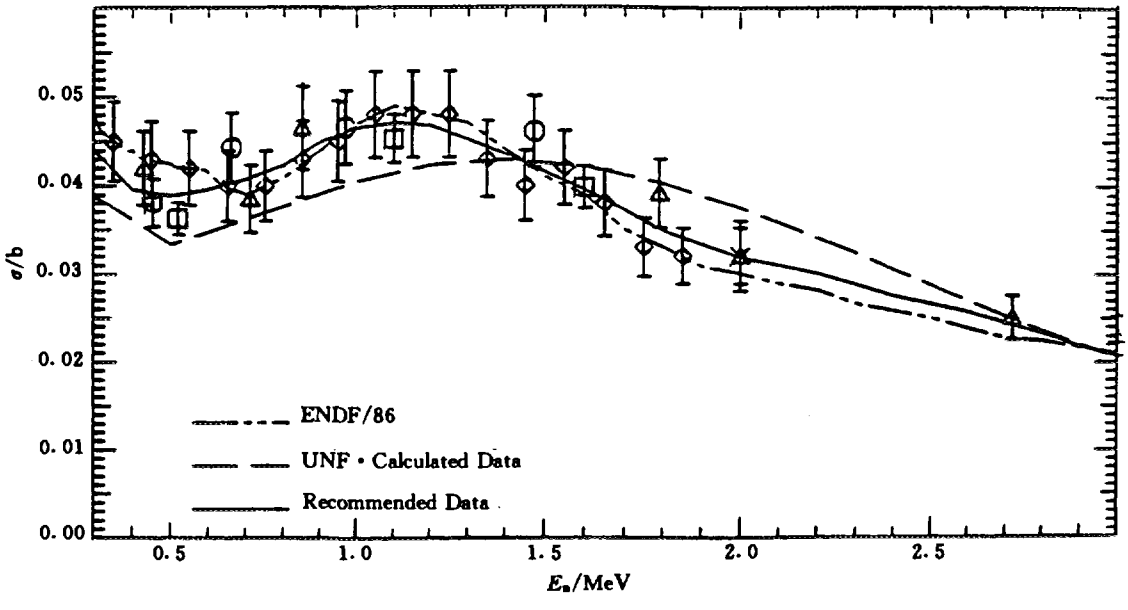

Fig.1 The cross section of $^{180}Hf(n,\gamma)$ reaction

Present Work. (96)
ZHOU ZU-YING,CPRAEP(8405)
J.A.MISKEL,USALRL(62)
YU.N.TROFIMOV,CCPRI(87)
H.BEER.USAORL,GERKFK(8210)

Table 4. The recommended data for $^{180}Hf(n,\gamma)^{181}Hf$

neutron energy/MeV	cross section/mb	neutron energy/MeV	cross section/mb
0.30	44.1 ± 1.8	1.40	43.5 ± 1.7
0.40	39.6 ± 1.6	1.60	39.6 ± 1.6
0.50	38.9 ± 1.6	1.80	34.8 ± 1.4
0.60	39.7 ± 1.6	2.00	31.8 ± 1.9
0.70	40.8 ± 1.6	2.20	30.1 ± 1.8
0.80	42.4 ± 1.7	2.40	27.4 ± 1.6
0.90	44.9 ± 1.8	2.60	25.7 ± 1.5
1.00	46.5 ± 1.9	2.80	23.2 ± 1.4
1.20	46.7 ± 1.9	3.00	21.1 ± 1.3

We thank the Chinese Nuclear Data Center for financial support. In addition, acknowledgement is also made to the crew of the 4.5 MV Van de Graaff accelerator at Peking University for numerous irradiations.

References

[1] Smith D. L. Cheng et al., ANL / NDM-123, Sept. 1991. p. 49
[2] Macklin R. L. et al., Phys. Rev., 1957, 107(2):504
[3] Miskel J. A. et al., Phys. Rev., 1962, 128(6):2717
[4] Beer H. et al., Phys. Rev., 1982, c26(4):1404
[5] Zhou Zuying et al., Chin. J. Nucl. Phys., 1984, 6(2):174
[6] Trofimov Yu N. 1st Internal. Conf. on Neutron Physics, Kief, Sept. 1987, p. 331
[7] R.B.Firestone, et al., Table of Isotopes, 18th editions(1996)
[8] Zhang Jingshang, Commu. Nucl. Data Progress, 1992, NO.7:14
[9] Han Yinlu et al., Commu. Nucl. Data Progress, 1995, NO.14:17

II THEORETICAL CALCULATION

SUNF Code for Fast Neutron Data Calculations

Zhang Jingshang

(China Nuclear Data Center, CIAE)

Introduction

The master equation theory of precompound and compound nuclear reaction has been generalized to the inclusion of the conservation of angular momentum and parity[1]. Based on this improved semi-classical multi-step compound theory the Hauser-Feshbach and Exciton Model was unified, with which the code UNF has been developed as an evaluation tool of the calculations of nucleon induced reaction cross sections and double differential cross sections at incident neutron energies below 20 MeV[2], it is demonstrated that the constructed model contains the Hauser-Feshbach model and the exciton models as the limiting cases. The unified treatment of equilibrium and pre-equilibrium reaction processes includes the introduction of formation factors of composite particle in calculations of pick-up type composite particle emissions.

Pre-equilibrium nuclear reaction theories have been developed with great success for the description of the double differential cross sections based on the exciton model. This success was mainly due to introducing a leading particle into the generalized exciton model[3,4] and application of the pick-up mechanism for composite particle emissions[5]. Since Iwamoto-Harada model overestimates the formation probabilities; it turns out that the phase space integration of the formation factor should be restricted by excitation energy E, the improved E-dependent formation factor has been proposed[6]. To keep the energy conservation the recoil nucleus effects are also taken into account. The discrete level effect in multiparticle emissions was taken into account to produce the reasonable energy spectra.

The more functions for a code needs more input information. In some cases users only concern the cross sections and neutron spectra, and may become aware of

lengthy and tedious for doing the UNF input files. For this reason a simplified UNF code was developed, which is named SUNF.

In the unified Hauser-Feshbach and Exciton Model the energy spectrum formula reads

$$\frac{d\sigma}{d\varepsilon} = \sum_{j\pi} \sigma_a^{j\pi} \sum_n P^{j\pi}(n) \frac{T_b^{j\pi}(n,E,\varepsilon)}{T_t^{j\pi}(n,E)} \tag{1}$$

where E is the excitation energy, ε is the energy of emitted particle b, $\sigma_a^{j\pi}$ stands for the absorption cross section in $j\pi$ channel. $T_b^{j\pi}(n, E, \varepsilon)$ is the T factor of emitted particle b with excitation energy E at n exciton state in $j\pi$ channel, $T_t^{j\pi}(n,E)$ is the total T factor. $P^{j\pi}(n)$ stands for the $j\pi$ channel occupation probability of n exciton state.

Obviously, if we do not consider the parity and angular momentum effects, Eq.(1) is reduced to the exciton model, while if the pre-equilibrium effect is omitted, it is reduced to the Hauser-Feshbach model. In the case of incident neutron energy below 20 MeV, the pre-equilibrium processes are described only by the exciton state $n = 3$, while the other part is described by the Hauser-Feshbach model. In practice the energy spectrum is calculated by the following formula

$$\frac{d\sigma}{d\varepsilon} = \sum_{j\pi} \sigma_a^{j\pi} \left\{ P^{j\pi}(3) \frac{T_b^{j\pi}(3,E,\varepsilon)}{T_t^{j\pi}(3,E)} + \left(1 - P^{j\pi}(3)\right) \frac{T_b^{j\pi}(E,\varepsilon)}{T_t^{j\pi}(E)} \right\} \tag{2}$$

1 The Functions of SUNF Code

SUNF code is developed for calculating fast neutron data for structural materials with incident energies from a few keV to 20 MeV, written in FORTRAN-77. The code may handle decay sequence (n,γ), (n,n'), (n,p), (n,α), (n,^{3}He), (n,d), (n,t), (n,2n), (n,np)+(n,pn), (n,nα)+(n,αn), (n,2p) and (n,3n) including 12 reaction channels. The physical quantities calculated by the SUNF code contain:

(1) Cross sections of total, elastic scattering, compound elastic scattering, nonelastic scattering and all reaction channels in which the discrete level emissions and continuum emission are included;

(2) Angular distributions of elastic scattering both in C. M. system and in Lab system;

(3) The energy spectra of emitted neutrons in laboratory system;

(4) If the direct inelastic scattering data and the direct reaction data are available from other codes, one can input the data so that the results may include the

direct reaction effect;

(5) The output form is in the ENDF/B-6 format, but in file 5 format.

The users manual of SUNF code is available. The typical running time is about 8 minutes at PC-586(120) for 40 neutron incident energy points from 1 keV to 20 MeV of (n,^{103}Rh). Now SUNF code is being used for calculating fast neutron data of fission production nuclei to develop CENDL.

References

[1] Zhang Jingshang and Wen Yuanqi, Chin. J. Nucl. Phys., 16, 153 (1994)

[2] J. S. Zhang Nucl. Sci. Eng. 114, 55(1993)

[3] G. Mantzouranis, H. Weidenmuller, D. Agassi, Z. Phys., A276, 145(1976)

[4] Sun Ziyang et al., Z. Phys., A305, 61(1982)

[5] A. Iwamoto, and K. Harada, Phys. Rev., C26, 1812(1982)

[6] J. S. Zhang, Chin. J. Nucl. Phys., 18, 28(1996)

Adjustment of the Parameters in the Calculations of the γ-Production Data

Liu Jianfeng Yao Ning
(Department of Physics, Zhengzhou University, Zhengzhou)

Liu Tingjin
(Chinese Nuclear Data Center, CIAE)

Introduction

The γ-production data are very important for the nuclear engineering, especially for the calculations of the radiation shielding. Because the experimental values of the γ-production data can not satisfy the needs of the nuclear engineering both in the quantity of the nuclei and in the energy region covered by them, as the supplement, the theoretical calculations of the γ-production data are indispensable.

The γ-production data in the nuclear reactions induced by neutrons include the γ-production cross sections, the γ-energy spectra, the γ-multiplicities and the reaction cross sections of the (n,γ) and the (n,xγ) reactions, where the (n,xγ) reactions mean the cascade γ-deexcitation processes of the residual nuclei formed after one or several particles are emitted. The process for (n,γ) reaction includes two parts, the one is the compound statistical process, i.e. the cascade γ-deexcitation process of the compound nucleus formed after the incident of the neutrons upon the targets, and the another is the non-statistical effect in which the incident neutron is captured into the unfilled low-lying excited single particle bound state and a γ-photon is emitted. Because of the differences of the γ production mechanisms in the statistical and non-statistical processes of the (n,γ) reactions, the adjustable parameters in the calculations are different. Though the γ photons are all created through the cascade γ-deexcitation processes of the excited nuclei both in the statistical (n,γ) processes and in the (n,xγ) reactions. Because of the differences way in which the nuclei are excited between the compound nuclei and the residual nuclei, the parameters which play the main parts in the calculations are different. In this paper, the basic principles of the parameter adjustment for different reactions in the calculations of the γ-production data are discussed.

1 Calculation Formulas

The γ-energy spectra of the cascade γ-deexcitation processes for both the compound nucleus (i.e. the (n,γ) reaction) and the residual nuclei (i.e. the (n,xγ) reactions) can be calculated in terms of the following relation[1]:

$$\begin{aligned}\frac{d\sigma^{\gamma}}{dE_{\gamma}} &= \sum_{i=1}^{N}\sum_{j=i+1}^{N}\sigma_j S^{ji}\delta(E_j - E_i - E_{\gamma}) \\ &+ \sum_{i=1}^{N}\sum_{J\pi}\sigma_c(E_i + E_{\gamma}, J'\pi')\frac{T_{\gamma}^{E_i+E_{\gamma}J'\pi', E_iJ_i\pi_i}}{T^{E_i+E_{\gamma}J'\pi'}} \\ &+ \int_{E_c+E_{\gamma}}^{E_m}\sum_{J\pi}\sum_{J'\pi'}\sigma_c(E', J', \pi')\frac{T_{\gamma}^{E'J'\pi', E'-E_r, J\pi}}{T^{E'J'\pi'}}\rho(E'-E_r, J\pi)dE'\end{aligned} \tag{1}$$

The γ-production cross section is

$$\sigma^{\gamma} = \int_0^{E_{\gamma\,max}}\frac{d\sigma_{\gamma}}{dE_{\gamma}}dE_{\gamma} \tag{2}$$

where S^{ji} represents the gamma transition branching ratio from j-th energy level to the i-th one, $\rho(E,J,\pi)$ the level density, $T^{EJ\pi}$ the total transmission coefficient, N the discrete level number, E_c the inferior limit of the energy level continuous region, E_m the highest excitation energy of the system, $T_{\gamma}^{EJ\pi, E'J'\pi'}$ and the gamma transmission coefficient from the energy level (E,J,π) to the energy level (E', J', π')

$$T_{\gamma}^{EJ\pi, E'J'\pi'} = \frac{1}{3\pi\hbar^2c^2}(E-E')^2\sigma_a(E-E')P(J,J';\pi,\pi') \tag{3}$$

and

$$\begin{aligned}\sigma_a(E_{\gamma}) &= \sum_{g=1}^{2}\sigma_g\frac{E_{\gamma}^2\Gamma_g^2}{(E_g^2 - E_{\gamma}^2)^2 + E_{\gamma}^2\Gamma_g^2} \\ P(J,J';\pi,\pi') &= \begin{cases}1 & \text{for } \pi\cdot\pi' = -1 \text{ and } |J-1| \le J' \le J+1 \\ 0 & \text{else}\end{cases}\end{aligned} \tag{4}$$

where σ_g, E_g, Γ_g are the peak cross section, peak energy and peak width of the giant dipole resonance respectively, $\sigma_c(E,J,\pi)$ is the total excitation cross section in an unit energy interval of the energy level in continuous region with spin J, parity π and energy E in the whole cascade γ-deexcitation process, σ_i is the total excitation cross section of i-th discrete level in the whole cascade γ-deexcitation process, σ_i and

$\sigma_c(E,J,\pi)$ can be calculated by th following integration equations:[1]

$$\begin{cases} \sigma_i = \sigma_{io} + \sum_{j=i+1}^{N} \sigma_j \cdot S^{ji} + \int_{E_c}^{E_m} \sum_{J\pi'} \sigma_c(E,J,\pi') \cdot \dfrac{T_\gamma^{EJ\pi',E_iJ_i\pi_i}}{T^{EJ'\pi'}} dE \\ \sigma_c(E,J,\pi) = \sigma_{co}(E,J,\pi) + \int_{E}^{E_m} \sum_{J\pi'} \sigma_c(EJ'\pi') \cdot \dfrac{T_\gamma^{EJ'\pi',EJ\pi}}{T^{EJ'\pi'}} \rho(E,J,\pi) dE \end{cases} \quad (5)$$

where σ_{io} and $\sigma_{co}(E,J,\pi)$ are their initial values respectively. For the (n,γ) reactions, they are the excitations to the energy levels created by the primary γ transitions when the neutrons are captured and the contributions to the γ energy spectra are

$$\frac{d\sigma^\gamma}{dE_\gamma} = \sigma_{io} \cdot \delta(E_m - E_i - E_\gamma) \quad (6)$$

and

$$\frac{d\sigma^\gamma}{dE_\gamma} = \sigma_{co}(E,J,\pi) \quad (7)$$

But for the (n,xγ) reactions, they are the excitations to the energy levels created by the particle emissions of the parent nuclei and, therefor, their values depend on the optical potentials of the emitted particles and the distributions of the energy levels of the residual nuclei.

From relations (1) and (5), the cross section can be calculated and the adjustment of the parameters can be discussed by analyzing the calculations of the cross sections. It can be seen from relation (5) that for the energy levels whose excitation energies are larger than the separation energies of the particles, the contributions of their cascade γ-deexcitations to the γ-production data are very small because their γ widths are much smaller than the particle widths. As a good approximation, we can only consider the contributions to the γ-production data from the primary γ-deexcitations of these energy levels. Therefor for the (n,γ) reaction, the cross section can be written as follows

$$\sigma_{n\gamma} \approx \sum_{i=1}^{N} \sigma_{io} + \sum_{J\pi} \int_{E_c}^{B_n} \sigma_{co}(E,J,\pi) dE \quad (8)$$

and for the (n,xγ) reactions,

$$\sigma_{nx\gamma} \approx \sum_{i=1}^{N}(\sigma_{io} + \sum_{J\pi'}\int_{B_n}^{E_m}\sigma_{co}(E,J,\pi')\cdot\frac{T_\gamma^{EJ\pi',E_iJ_i\pi_i}}{T^{EJ\pi'}}dE)$$
$$+\sum_{j\pi}\int_{E_c}^{B_n}(\sigma_{co}(E,J,\pi)+\int_{B_n}^{E_m}\sum_{j'\pi'}\sigma_{co}(E,J,\pi')\cdot\frac{T_\gamma^{EJ\pi',EJ\pi}}{T^{EJ\pi'}}\rho(E,J,\pi)dE)dE \quad (9)$$

In relation (9), the second term in each bracket is much smaller than the first one. B_n represents the separation energy of the particle.

σ_{io} and $\sigma_{co}(E,J,\pi)$ in relation (9) are all calculated in terms of the optical model parameters and the calculation formulas can be found in the theory on the nuclear reactions[3]. The relation (8) can further be written as[4]

$$\sigma_{n\gamma} \approx \sum_{i=1}^{N}\sigma_{io}^{non} + (\sum_{i=1}^{N}\sigma_{io}^{st} + \sum_{J\pi}\int_{E_c}^{B_n}\sigma_{co}(E,J,\pi)dE)$$
$$= \sum_{f}\sigma_{n\gamma f} + \sum_{J\pi}\sigma_a(J,\pi)\cdot\frac{T_\gamma^{J\pi}}{T^{J\pi}} \quad (10)$$

where the first term is the contributions from the non-statistical effects, the second term from the compound statistical processes. $\sum_f$ represents the summation for the f single particle bound states. $\sigma_a(J,\pi)$ is the absorption cross section of the $J\pi$ state of the compound nucleus. For σ_{nrf}, the calculation formula is[5]

$$\sigma_{nrf} = \frac{2\pi me^2z^2k_r^2}{3\pi^2k^3A^2}S_{dpf}\sum_{ljJ}\frac{(2l+1)(2j_f+1)(2J+1)}{2I+1}\cdot\left[C_{l010}^{l_f0}W(l_jl_fj_f;\frac{1}{2}l)\right]^2\cdot$$
$$\left\{\left|\int r^2U_{l_fj_f}(r)U_{lj}(r)dg\right|^2+\left|(\alpha-i\beta)\cdot\int rU_{l_fj_f}(r)h(r)U_{lj}(r)dr\right|^2\right.$$
$$\left.+2\,\mathrm{Re}\left[\left(\int r^2U_{l_fj_f}(r)U_{lj}(r)dr\right)(\alpha+i\beta)\left(\int rU_{l_fj_f}(r)h(r)U_{lj}(r)dr\right)^*\right]\right\} \quad (11)$$
$$+\frac{2\pi me^2z^2k_r^3}{3\pi^2k^3A^2}S_{dpg}\sum_{ljJl'j'}\frac{(2l'+1)(2j_f+1)(2J+1)}{2I+1}\cdot\left[C_{l'010}^{l_f0}W(l'j'l_fj_f;\frac{1}{2}l)\right]^2\cdot$$
$$\left|\int r^2U_{l_fj_f}(r)Q_{l'j'}(r)dr\right|^2\cdot\frac{T_{\alpha lj}\cdot T_{\alpha'l'j'}}{T^{Jp}}$$

where the first part is the capture of the shape-elastic scattering channels and the three terms in the part are the direct capture, the semi-direct capture and the interference term of them respectively. The second part is the capture of the compound elastic scattering channels. Both $U_{lj}(r)$ and $Q_{l'j'}(r)$ are the wave functions of the scattering waves and calculated in terms of the optical model parameters.

$U_{l_f j_f}(r)$ and K_τ are the eigen-function and the photon wave number, they are calculated in terms of the real part of the optical potential. $h(r)$ is the nucleon-phonon coupling potential. The meaning of the other symbols can be found in the references listed in this paper.

2 Discussions on the Parameter Adjustments

It can be seen from the formulas given above that, first of all, the reliability of the calculated γ-production data depends on the reliability of the calculations of the absorption cross sections of every $J\pi$ states of the compound nucleus. At the same time, when the excitation energy is larger than the separation energy of the particle, the transmission coefficients of the particle emissions of the level are much larger than the γ transmission coefficients, therefor the changes of the γ transmission coefficients nearly do not influence the total transmission coefficients, in other words, the calculations of the particle channels will influence the γ channels but the calculations of the γ channels will nearly have no influence on the particle channels. Therefor:

(1) First of all, the optical potential parameters of the incident neutrons must be adjusted to give the reasonable values of the total cross section, the elastic cross section, the absorption cross section and so on and to ensure the reliability of the optical potential parameters of the incident channels.

(2) For each nucleus, either the compound nucleus or the residual nuclei, the particle emissions ought to be calculated first and then the γ emissions.

(3) For the (n,γ) reaction, the non-statistical effects ought to be calculated first. Because the optical potential parameters of the scattering neutron have been adjusted, the scattering wave functions have also been given. We only need to adjust the potentials of the single particle bound states to give the reasonable eigenvalues and to adjust the nucleon-phonon coupling potentials and the giant dipole resonance parameters (if there are no experimental values, the same below) to make calculated excitation curves of the semi-direct capture fit the experimental values. For the statistical processes of the (n,γ) reactions, only the energy level density parameters and the giant resonance parameters need to be adjusted to make the total (n,γ) cross sections (the sum of the statistical and non-statistical processes) fit the experimental values but the optical potentials of the particles should not be adjusted again.

(4) For the (n,xγ) reactions, it can be seen from relation (9) that the optical potential

parameters and the energy level density parameters ought to be adjusted mainly to give the reasonable values of σ_{io} and $\sigma_{\infty}(E,J,\pi)$. Because $T_{\gamma}^{EJ\pi',EJ\pi}$ is much smaller than $T^{EJ'\pi'}$, the calculated values of the γ-production data will not be improved obviously if the giant dipole resonance parameters are adjusted to change the γ transmission coefficients.

References

[1] Liu Jianfeng et al., CNDP, 10,28(1993)

[2] R. E. Chrien, Neutron Radiative Capture, Pergamon Press, (1984)

[3] Hu Jimin et al., Nuclear Theory(in Chinese), Beijing: Atomic Energy Press, (1987)

[4] Liu Jianfeng et al., Chinese Journal of Nuclear Physics, 2, 127(1992)

[5] Liu Jianfeng et al., High Energy Physics and Nuclear Physics, 5, 469(1990)

Analysis and Prediction of the Cross Sections of d+^{6}Li and d+^{7}Be Reactions for Energy up to 30 MeV

Han Yinlu Shen Qingbiao Zhang Jingshang
(Chinese Nuclear Data Center, CIAE)

Zhang Zhengjun Sun Xiuquan
(Physics Department, Northwest University, Shannxi)

Abstract

A set of deuteron optical potential parameters is obtained based on the relevant experimental data, and various nuclear data of d+^{6}Li reaction at incident energies spanning 0.1~30 MeV were calculated with the Distorted Wave Born Approximation, preequilibrium nuclear reaction and Hauser-Feshbach (HF) theory. The cross sections of d+^{7}Be reaction were predicted. The results show that the experimental measurement for d+^{7}Be reaction is feasible at HI-13 tandem accelerator.

Introduction

The production and use of unstable radioactive nuclear ion beams are of considerable interest, because they can provide a new opportunity for studying nuclear phenomena in a wider field. The nuclear data of the secondary radioactive beam induced reactions are of fundamental importance for astrophysical studies and some nuclear engineering designs. Many laboratories have made a lot of effort in producing the secondary radioactive beams for nuclear physical research[1~3]. The theoretical predictions of the nuclear data for secondary reactions have important reference value to experimental scientists.

In order to predict and analyse the production of ^{7}Be radioactive beams and the deuteron induced reaction on the unstable radioactive nuclei ^{7}Be, the theoretical calculations and analysis of d+^{6}Li reaction are needed. The purpose of this paper is to calculate and analyse deuteron reaction data of ^{6}Li, and to predict d+^{7}Be reaction.

1 Theoretical Calculation and Analysis of the Reaction d+^{6}Li

The reaction d+^{6}Li in the incident deuteron energy region of 0.1~30 MeV were studied with the distorted wave Born approximation, preequilibrium nuclear reaction and Hauser-Feshbach theory. The charged particle induced reaction code CUNF[4], the searching optimal charged particle optical potential parameter code APCOM[5] and the distorted wave Born approximation code DWUCK4[6] were used in our calculations.

Based on the experimental reaction cross sections of d+^{9}Be[7,8] and elastic scattering angular distributions of d+^{6,7}Li[9~11] and d+^{9}Be[12], a set of optimum deuteron optical potential parameters up to 30 MeV with the code APCOM was obtained as follows:

$$V = 150.76-0.5892E-0.1375E^2+0.0031(N-Z)/A+0.0147Z/A^{1/3}$$
$$W_s = \max\{0.0,17.6415062-0.1743441E+0.0002105(N-Z)/A\}$$
$$W_v = \max\{0.0,3.6999149+0.3003237E+0.1599908E^2\}$$
$$V_{so} = 7.0$$
$$\alpha_R = 0.854794, \quad \alpha_S = 0.7554354, \quad \alpha_V = 0.29, \quad \alpha_{SO} = 0.81,$$
$$\gamma_R = 1.0155202, \quad \alpha_S = 1.3132277, \quad \gamma_V = 1.6377302, \quad \gamma_{SO} = 1.64,$$
$$\gamma_C = 1.05.$$

The calculated reaction cross sections σ_R of d+^{9}Be reaction and elastic scattering angular distribution of d+^{6,7}Li and d+^{9}Be reaction with this set of optical potential parameters are shown in Fig.1~3, respectively, which fit the experimental data well.

Fig.4 shows the comparison of the calculated discrete level (d,d$_1$) angular distribution of d+^{6}Li reactions at the energy 5.03 MeV with the experimental data[10]. The theoretical calculated values are basically in agreement with the experimental data. The contributions of the direct reaction is larger than those of the compound-nucleus reaction. The ^{6}Li(d,t$_0$)^{5}Li reaction angular distributions for the deuteron energies 3.7 MeV and 5.03 MeV are shown in Fig.5. It can be seen that to theoretical calculated values are in agreement with the experimental data[9,10]. The angular distribution of the ^{6}Li(d,t$_0$)^{5}Li reaction is mainly from the contribution of the direct reaction, the contribution of the compound-nucleus reaction is small.

Fig.6 shows the comparison of the calculated ^{6}Li(d,n)^{7}Be reaction cross sections with the experimental data[13,14]. The calculated curve pass through the existing experimental data and the reaction cross sections are mainly contributed from the compound-nucleus reactions. The comparison of ^{6}Li(d,α)^{4}He reaction cross sections with the experimental data[15~17] is shown in Fig.7. The calculated results and experimental data have some difference, this difference needs to be studied further in theory and experiment. The ^{6}Li(d,t)^{5}Li reaction cross sections are given in Fig.8. The

calculated value fit experimental data[18] well. The compound-nucleus contribution for the cross sections of ^{6}Li(d,t)^{5}Li reaction is larger than the direct contribution for the energy E_d<1.5 MeV, while for the energy E_d>1.5 MeV, the direct contribution is the most.

Besides, the cross sections without any experimental data are calculated for d+^{6}Li reaction and shown in Fig.9. Because of the discrete level effect the curve of reaction cross section presents some small peak in above figures. The ^{7}Be radioactive beam were produced through ^{6}Li(d,n)^{7}Be reaction. The ^{6}Li(d,n)^{7}Be reaction channels is open at incident deuteron energy 0.1 MeV. The results show that the ^{6}Li(d,n)^{7}Be reaction is feasible to get the ^{7}Be radioactive beam in experimental measurement.

2 Prediction of the Cross Section of the Reaction d+^{7}Be

We especially paid attention to the measurement of the secondary reaction induced by the radioactive ^{7}Be. Fig.10 shows the calculated cross section of the reaction d+^{7}Be in the incident deuteron energy region 0.1~30.0 MeV. When the incident deuteron energy is less than 1.0 MeV, the (d,p) and (d,α) channel are open. This result are easy to be understood because the compound-nuclei ^{9}B of d+^{7}Be reaction is easy to emit p and α particles. The reaction channels (d,n), (d,p), (d,α), (d,He^{3}), (d,d'), (d,t),(d,2p), (d,np) and (d,nα) are all open for incident deuteron energy E_d<12.0 MeV, and the cross sections of (d,p), (d,2p) and (d,np) channels are larger than those in most other parts of the energy region. The ions of ^{8}B, ^{8}Be, ^{7}Be, ^{7}Li, ^{6}Li, ^{5}Li and ^{4}Li may be detected to obtain some nuclear data on the reaction d+^{7}Be. The calculated ^{7}Be (d,n)^{8}B reaction cross section pass through the existing experimental data[19], and shows clearly that the (d,n) reaction cross sections are all contributed by the ground state of ^{8}B. The angular distribution of (d,n) reaction is also predicted in our calculated.

3 Summary

The various nuclear data of the reaction d+^{6}Li in the incident deuteron energy region 0.1~30.0 MeV were obtained with DWBA, preequilibrium reaction and HF theory. The calculated results basically agree with the experimental data. The nuclear data for some incident energies, for which there is no any experimental data, were reasonably predicted. The calculated results show that the contribution of compound- nucleus is important for light nucleus, and the reaction cross sections come from the contribution of the discrete level. The cross sections of the secondary reaction d+^{7}Be were also predicted. The calculated results show that the

experimental measurement for d+^{7}Be reaction is feasible at HI-13 tandem accelerator. These theoretical results have important reference value to experimental scientists.

One of the authors would like to thank Prof. Cai Dunjiu for helpful discussions and suggestions.

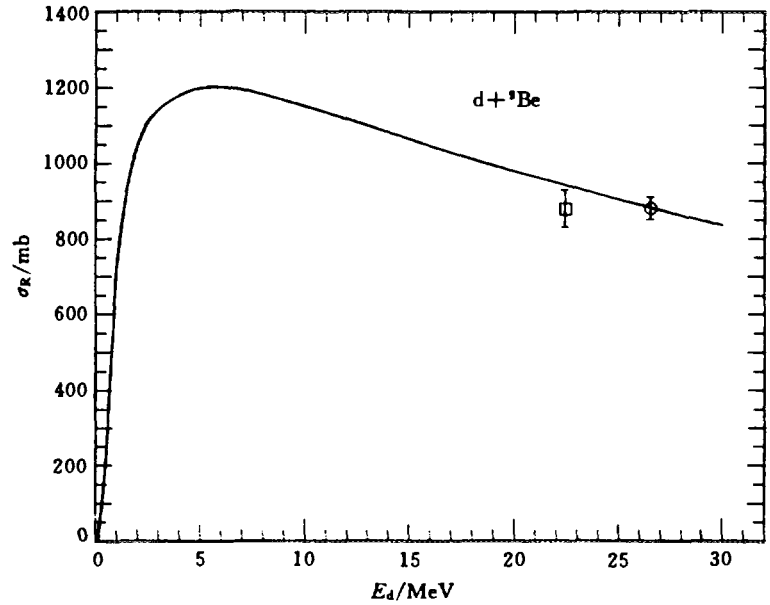

Fig.1 The reaction cross sections of d+^{9}Be reaction.

The line is for theoretical value, the dots are for experimental data.

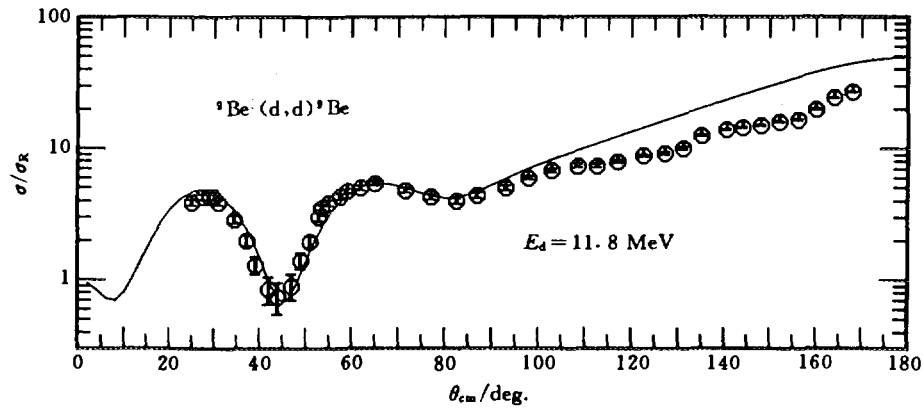

Fig.3 The elastic scattering angular distribution of d+^{9}Be.

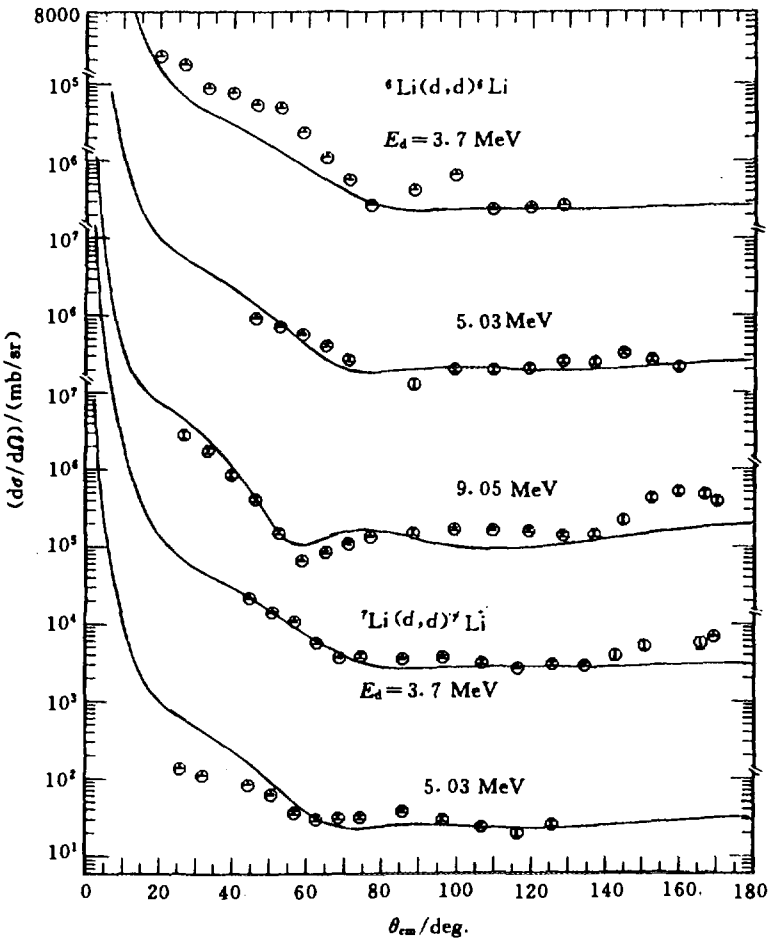

Fig.2 The elastic scattering angular distribution of d+^{6}Li and d+^{7}Li.

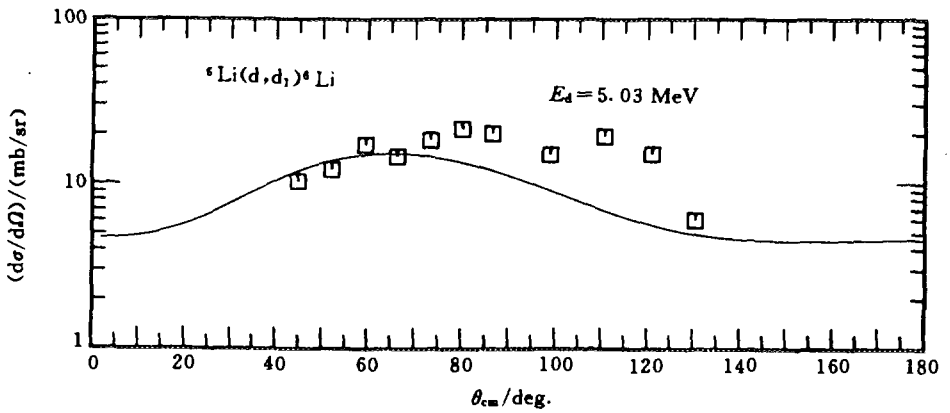

Fig.4 The discrete level angular distributions of^{6}Li(d,d)^{6}Li reaction.

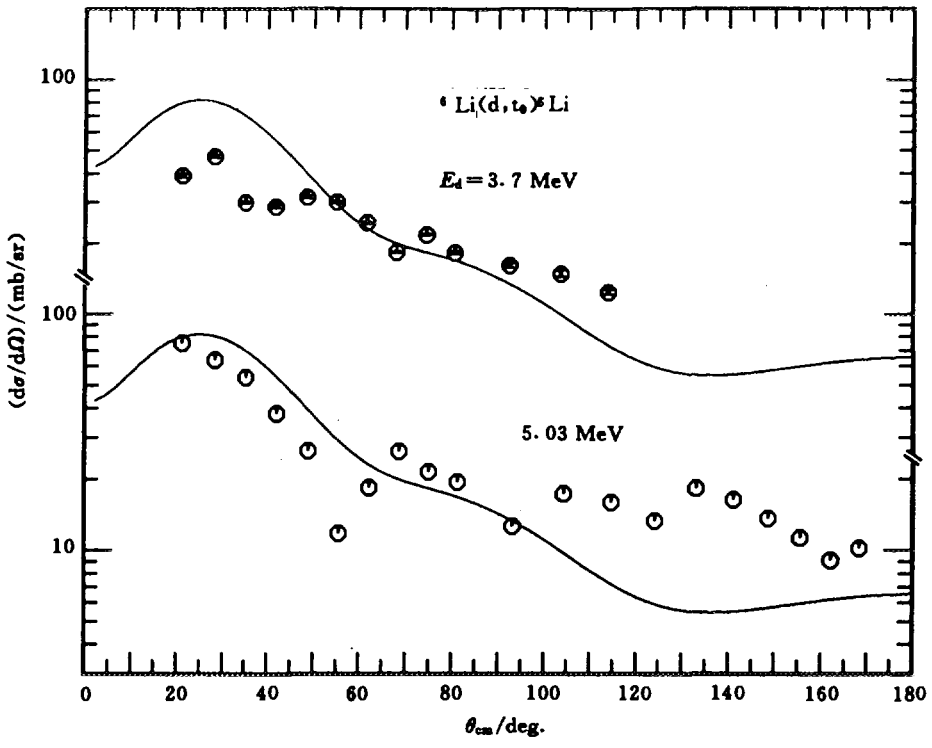

Fig.5 The discrete level angular distributions of ^{6}Li(d,t)^{5}Li reaction.

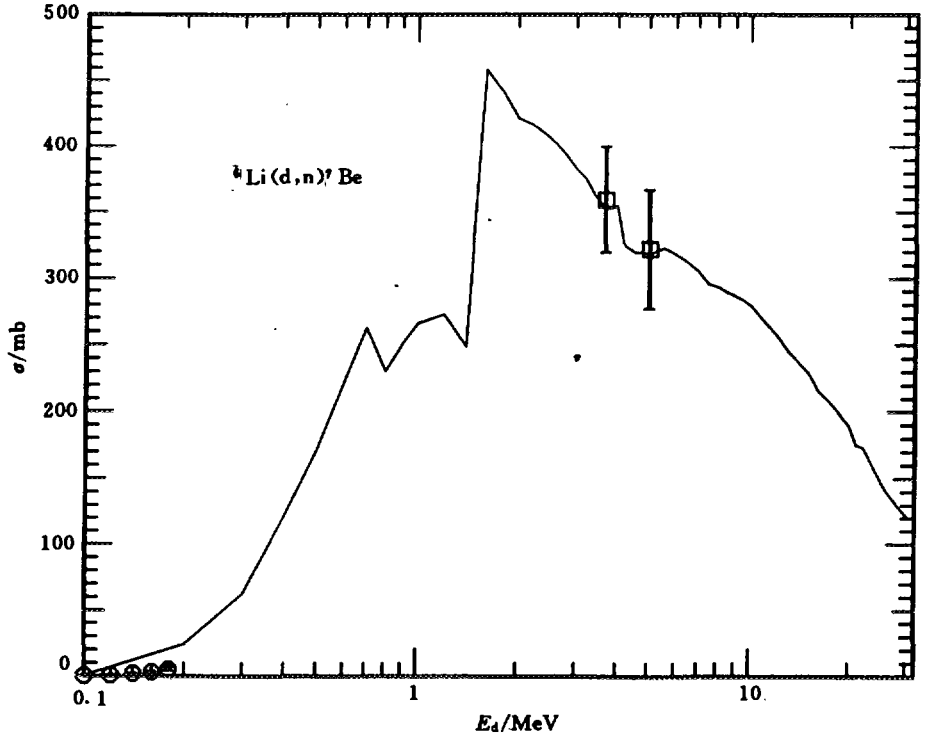

Fig.6 The cross section of ^{6}Li(d,n)^{7}Be reaction.

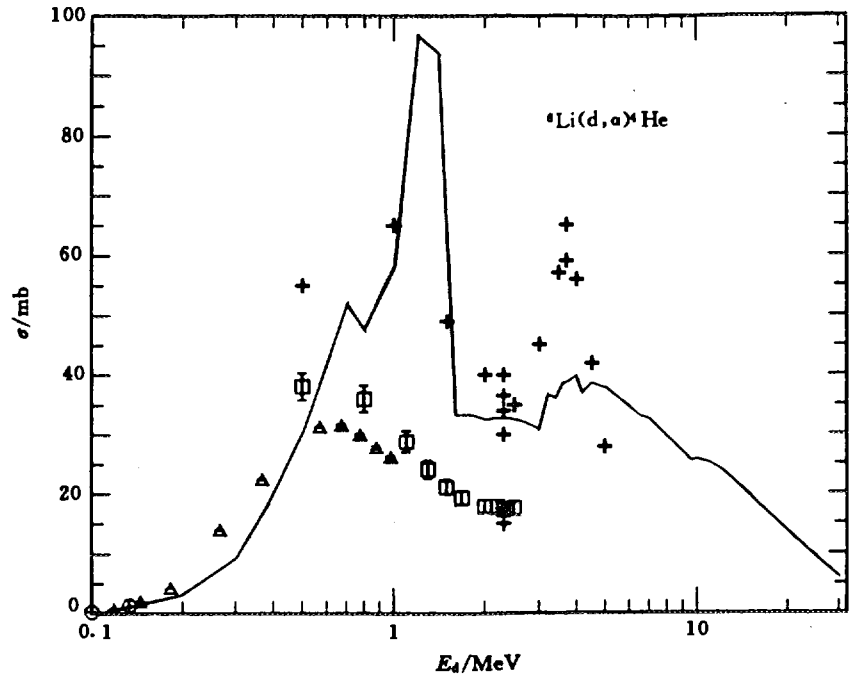

Fig.7 The cross section of $^{6}Li(d,\alpha)^{4}He$ reaction.

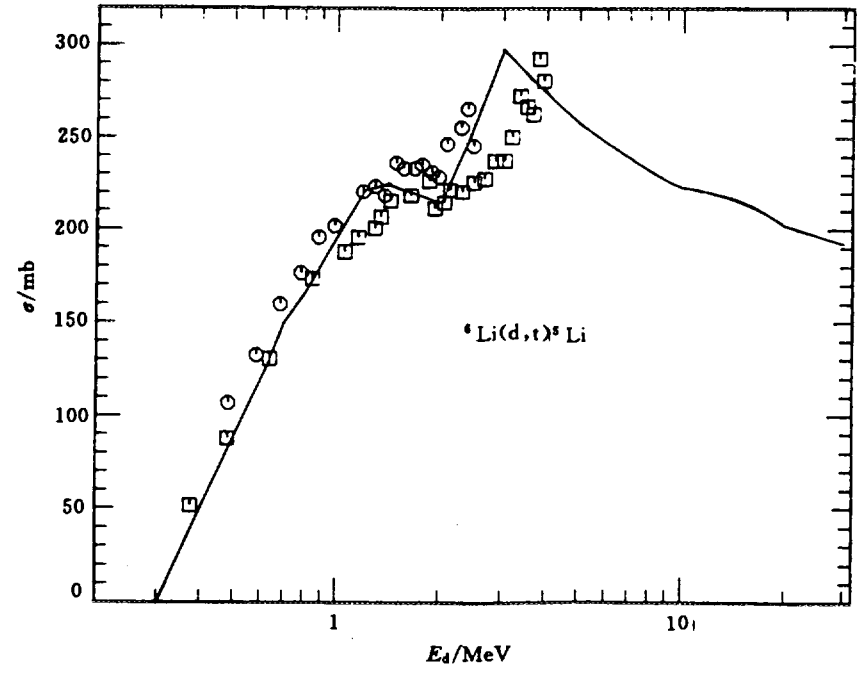

Fig.8 The cross section of $^{6}Li(d,t)^{5}Li$ reaction.

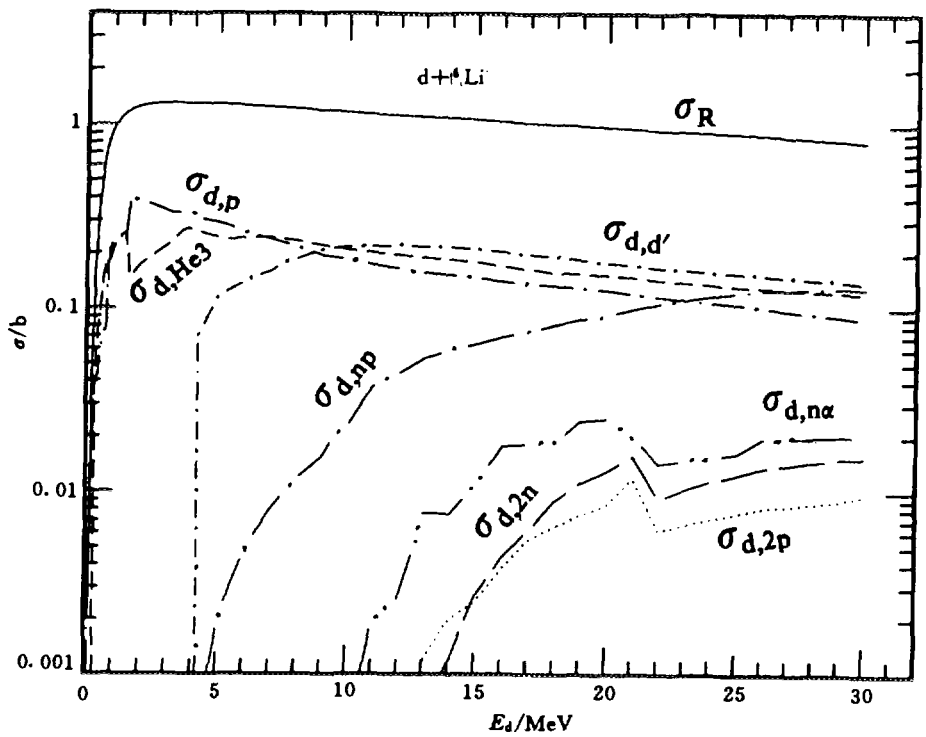

Fig.9 The cross section of d+^{6}Li reaction.

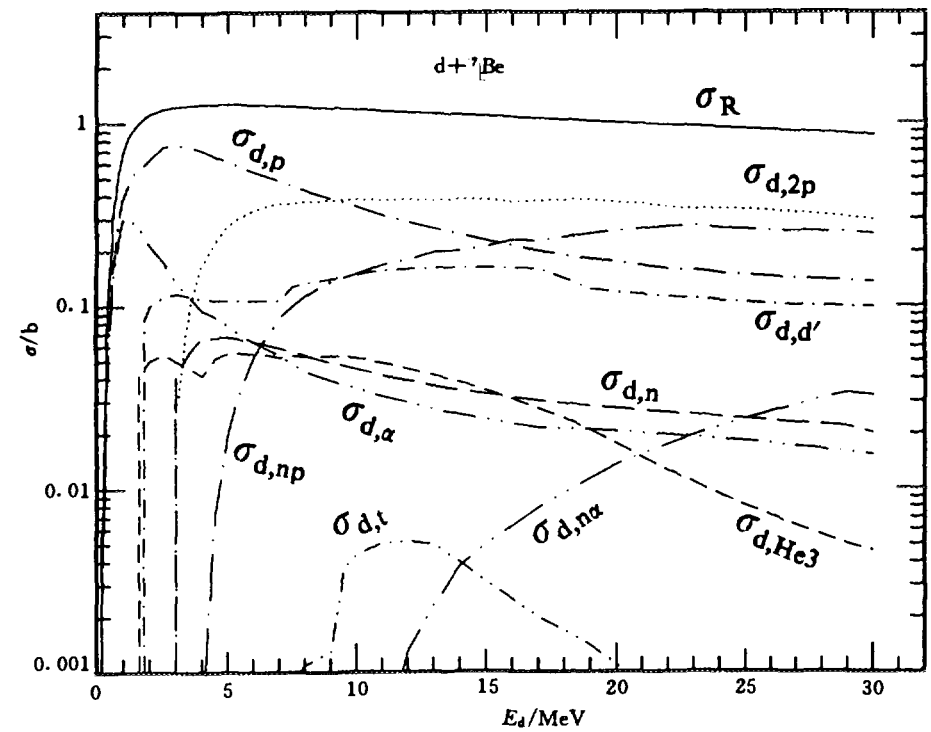

Fig.10 The calculated cross section of the d+^{7}Be reaction.

References

[1] W.D. Myers, et al., Proc. of First Int. Conf. on Radioactive Nuclear Beams, Singapore, World Scientific, 1990.

[2] Bai Xixiang, Liu Weiping. Atomic Energy Sci. and Technol. 27, 385(1993).

[3] Bai Xixiang et al., Chin. J. Nucl. Phys. 16, 100(1994).

[4] Zhang Jingshang, The Charged Particle Induced Reaction Code CUNF(unpublished).

[5] Shen Qingbiao, Lu Congshan, Commun. of Nucl. Data Prog., 7, 41(1992).

[6] P.D. Kunz, Distorted Wave Code DWUCK4. University of Colorado, USA (unpublished).

[7] B. Wilkins, G. Igo., Phys. Lett.3, 48(1962).

[8] S. Mayo, W. Schimmerling, M.J. Sametband., Nucl. Phys. 62, 393(1965).

[9] Huang Bingyin et al., Conf. on Nucl. Phys., Shanghai, 1974.

[10] Mao Zhenlin et al., Conf. on Low Energy Nucl. Phys., Lanzhou, 1972.

[11] Yuan Rongfeng et al., Chin. J. Nucl. Phys., 3, 155(1981).

[12] W. Fitz, R. Jahr, R. Santo., Nucl. Phys., A101, 449(1967).

[13] J. Szab et al., Nucl. Phys., A289, 526(1977).

[14] Liang Qichang et al., Atomic Energy Sci. and Technol., 1, 10(1977).

[15] A.J. Elwyn et al., Phys. Rev., C16, 1744(1977).

[16] J.M.F. Jeronymo et al., Nucl. Phys., 38, 11(1962).

[17] Cai Dunjiu et al., Exfor-S00171, 1985.

[18] R.L. Macklin, H.E. Banta, Phys. Rev. 97, 753(1955).

[19] Liu Weiping et al., Phys. Rev. Lett., 77, 611(1996).

CN9702238

DEUTERON INDUCED REACTIONS EXCITATION FUNCTIONS ON ^{51}V, ^{52}Cr, ^{56}Fe AND ^{57}Fe

Xu Xiaoping Han Yinlu Zhuang Youxiang

(China Nuclear Data Center, CIAE)

Abstract

Deuteron induced reactions on ^{56}Fe, ^{57}Fe, ^{51}V and ^{52}Cr have been widely used in medical radioisotope production, research on radiation damage and activation analysis. The excitation functions and energy spectra were evaluated and calculated for ^{56}Fe, ^{57}Fe, ^{51}V and ^{52}Cr(d,n), (d,p), (d,α), (d,^{3}He), (d,d'), (d,t), (d,2n), (d,np+pn), (d,nα+αn), (d,2p) and (d,3n) from respective threshold to 30.0 MeV.

Introduction

Because of applications to astrophysics, neutron source, radiation therapy, isotope production, radiation damage, accelerator shielding, neutral or charged particle beam spectroscopy, etc., there is considerable interest in proton and deuteron reaction data. The purpose of this paper is to report the set of calculated results of $^{56,57}Fe$, ^{51}V and ^{52}Cr in the deuteron energy up to 30.0 MeV and to test the applicability of nuclear model calculations.

1 Evaluation of Experimental Data

There are a few deuteron absorption cross sections for d+^{56}Fe and d+^{51}V measured by some laboratories[1~3]. Because the isotope abundances of natural iron are ^{58}Fe: 0.3%, ^{57}Fe: 2.2%, ^{56}Fe: 91.7%, ^{54}Fe: 5.8%, most of the iron samples are not pure ^{56}Fe.

Excitation functions of $^{56}Fe(d,n)^{57}Co$[4], $^{56}Fe(d,\alpha)^{54}Mn$[2,4,5,6], $^{56}Fe(d,2n)^{56}Co$[2,4,5,6], $^{56}Fe(d,3n)^{55}Co$[6] were reported at low bombarding energies. $^{57}Fe(d,2n)^{57}Co$[6], $^{52}Cr(d,2n)^{52}Mn$[5] and $^{51}V(d,2n)^{51}Cr$[5] reactions cross sections were reported in some laboratories. The errors for these experimental data are between 6% and 15%. The measured data are available from threshold energy to 30.0 MeV. Most of these data were measured using the stacked-foil technique. There are two major sources of errors in this technique: (1). Beam current measurement via monitor reactions;

(2). Mean particle energy determination in a thick sample. These two points were considered in Ref.[2] which used high enriched ^{56}Fe foils (99.95%) as samples. In recent years, in order to check the incident deuteron energy, the energy degradation in the stack, and the beam intensity, appropriate monitor foils were inserted in each stack. The foils used were Al for the deuteron beam. The chemical separation, coincidence technique, Ge-Li detector are used in these experiments.

2 Theories and Parameters

The optimum deuteron optical potential parameters of iron were searched automatically by APCOM[7] to fit the experimental data of deuteron absorption cross sections for d+^{56}Fe with incident deuteron energies of 2.0 ~ 65.0 MeV. The excitation functions were calculated by code CUNF[8] which is based on the optical model, evaporation model, exciton model of preequibrium emission theory, the multiparticle and hole state densities and the Pauli exclusion principle are considered. Because the experimental data of d+^{56}Fe are scarce, the experimental data of d+^{nat}Fe absorption cross sections are also used in our calculation, the set of best deuteron optical potential parameters on ^{56}Fe is obtained as follows:

$$V = 119.1264 - 0.0001E - 0.026784E^2 + 18.2441\,(N - Z)/A$$
$$W_s = \{\, 0.0,\ 5.4464 - 0.00001E + 11.8333\,(N - Z)/A \,\}$$
$$W_v = 0.023983, \quad U_{so} = 7.0, \quad R_c = 1.172,$$
$$R_{so} = R_r = 0.9000, \quad R_s = 1.5089, \quad R_v = 0.9000,$$
$$A_{so} = A_r = 0.6676, \quad A_s = 0.7471, \quad A_v = 0.9000.$$

Using this set of deuteron optical potential parameters on ^{56}Fe, all reaction cross sections on ^{56}Fe, ^{57}Fe, ^{51}V and ^{52}Cr were calculated by code CUNF. The pair corrections, the level densities parameters and the discrete levels with their spins and parities are obtained from Ref.[9] in our calculation. Other charged particles and neutron optical potential parameters, the level density parameter and the free parameter of square of the average two-body interaction matrix element K in pre-equilibrium exciton model were adjusted. The exciton model parameter K is taken as 200 MeV^3. The direct inelastic cross sections were calculated by DWUCK-4[10].

3 Results and Discussion

Fig.1 shows the comparison of deuteron absorption cross sections on ^{56}Fe in the deuteron energy region 2.0 ~ 65.0 MeV between the theoretical values (solid line)

and the experimental data. There is good agreement between them.

Because some different channels have the same residual nuclei, such as (d,np), (d,pn) and (d,d); (d,nα) and (d,αn) et al.; (d,^{3}He) and (d,2pn); (d,α) and (d,2d) et al., the cross sections obtained by measuring the residual nuclei were the sum of all the corresponding reaction channels.

The cross sections for ^{56}Fe(d,n)^{57}Co reaction are also shown in Fig.1. The theoretical results (solid line) are in good agreement with the experimental values. The experimental data at E_d>15.0 MeV include those of the other channel. Fig.1 shows the comparisons between the calculated and experimental data of the cross sections of ^{56}Fe(d,α)^{54}Mn reactions. Fig.2 shows the reaction cross section of ^{56}Fe(d,2n)^{56}Fe. The theoretical results are larger than the experimental data at the incident deuteron energy E_d<13.0 MeV which are to be researched in the future. There are excellent agreements between the experimental and calculated data at E_d≥13.0 MeV. The cross sections of ^{56}Fe(d,3n)^{55}Co reaction are shown in Fig.2. There are excellent agreements between the experimental and calculated data at the incident deuteron energy E_d<30.0 MeV. The calculation results are larger than the experimental data at E_d≥30.0 MeV because the theoretical calculation codes used here have not considered the fourth-chance particles emission.

Fig.3 shows the absorption cross section of d+^{51}V. There is excellent agreement between the theoretical result and the experimental data. Fig.3 also shows the reaction cross section of ^{51}V(d,2n)^{51}Cr. There is good agreement between the theoretical result and the experimental data at the incident deuteron energy E_d<25.0 MeV and there is big difference at E_d≥25.0 MeV. Fig.4 shows the reaction cross section of ^{57}Fe(d,2n)^{57}Co. There is good agreement between the theoretical result and the experimental data at the incident deuteron energy E_d<20.0 MeV and there is big difference at E_d≥20.0 MeV because the fourth-chance emission particles are not considered in the theoretical calculation codes. ^{52}Cr(d,2n)^{52}Mn reaction cross section is shown in Fig.5. The experimental data are of ^{52}Cr(d,2n)^{52g}Mn and ^{52}Cr(d,2n)$^{52\,m}$Mn, respectively. The theoretical results are of ^{52}Cr(d,2n)$^{52\,g+m}$Mn. The experimental data of S. J. Nassiff (1973) are to be researched in other papers.

Figs.6 ~ 9 show the reactions cross sections of (d,n), (d,p), (d,α), (d,^{3}He), (d,d'), (d,t), (d,2n), (d,np+pn), (d,nα+αn), (d,2p), (d,3n) reactions on ^{56}Fe, ^{51}V, ^{57}Fe and ^{52}Cr, respectively. The curves' trends of the channels which have no experimental data are reasonable. These results could predict some characteristics of the reaction channels which have no experimental data upto now.

4 Conclusions

Based on the available deuteron induced reactions experimental data of iron, a set of deuteron optical potential parameters on iron at 2.0 ~ 65.0 MeV has been obtained. With adjusting the level densities parameters, the calculated reaction cross sections of $^{56}Fe(d,n)^{57}Co$, $^{56}Fe(d,\alpha)^{54}Mn$, $^{56}Fe(d,2n)^{56}Co$, $^{56}Fe(d,3n)^{55}Co$, $^{57}Fe(d,2n)^{57}Co$, $^{52}Cr(d,2n)^{52}Mn$ and $^{51}V(d,2n)^{51}Cr$ are in reasonable agreements with the experimental data and might predict some characteristics of reaction channels of d+^{56}Fe, ^{57}Fe, ^{52}Cr and ^{51}V which have no experimental data up to now. These conclusions also proved the reasonability and dependability of these theoretical calculation programs which could possibly help in selecting the best experimental data for evaluation purposes in cases where several inconsistent experimental data sets are available.

Acknowledgments

One of the author (Xu) thanks to Drs. Zhang Jingshang, Shen Qingbiao, Liu Tong and Su Zongdi for their very kind help and suggestions. This work was supported by CNDC.

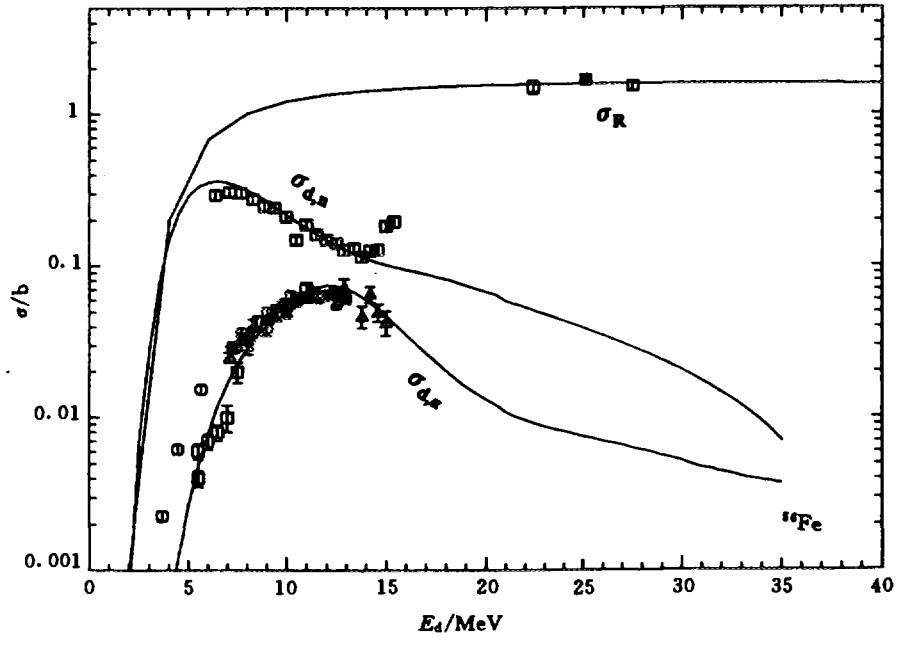

Fig.1 ^{56}Fe deuteron absorption cross section

□ S. Maya 65 $^{56}Fe(d,\alpha)^{54}Mn$ reaction cross section

$^{56}Fe(d,n)^{57}Co$ reaction cross section ▫ J. W. Clark 69 ○ S. Sudar 94 ▲ Tao Zhenlan 83

▫ Tao Zhenlan 83

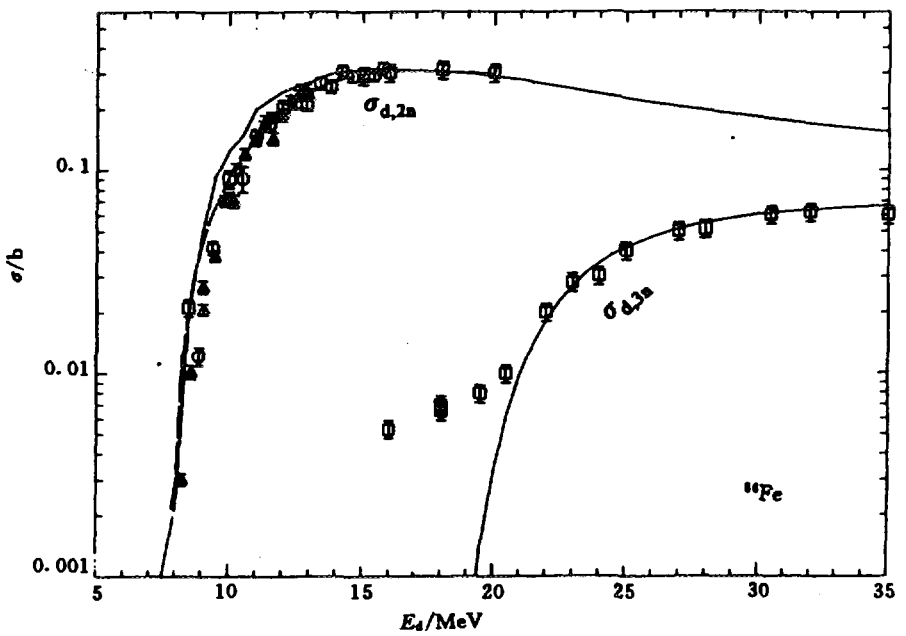

Fig.2 $^{56}Fe(d,2n)^{56}Co$ reaction cross section

▫ J. W. Clark 69 ○ Tao Zhenlan 83 ▲ S. Sudar 94

$^{56}Fe(d,3n)^{55}Co$ reaction cross section

▫ J. W. Clark 69

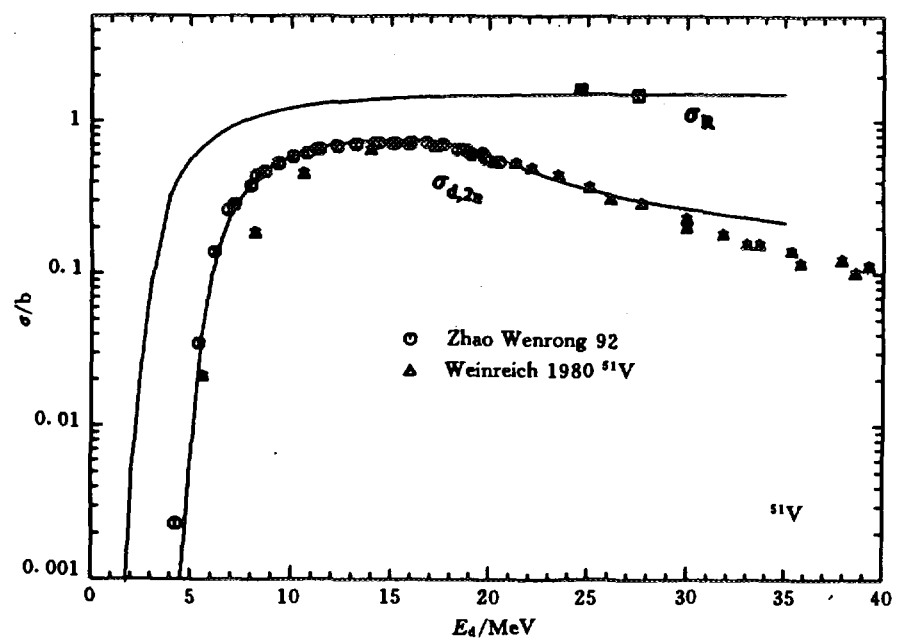

Fig.3 ^{51}V deuteron absorption cross section

▫ S. Maya 65

$^{51}V(d,2n)^{51}Cr$ reaction cross section ▫ Zhao Wenrong 92 ○ Weinreich 80

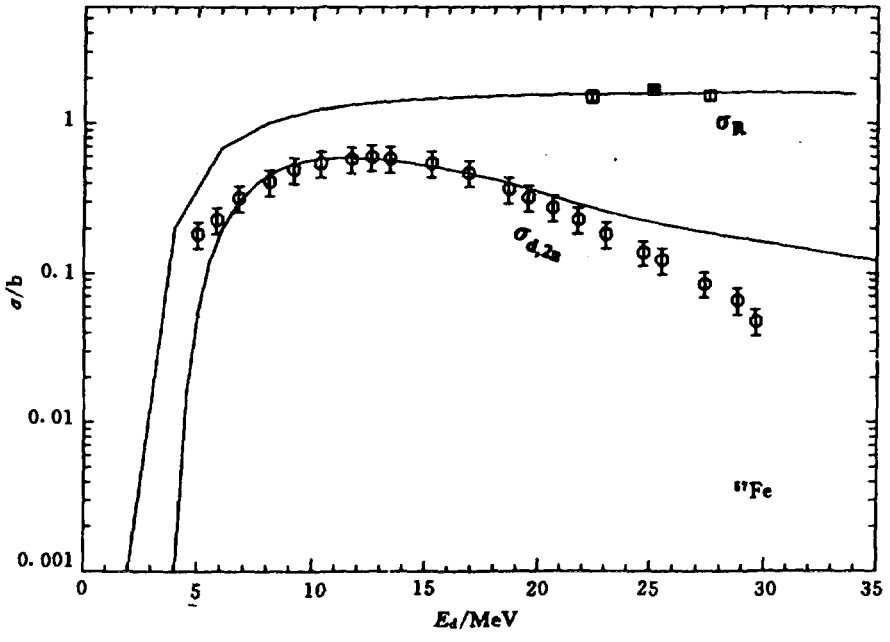

Fig.4 ^{57}Fe(d,2n)^{57}Co reaction cross section

▫ J. W. Clark 69

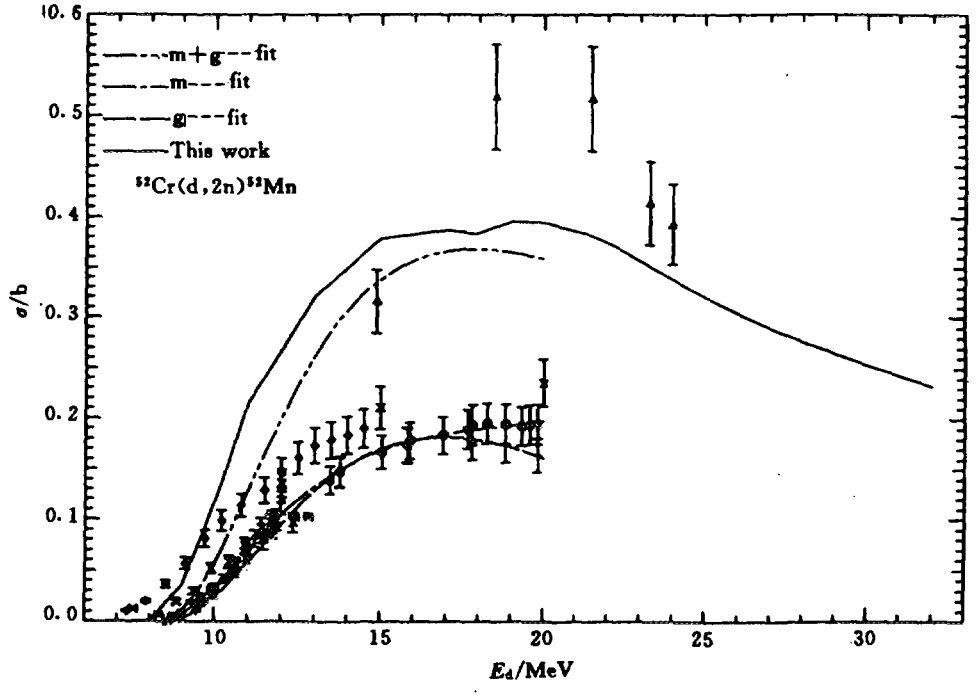

Fig.5 ^{52}Cr(d,2n)^{52}Mn reaction cross section

▫ H. I. West 87 ○ S. J. Nassiff 73 ▲ H. I. West 87

+ W. H. Burgus 54 × P. Kafalas 56 ◦ M. Cogreau 66

✦ Chen Xiaowu 66

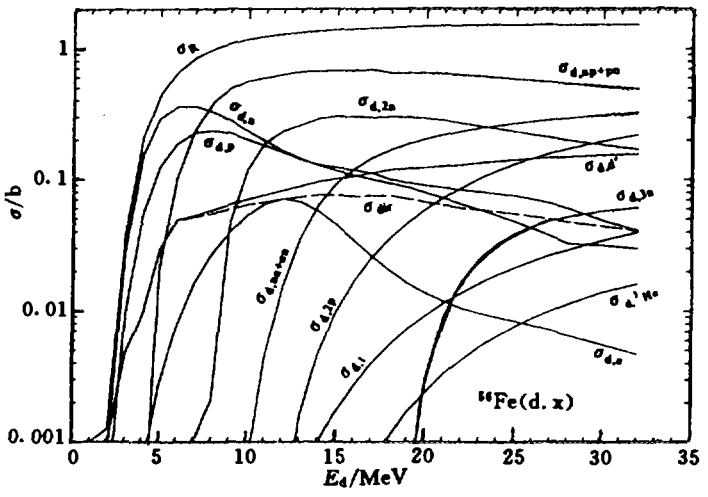

Fig.6 ^{56}Fe(d,x) reaction cross sections

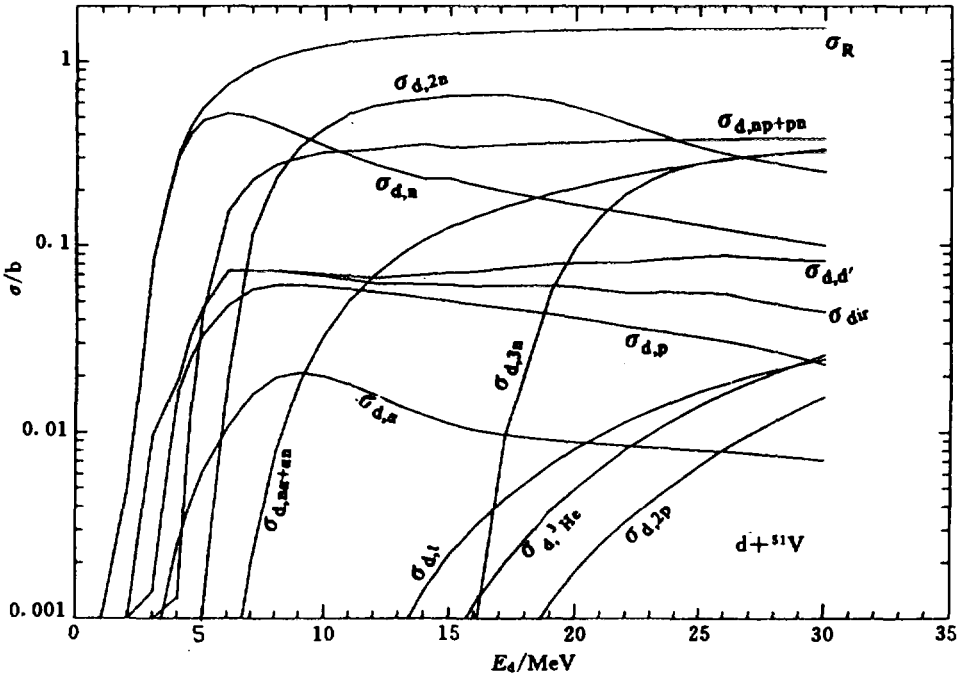

Fig.7 ^{51}V(d,x) reaction cross sections

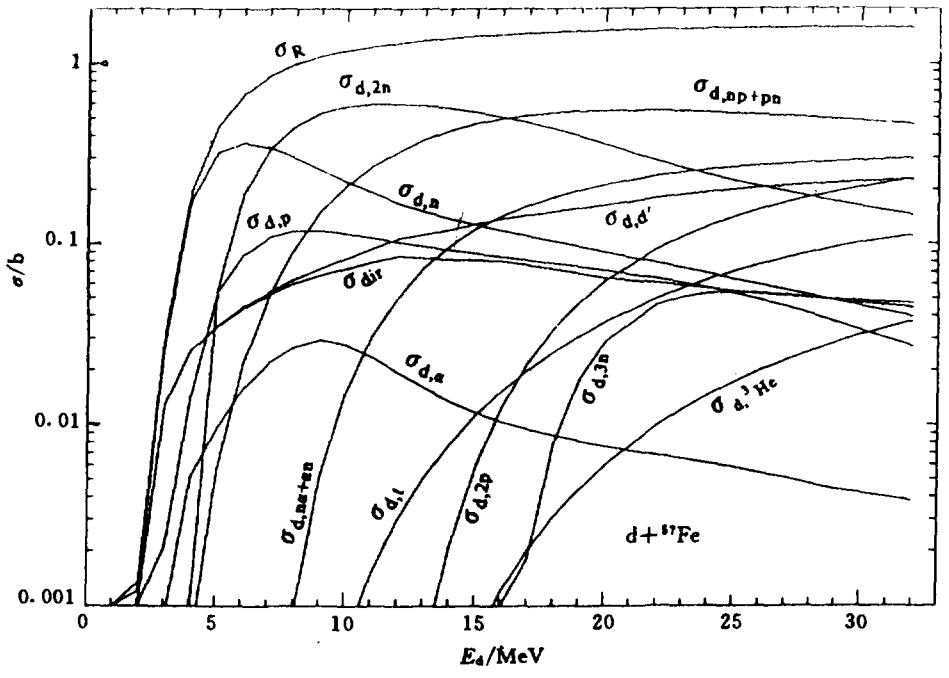

Fig.8 ^{57}Fe(d,x) reaction cross sections

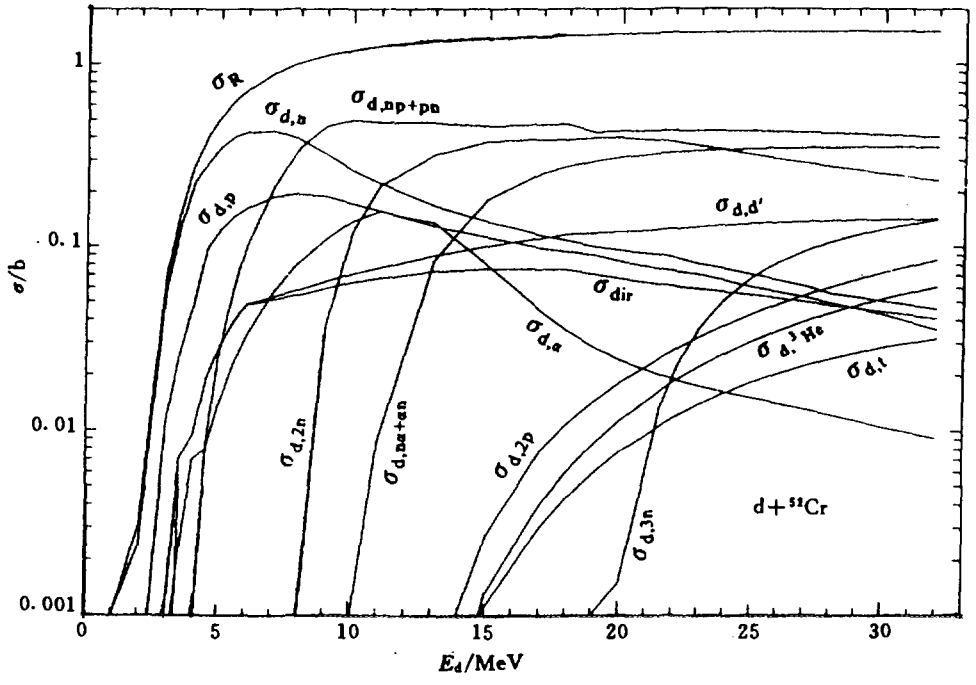

Fig.9 ^{52}Cr(d,x) reaction cross sections

References

[1] W. Bauhoff, Atomic Data and Nuclear Data Tables, 35, No.3, (1986)

[2] S. Sudar et al., Phys. Rev., C50, 2408, (1994)

[3] S. Maya et al., Nucl. Phys., 62, 393, (1965)

[4] Tao Zhenlan et al., Atom. Ener. Sci. and Tech. 5, 506, (1983)

[5] Experimental Nuclear Data Master File in EXFOR Format.

[6] J. W. Clark et al., Phys. Rev., 179, 1104, (1969)

[7] Shen Qingbiao, Commu. Nucl. Data Progress 7, 41 (1992)

[8] Zhang Jingshang, Commu. Nucl. Data Progress 7, 14 (1992)

[9] Su Zongdi et al., Commu. Nucl. Data Progress 12, 83 (1994)

[10] P. D. Kunz, "Distorted Wave Code Dwuck 4", University of Colorado.

[11] W. H. Burgus et al., Phys. Rev., 95, 750, (1954)

[12] P. Kafaras et al., Phys. Rev., 104, 703, (1956)

[13] Cheng Xiaowu et al., Physics Journal, 22(2), 250, (1966)

[14] M. Cogneau et al., Nucl. Phys., 79, 203, (1966)

Calculation and Analysis of d+^{7}Li Reaction

Han Yinlu Shen Qingbiao Zhang Jingshang
(Chinese Nuclear data Center, CIAE)

Zhang Zhengjun Sun Xiuquan
(Physics Department, Northwest University, Shannxi)

Abstract

The cross sections of d+^{7}Li reaction at incident energies spanning 0.1 ~ 30 MeV were obtained by calculation with the Distorted Wave Born approximation, preequilibrium nuclear reaction and Hauser-Feshbach (HF) theories. The calculated results are compared with experimental data.

Introduction

The production and use of unstable radioactive nuclear ion beams are of considerable interest, because they can provide a new opportunity for studying nuclear phenomena in a wider field. The cross sections of d+^{7}Li reaction are important for some nuclear engineering designs.

In order to predict and analyse the production of ^{6}He, ^{8}Li and ^{7}Be radioactive beams, theoretical calculations and analysis of the d+^{7}Li reaction are needed. The purpose of this paper is to calculate and analyse the data of d+^{7}Li reaction.

1 Theoretical Calculation and Analysis of Reaction d+^{7}Li

The reaction d+ ^{7}Li at the incident deuteron energy region of 0.1~30 MeV were studied with the distorted wave Born approximation, preequilibrium nuclear reaction and Hauser-Feshbach theories. The charged particle induced reaction code CUNF[1], the searching optimal charged particle optical potential parameter code APCOM[2] and the distorted wave Born approximation code DWUCK4[3] were used in the calculations.

Based on the experimental reaction cross sections of d+^{9}Be[4,5] and elastic scattering angular distributions of d+^{6,7}Li[6~8] and d+^{9}Be[9], a set of optimum deuteron optical potential parameters up to 30 MeV with the code APCOM has been obtained in Ref.[10]. The cross sections of d+^{7}Be reaction were calculated with this set of optical potential parameters.

Fig.1 shows the comparison of the calculated discrete level (d,p_0), (d,p_1) and (d,p_2) angular distribution of d+^{7}Li reactions at the energy 3.7 MeV and 5.05 MeV with the experimental data[6,7]. The theoretical calculated values at deuteron energy 3.7 MeV are in agreement with the experimental data, and at deuteron energy 5.03 MeV the calculated values are basically in agreement with the experimental data. The contribution of the direct reaction is large than those of the compound-nucleus reaction at the energy 3.7 MeV, while at the energy 5.03 MeV, the contribution of the compound-nucleus reaction is large than those of the direct reaction. The angular distribution for (d,p_1) and (d,p_2) reaction are mainly contributed by the compound-nucleus reaction. The comparison of the calculated discrete level (d,d_1) reaction angular distribution at the energy 3.7 MeV and 5.05 MeV with the experimental data[6,7] were given in Fig.2. The theoretical calculated values at deuteron energy 3.7 MeV are low than the experimental data, and at deuteron energy 5.03 MeV the calculated value are basically in agreement with the experimental data. The ^{7}Li$(d,t_0)^6$Li reaction angular distributions for the deuteron energies 3.7 MeV and 5.03 MeV are shown in Fig.3, and the theoretical calculated value are in agreement with the experimental data[6,7].

Fig.4 shows the comparison of the calculated ^{7}Li$(d,n)^8$Be reaction cross sections with the experimental data[11,12]. The theoretical calculated curve pass through the existence experimental data and the reaction cross sections are mainly contributions of the compound-nucleus reactions. The ^{7}Li$(d,p)^8$Li and ^{7}Li$(d,t)^6$Li reaction cross sections are given in Fig.5 and Fig.6, respectively. The calculated value fit the experimental data[13~15] well. The direct and compound-nucleus reaction are corre-spondence for the cross sections of the ^{7}Li$(d,p)^8$Li and ^{7}Li$(d,t)^6$Li reaction. The cross section of the ^{7}Li$(d,\alpha)^5$He reaction is shown in Fig.7. The calculated value are low than the experimental data[16]. The cross section of the ^{7}Li$(d,2n)^7$Be reaction is shown in Fig.8. The calculated value are basically in agreement with experimental data[17].

Besides above results, the cross sections without experimental data, are predicted for d+^{7}Li reaction, the calculated results were shown in Fig.9. Because of the discrete level effect, the curve of reaction cross section presents some small peak in above figures, it is reasonable in physically. The ^{6}He, ^{8}Li and ^{7}Be radioactive beam were produced through ^{7}Li$(d,He^3)^6$He, ^{7}Li$(d,p)^8$Li and ^{7}Li$(d,2n)^7$Be reactions, respec- tively. The ^{6}Li$(d,n)^7$Be[10] and ^{7}Li$(d,2n)^7$Be reactions channels are open at inci- dent deuteron energy 0.1 MeV and 5.0 MeV, respectively, and the cross sections of ^{7}Li$(d,n)^7$Be reaction are large than those of ^{7}Li$(d,2n)^7$Be reaction. The results show that the ^{6}Li$(d,n)^7$Be reaction is more feasible than the ^{7}Li$(d,2n)^7$Be reaction to get the ^{7}Be radioactive beam, and the ^{7}Li$(d,p)^8$Li reaction is more feasible than the ^{9}Be$(d,He^3)^8$Li reaction to get the ^{8}Li radioactive beam in experimental

measurement.

2 Summary

The various nuclear data of the reaction d+^{7}Li in the incident deuteron energy region 0.1~30.0 MeV were obtained with DWBA, preequilibrium reaction and HF theory. The calculated results basically agree with the experimental data. The nuclear data for some incident energies, for which there is no experimental data, were reasonably predicted. The calculated results show that the contribution of compound- nucleus reaction is important, and the reaction cross sections come from contribution of the discrete level for light nucleus. These theoretical results have important reference value to experimental scientists.

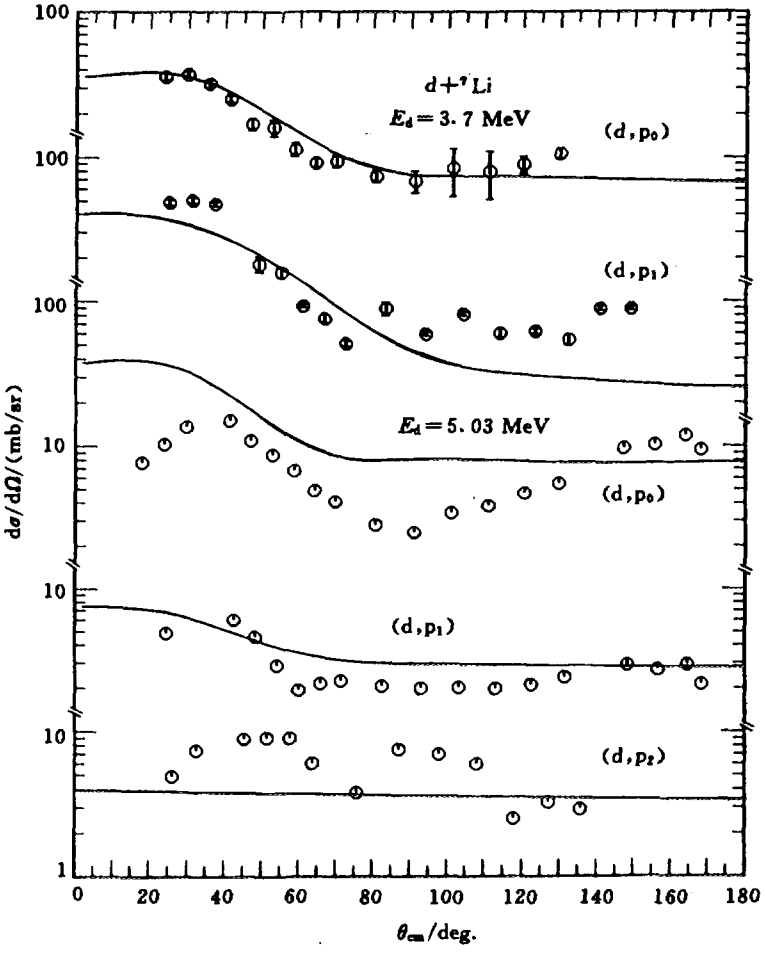

Fig.1 The discrete level angular distributions of ^{7}Li(d,p)^{8}Li reaction.

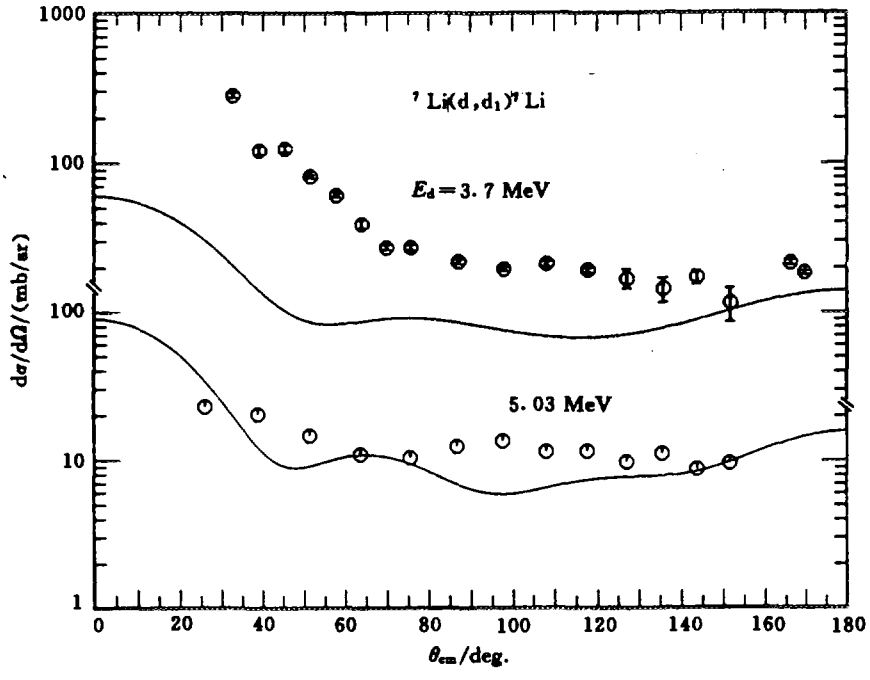

Fig.2 The discrete level angular distributions of $^{7}Li(d,d_1)^{7}Li$ reaction.

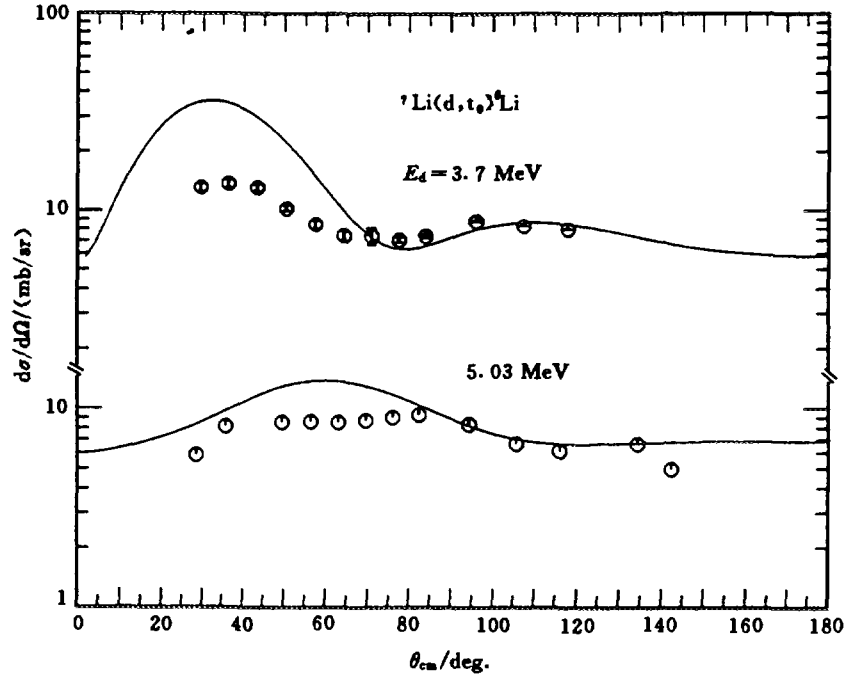

Fig.3 The discrete level angular distributions of $^{7}Li(d,t)^{6}Li$ reaction.

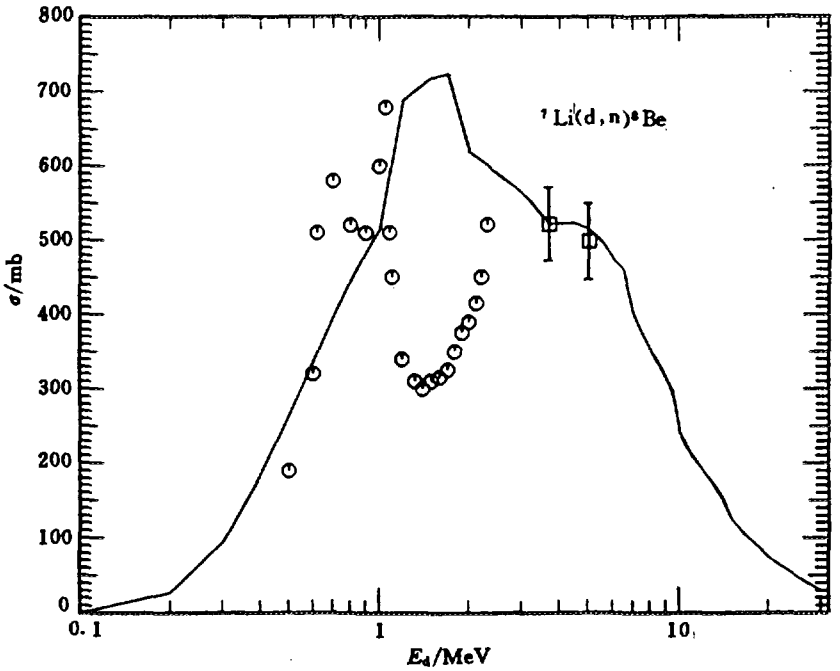

Fig.4 The cross section of ^{7}Li(d,n)^{8}Be reaction

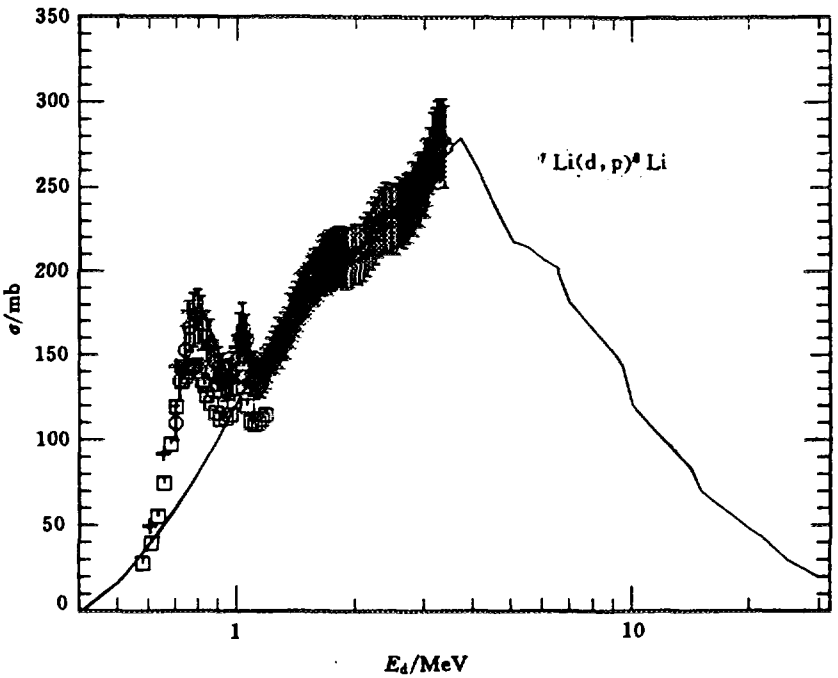

Fig.5 The cross section of ^{7}Li(d,p)^{8}Li reaction.

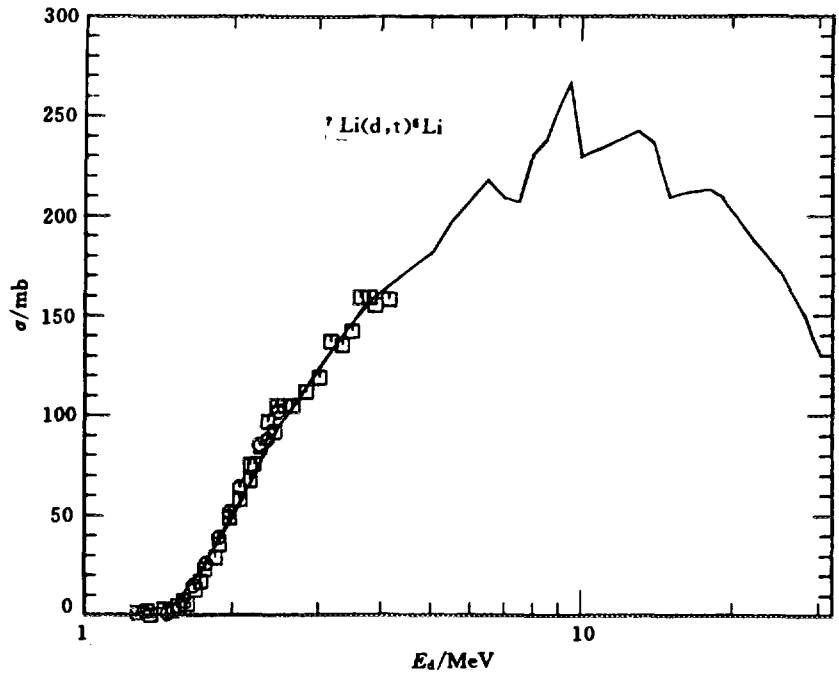

Fig.6 The cross section of $^{7}Li(d,t)^{6}Li$ reaction.

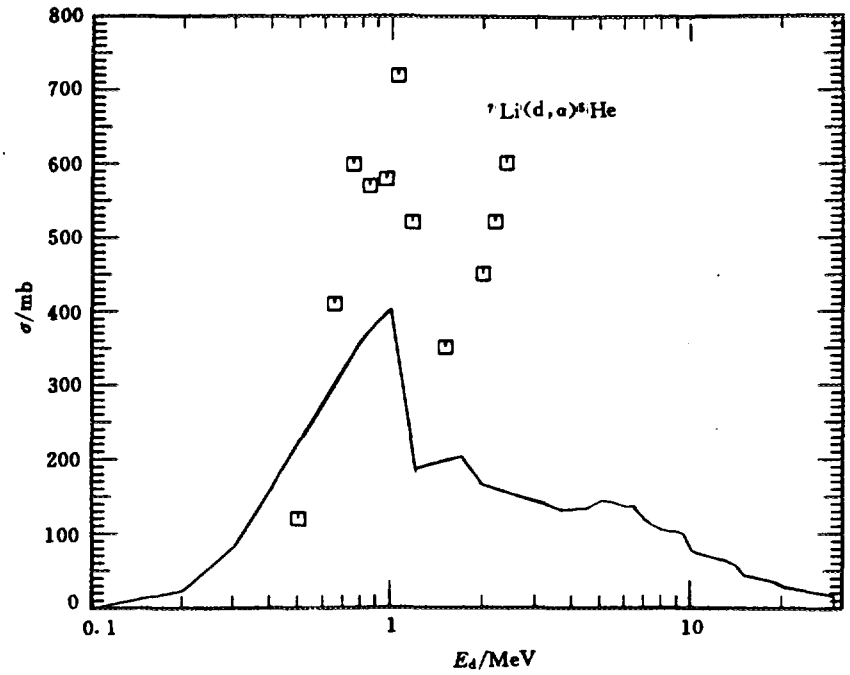

Fig.7 The cross section of $^{7}Li(d,\alpha)^{5}He$ reaction.

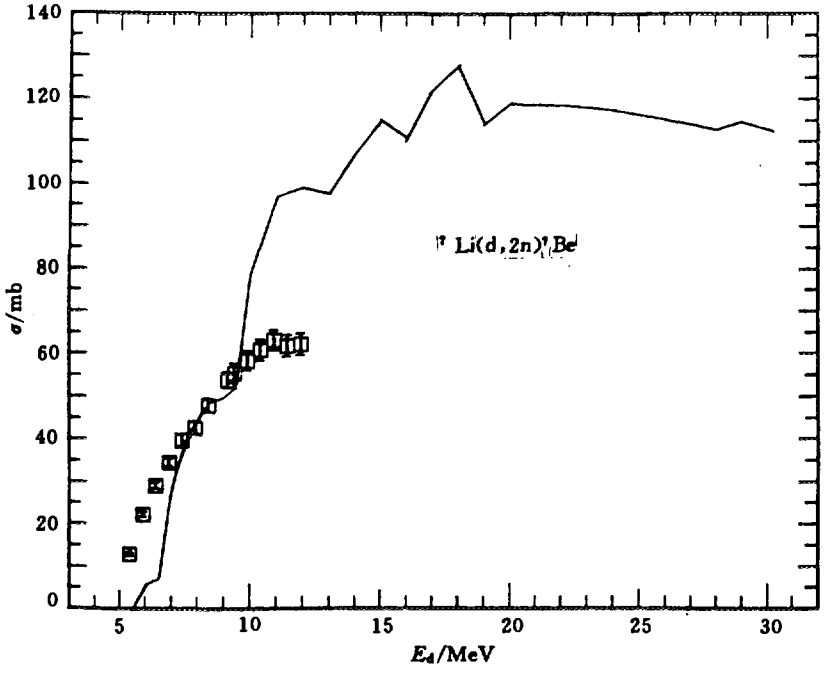

Fig.8 The cross section of ^{7}Li(d,2n)^{7}Be reaction.

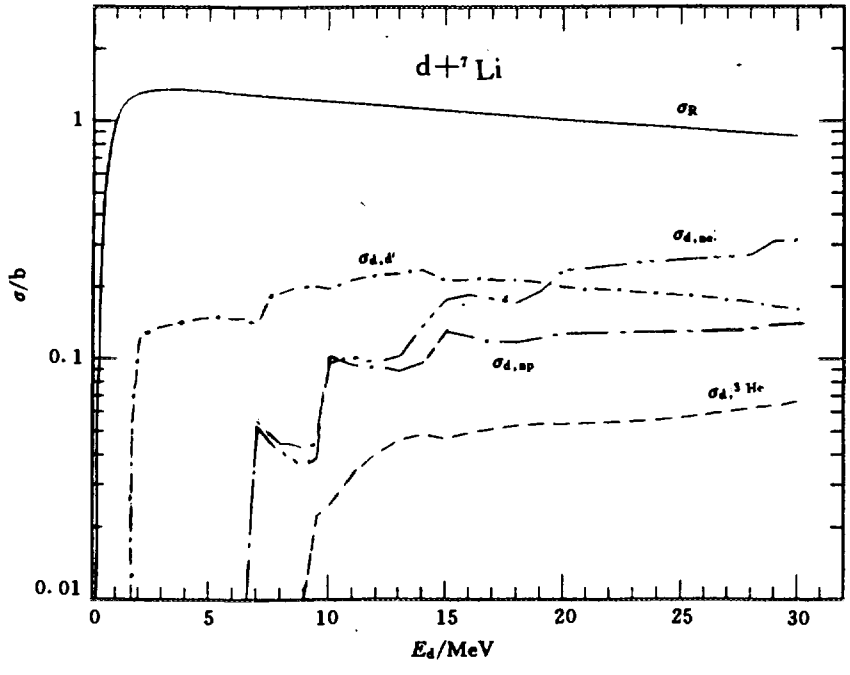

Fig.9 The calculated cross section of the d+^{7}Li reaction.

References

[1] Zhang Jingshang. The Charged Particle Induced Reaction Code CUNF. (unpublished).
[2] Shen Qingbiao, Lu Congshan. Commun. Nucl. data Prog., 7 , 41(1992).
[3] P. D. Kunz, Distorted Wave Code DWUCK4. University of Colorado, USA (unpublished).
[4] B. Wilkins, G. Igo. Phys. Lett., 3, 48(1962).
[5] S. Mayo, W. Schimmerling, M. J. Sametband. Nucl. Phys., 62, 393(1965).
[6] Huang Bingyin et al., Conf. on Nucl. Phys., Shanghai, 1974.
[7] Mao Zhenlin at al., Conf. on Low Energy Nucl. Phys., Lanzhou, 1972.
[8] Yuan Rongfeng et al., Chin. J. Nucl. Phys., 3, 155(1981).
[9] W. Fitz, R. Jahr, R. Santo. Nucl. Phys., A101, 449(1967).
[10] Han Yinlu et al., Commun. Nucl. Data Prog. to be published.
[11] Liang Qichang et al., Atomic Energy Sci. and Technol., 1, 10(1977).
[12] Yuan Hanrong et al., The Cross Section for ^{6}Li(d,n) and ^{7}Li(d,n). (unpublished).
[13] B. W. Filippone et al., Phys. Rev., C25, 2174(1982).
[14] R. W. Kavanagh. Nucl. Phys., 15, 411(1960).
[15] R. L. Macklin, H. E. Banta. Phys. Rev., 97, 753(1955).
[16] The charged particle group, Atomic Energy Sci. and Technol., 1,1(1975).
[17] B. JA. Guzhovskij et al., Izvestiya Akad. Nauk. SSSR, Ser. Fiz, 44, 1983(1980)

Excitation Functions and Energy Spectra of Proton Induced Reactions on ^{56}Fe and ^{57}Fe in the Energy up to 30 MeV

Xu Xiaoping Han Yinlu Zhuang Youxiang

(China Nuclear Data Center, CIAE)

Abstract

A set of proton optical potential parameters was obtained on ^{56}Fe from threshold to 65.0 MeV based on the available experimental data, and the excitation functions and energy spectra were evaluated and calculated for ^{56}Fe, ^{57}Fe(p,n), (p,p'), (p,α), (p,^{3}He), (p,d), (p,t), (p,2n), (p,np+pn), (p,nα+αn), (p,2p) and (p,3n) from respective threshold to 30.0 MeV. There are good agreements between the experimental data and the calculated data.

Introduction

Studies of excitation functions of charged particles induced reactions are of considerable significance for nuclear science and technology, such as activation analysis. Compared with neutron experimental data, the charged particles data are scarce, it is necessary to calculate the cross sections according to some theoretical models. The purpose of this paper is to report the set of calculated results of $^{56,57}Fe$ in the proton energy up to 30.0 MeV.

1 Evaluation of Experimental Data

The angular distributions of proton elastically scattering on iron have been reported at 10.93, 11.7, 17.0, 19.1, 20.4, 24.6, 30.3, 35.2 and 65.0 MeV[1,2]. There are a few proton absorbed cross sections for p+$^{56,57}Fe$ measured by some laboratories[2,3]. Because the isotope abundances of natural iron are ^{58}Fe: 0.3%, ^{57}Fe: 2.2%, ^{56}Fe: 91.7%, ^{54}Fe: 5.8%, most of the iron samples are not pure ^{56}Fe or ^{57}Fe.

Excitation functions of ^{56}Fe(p,n)^{56}Co, ^{56}Fe(p,p')^{56}Fe, ^{56}Fe(p,^{3}He)^{54}Mn, ^{56}Fe(p,2n)^{55}Co, ^{56}Fe(p,np+pn)^{55}Fe, ^{56}Fe(p,nα+αn)^{52}Mn[2~10] were reported at low bombarding energies. There were experimental data for the energy spectra of ^{56}Fe(p,xp) and ^{56}Fe(p,xα) reactions at the proton energy of 14.0 MeV. The error for these experimental data

was between 6% and 15%. The measured data were available from threshold energy to 30.0 MeV. Most of these data were measured using the stacked-foil technique. In recent years, in order to check the incident proton energy, the energy degradation in the stack, and the beam intensity, appropriate monitor foils were inserted in each stack. The foils used were Cu and Ni for the proton beam. The chemical separation, coincidence technique, Ge-Li detector are used in these ex- periments.

There were big differences between the experimental data for excitation functions of $^{57}Fe(p,n)^{57}Co$[2,4,5,7] reaction in different laboratories because it was very difficult to obtain pure ^{57}Fe samples. So did that of $^{57}Fe(p,\alpha)^{54}Mn$[2,4,5,7] reaction. There were only one group of experimental data for $^{57}Fe(p,2n)^{56}Fe$[2], $^{57}Fe(p,2p)^{56}Mn$[2] and $^{57}Fe(p,3n)^{55}Co$[2] reactions, respectively.

2 Theories and Parameters

The optimum proton optical potential parameters of iron were searched automatically by APCOM[13] to fit the experimental data of proton absorbed cross sections and differential cross sections simultaneously for p+^{56}Fe with incident proton energies of 2.0 ~ 65.0 MeV. The excitation functions were calculated by code CUNF[14] which was based on the optical model, evaporation model, exciton model of preequibrium emission theory, the multi-particle and hole state densities and the Pauli exclusion principle were considered. Because the experimental data of p+^{56}Fe were scarce, the experimental data of p+^{nat}Fe absorbed cross sections were also used in our calculation, the set of best proton optical potential parameters on ^{56}Fe is obtained as follows:

$$V = 45.49163 - 0.3007E - 0.00090336E^2 + 24(N\text{-}Z)/A + 0.4Z/A^{1/3}$$
$$W_s = \{\ 0.0,\ 10.04466 - 0.14224E + 12(N\text{-}Z)/A\ \}$$
$$W_v = \{\ 0.0,\ -0.44281 + 0.07084E - 0.0006293E^2\ \}$$
$$U_{so} = 6.2, \quad R_c = 1.85,$$
$$R_{so} = R_\gamma = 1.25845, \quad R_s = 1.25118, \quad R_v = 1.84970,$$
$$A_{so} = A_\gamma = 0.57880, \quad A_s = 0.44362, \quad A_v = 0.90000.$$

Using this set of proton optical potential parameters on ^{56}Fe, all reaction cross sections and energy spectra were calculated by code CUNF. The pair corrections, the level densities and the discrete levels with their spins and parities are obtained from Ref.[15] in our calculation. Other charged particles and neutron optical potential parameters, the level density parameter and the free parameter of square of the average two-body interaction matrix element K in pre-equilibrium exciton model were adjusted. The exciton model parameter K was taken as 900 MeV^3 and 600

MeV[3] for ^{57}Fe(p,x) and ^{56}Fe(p,x), respectively.

The direct inelastic cross sections were calculated by DWUCK-4[16] and the proton performance factor was taken as 0.25.

3 Results and Discussion

The differential cross sections for p+^{nat}Fe are shown in Fig.1 and Fig.2, we observed that the theoretical calculation were in good agreement with the measured data at the proton energy from 10.93 MeV to 65.0 MeV. Fig.2 shows the comparison of proton absorption cross sections on ^{56}Fe in the energy region 2.0 ~ 65.0 MeV between the theoretical values (solid line) and the experimental data. There is good agreement between both of them.

The cross sections for ^{56}Fe(p,n)^{56}Co reaction are shown in Fig.4. The theoretical results (solid line) are in good agreement with the experimental values. Because some different channels have the same residual nuclei, such as (p,np), (p,pn) and (p,d); (p,nα), (p,αn) and (p,2dn) et al; (p,^{3}He) and (p,2pn); (p,α), (p,2d), (p,pnd), (p,2n2p) et al., the cross sections obtained by measuring the residual nuclei were the sum of all the corresponding reaction channels.

Fig.3 show the comparisons between the calculated and experimental data of the cross sections of ^{56}Fe(p,p')^{56}Fe and ^{56}Fe(p,2n)^{55}Co reactions. Fig.4 shows the reaction cross section of ^{56}Fe(p,np+pn)^{55}Fe. Fig.5 and Fig.6 show the energy spectra of ^{56}Fe(p,xp) reaction and ^{56}Fe(p,xα) reaction. In Fig.5, the first peak that occurs at about 2.0 MeV is due to second-chance proton emission, the second peak at about 5.0 MeV is due to ^{56}Fe(p,p')^{56}Fe reaction energy spectra. The energy spectra at the emission proton energy E_p>9.0 MeV included the contributions of direct reaction and discreet energy levels. Because we did not consider the direct reaction for ^{56}Fe(p,α)^{53}Mn, there are big differences between the calculated results and the experimental data of ^{56}Fe(p,xα) reaction at the emission proton energy E_p>11.0 MeV. Because there are good agreements between the calculated results and the experimental data of ^{56}Fe(p,n)^{56}Co reaction cross sections and ^{56}Fe(p,xp) energy spectra, the neutron and proton parameters used in the code were reasonable, therefore the calculated results for ^{56}Fe(p,np+pn)^{55}Fe, ^{56}Fe(p,p')^{56}Fe (including the direct inelastic cross section) and ^{56}Fe(p,2n)^{55}Co reaction cross sections were reasonable, too.

The cross sections of ^{56}Fe(p,^{3}He)^{54}Mn and ^{56}Fe(p,nα+αn)^{52}Mn reactions are shown in Fig.4 and Fig.7, respectively. There are excellent agreements between the experimental and calculated data.

The proton absorption cross sections of ^{57}Fe were shown in Fig.8. There is good agreement between the experimental data and the calculated data. Fig.8 and Fig.9 showed the reaction cross sections of ^{57}Fe(p,n)^{57}Co, ^{57}Fe(p,α)^{54}Mn, ^{57}Fe(p,2n)^{56}Co,

^{57}Fe(p,2p)^{56}Mn and ^{57}Fe(p,3n)^{55}Co, respectively. There are good agreements between the calculated data and the experimental data, except for ^{57}Fe(p,3n)^{55}Co reaction cross section which was very small.

Fig.10 and Fig.11 illustrated (p,n), (p,p'), (p,α), (p,^{3}He), (p,d), (p,t), (p,2n), (p,np+pn), (p,nα+αn), (p,2p), (p,3n) of ^{56}Fe and ^{57}Fe. The curves' trends of the channels which have no experimental data were reasonable. These results could predict some characteristics of the reaction channels which have no experimental data upto now.

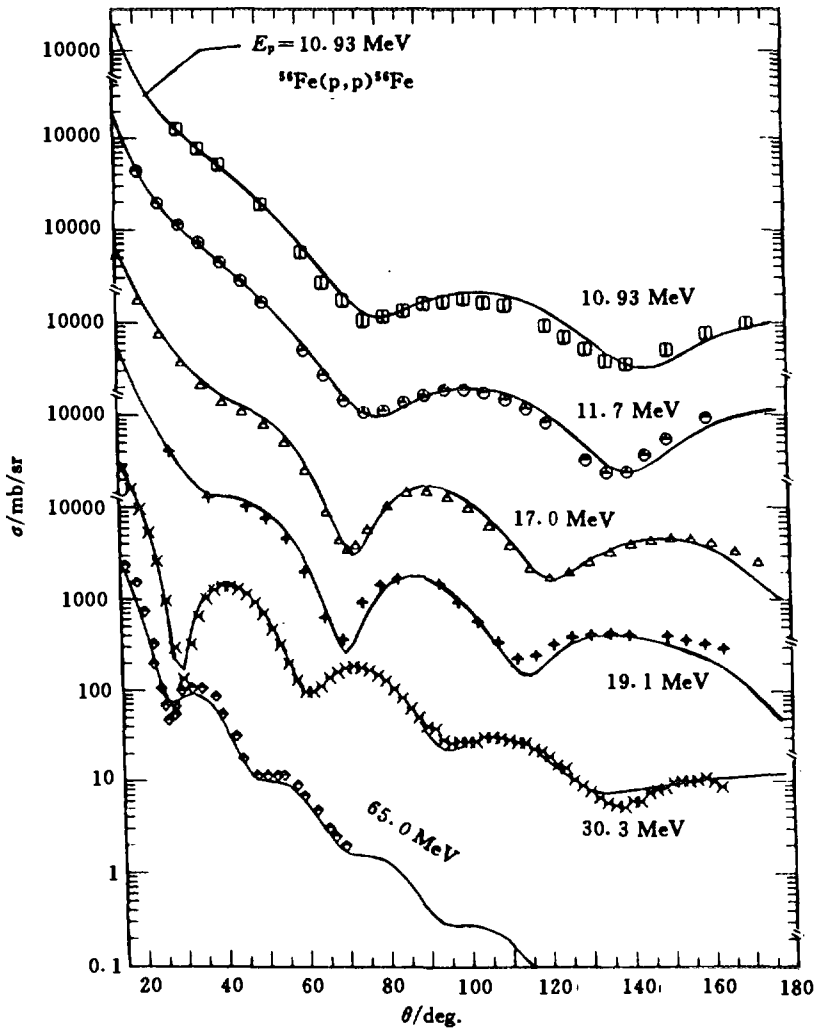

Fig.1 ^{56}Fe(p,p)^{56}Fe differential cross sections

□ J. Benveniste 63 ○ J. Benveniste 63 △ I. E. Dayton 56

+ S. F. Eccles 66 × B. W. Ridley 64 ◇ H. Sakaguchi 82

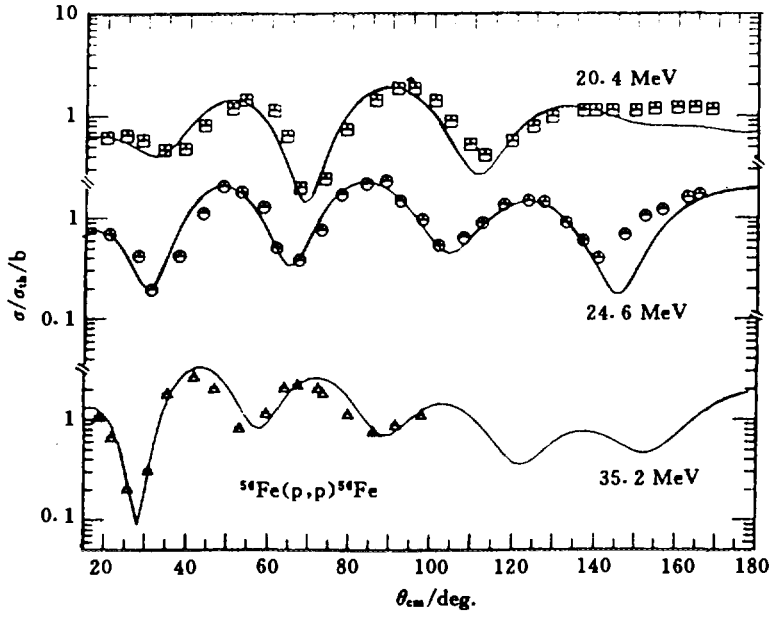

Fig.2 ^{56}Fe(p,p)^{56}Fe differential cross sections

□ P. J. Van Hall 77 ○ P. J. Van Hall 77 △ E. Colombo 77

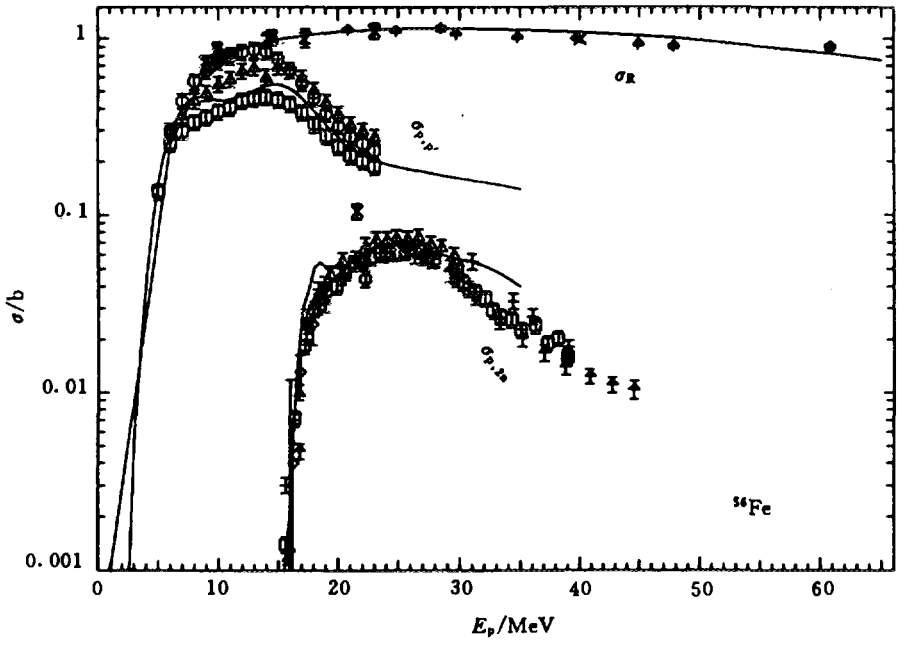

Fig.3 ^{56}Fe proton absorption cross section

□ K. Bearpark 65 ○ B. D. Wilkins 63 △ J. F. Dicello 67 + J. F. Turner 64

× P. J. Bulman 64 ◇ J. J. Menet 71 ✦ R. H. Mccamic 86 ⧗ B. Buck 63

^{56}Fe(p,p')^{56}Fe reaction cross section ▫ P. Dyer 81

^{56}Fe(p,2n)^{55}Co reaction cross section

▫ M. C. Lagunas 79 ○ B. V. Zhurazlev 84 △ V. N. Levkovskij 91 + I. J. Jenkins 70

× B. L. Cohen 55 ◇ Zhao Wenrong 93 ✦ R. Michel 79 ⧗ I. R. Williams 67

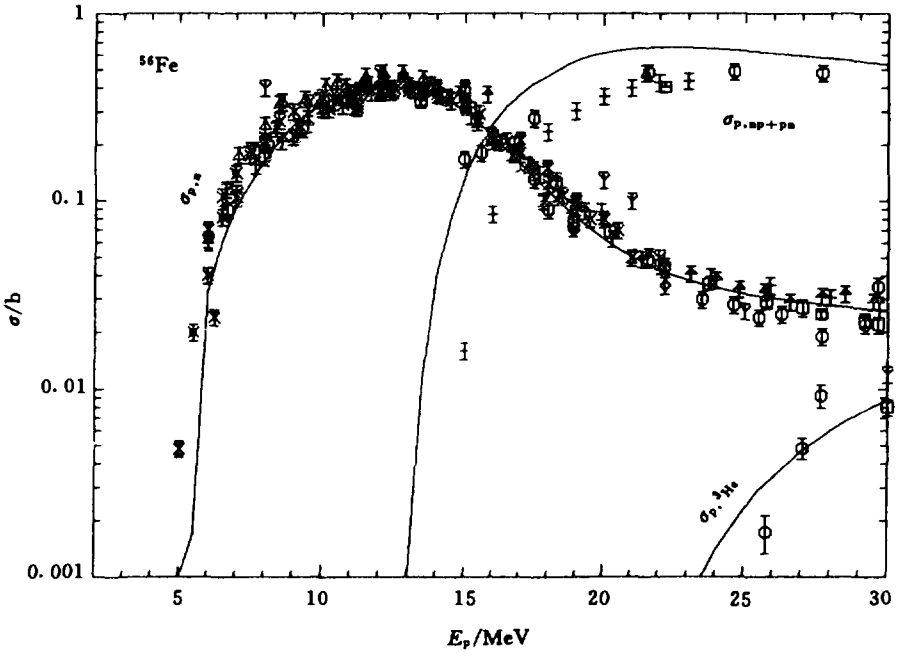

Fig.4 ^{56}Fe(p,n)^{56}Co reaction cross section

□ B. Michel 79 ○ I. J. Jenkins 70 △ S. Tanaka 59 + E. Gadioli 74
× Tao Zhenlan 83 ◇ B. V. Zhurazlev 84 ✦ V. N. Levkovskij 91 ⊼ A. E. Antropov 85
⧗ Zhao Wenrong 93 ▽ I. R. Williams 67 ✕ S. Sudar 94 ⧗ R. L. Brodzinski 71

^{56}Fe(p,np+pn)^{55}Fe reaction cross section

□ B. V. Zhurazlev 84 ○ I. J. Jenkins 70 △ P. Dyer 81 + C. C. Chang 74

^{56}Fe(p,^{3}He)^{54}Mn reaction cross section □ I. R. Williams 67 ○ R. Michel 79

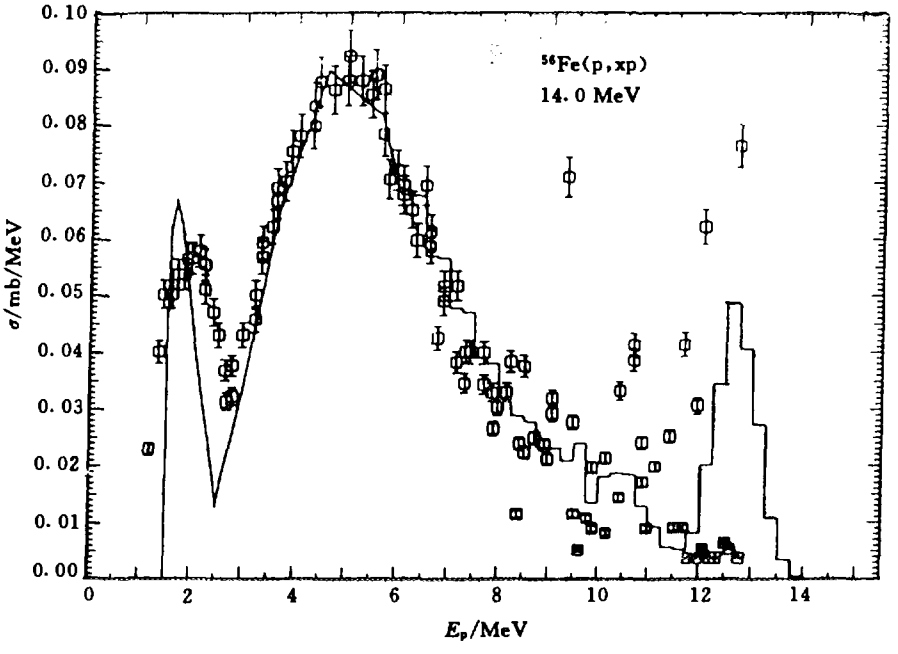

Fig.5 The energy spectra of ^{56}Fe(p,xp) reaction at E_p = 14.0 MeV

□ A. Sprinzak 73

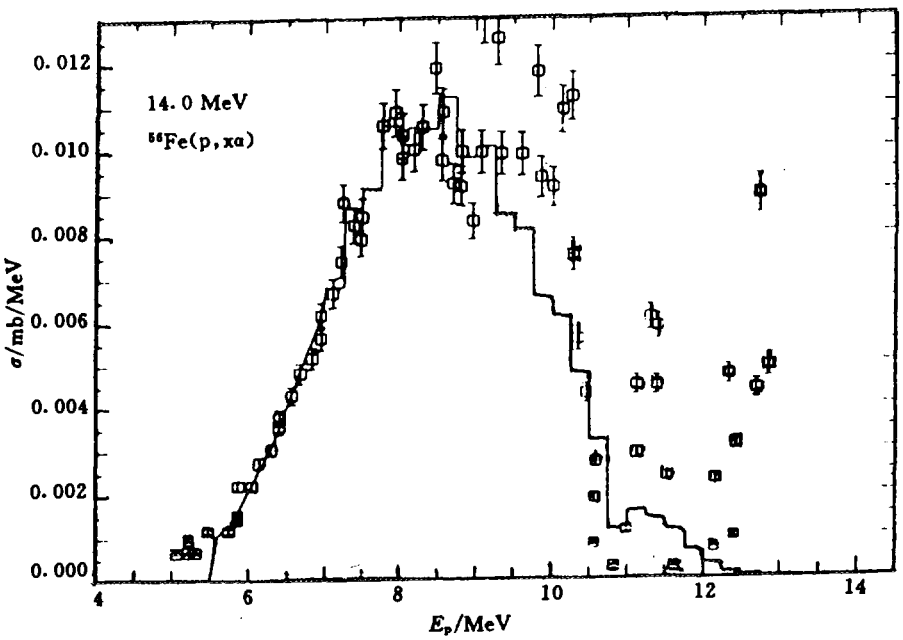

Fig.6 The energy spectra of ^{56}Fe(p,xα) reaction at E_p = 14.0 MeV

□ A. Sprinzak 73

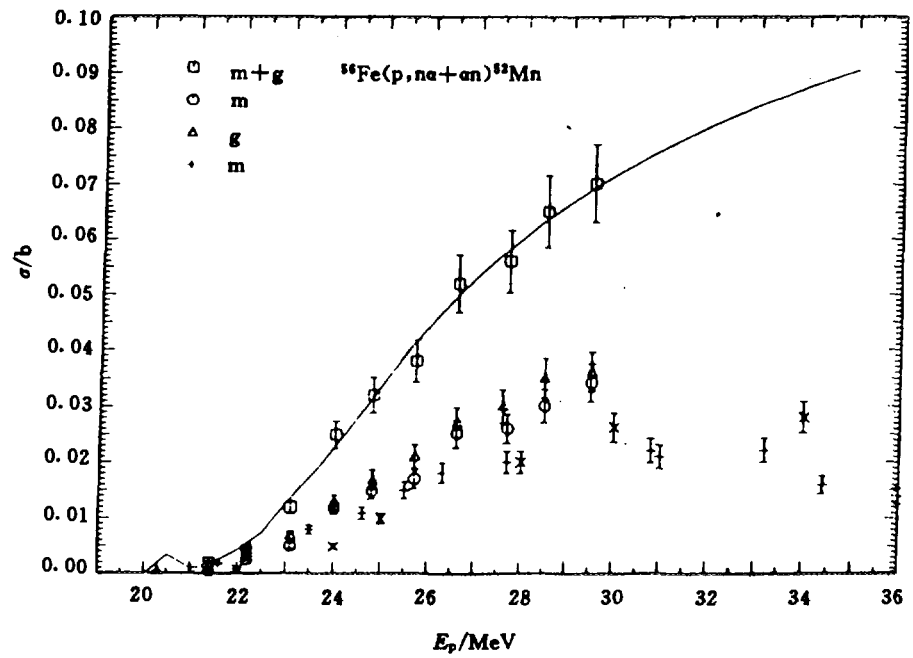

Fig.7 ^{56}Fe(p,nα+αn)^{52}Mn reaction cross section

□ V. N. Levkovskij 91 (m+g)

○ V. N. Levkovskij 91 (m)

△ V. N. Levkovskij 91 (g)

+ I. J. Jenkins 70 (m)

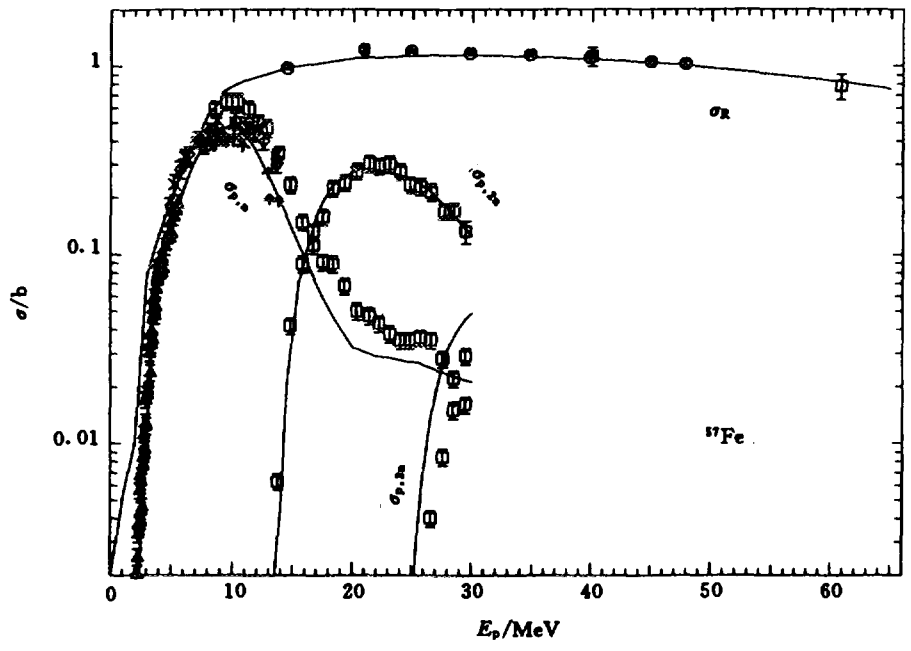

Fig.8 ^{57}Fe proton absorption cross section

□ J. J. Menet 71 ○ R. H. Mccamic 86

$^{57}Fe(p,n)^{57}Co$ reaction cross section ⊏ V. N. Levkovskij 91 ⊙ C. H. Johnson 60

△ A. E. Antropov 80 + A. A. Kovlozhvari 91 × S. Sudar 94 ◇ S. Tanaka 59

$^{57}Fe(p,2n)^{56}Co$ reaction cross section ▫ V. N. Levkovskij 91

$^{57}Fe(p,3n)^{55}Co$ reaction cross section ▫ V. N. Levkovskij 91

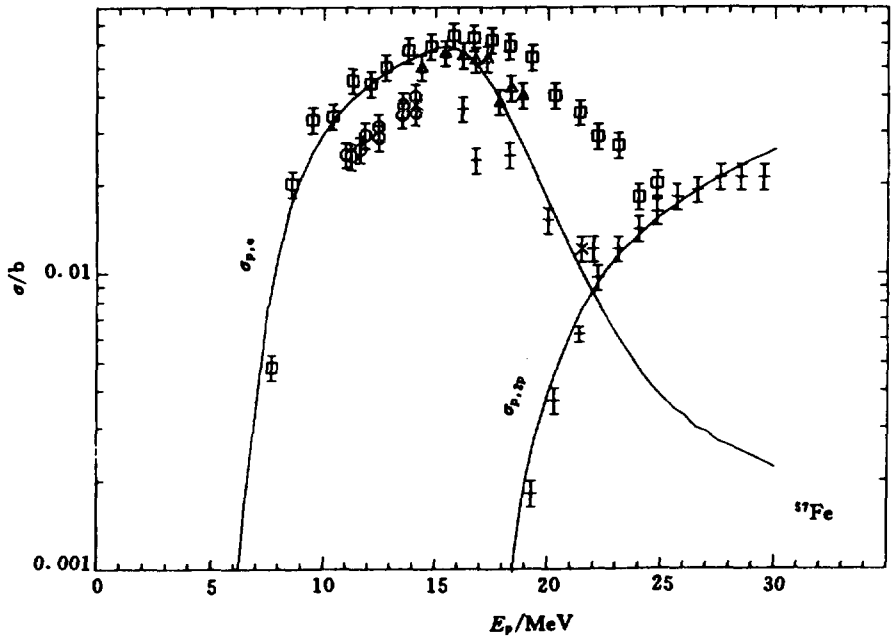

Fig.9 $^{57}Fe(p,\alpha)^{54}Mn$ reaction cross section

⊏ V. N. Levkovskij 91 ○ S. Sudar 94 △ Zhao Wenrong 93 + R. Michel 79

$^{57}Fe(p,2p)^{56}Mn$ reaction cross section ▫ V. N. Levkovskij 91

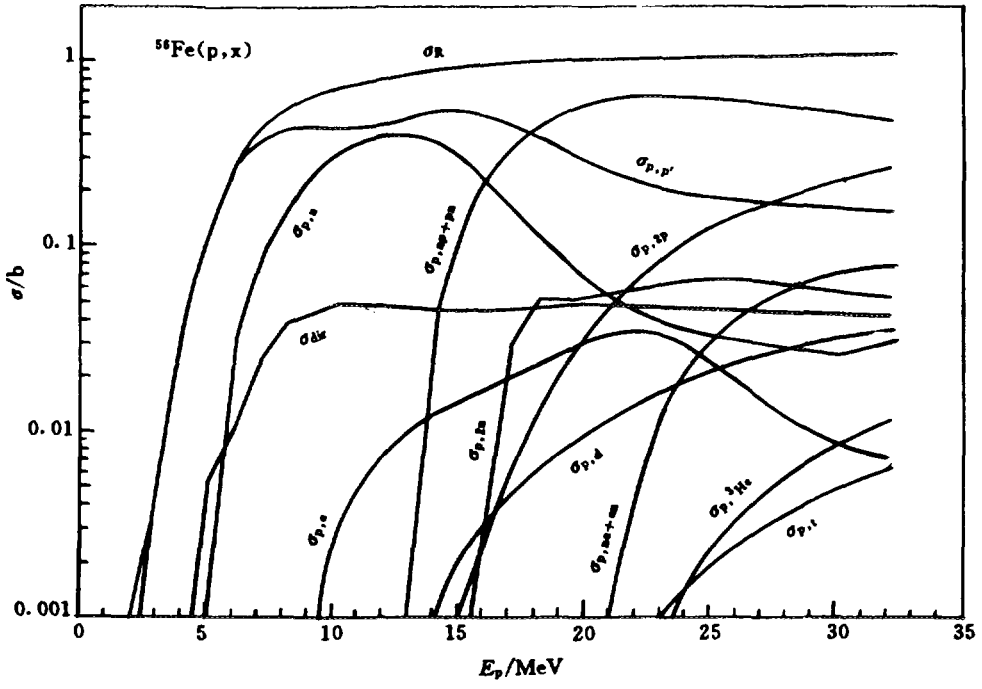

Fig.10 ^{56}Fe(p,x) reaction cross sections

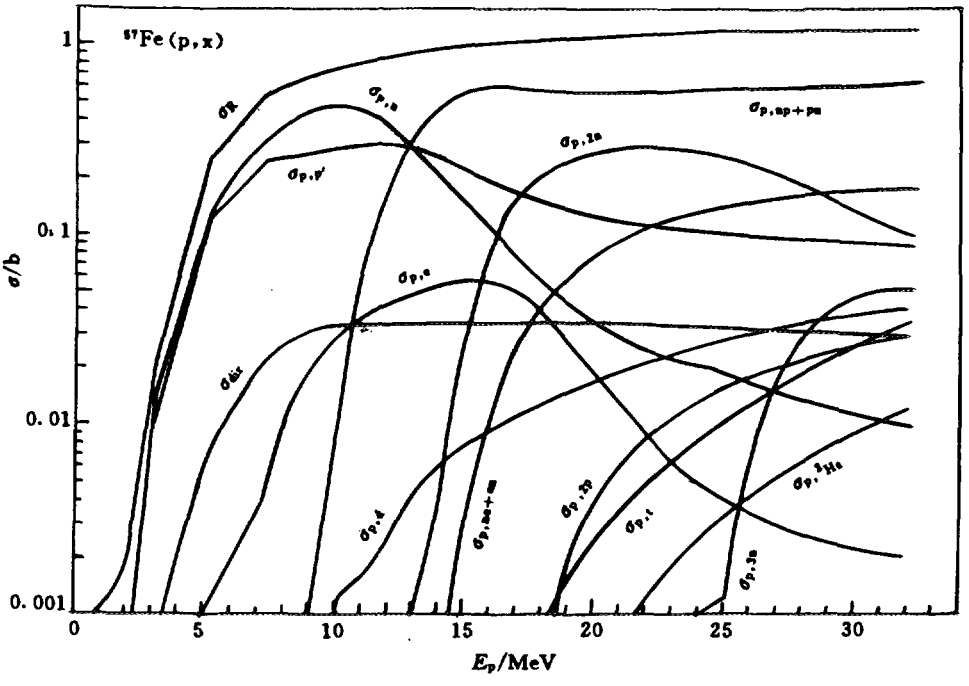

Fig.11 ^{57}Fe(p,x) reaction cross sections

4 Conclusions

Based on the available experimental data of iron, a set of proton optical potential parameters on iron at 2.0 ~ 65.0 MeV has been obtained. With adjusting the level densities parameters, the calculated reaction cross sections and energy spectra were in reasonable agreements with the experimental data and might predict some characteristics of some reaction channels of ^{56}Fe and ^{57}Fe which have no experimental data up to now. These conclusions also proved the reasonability and dependability of these theoretical calculation programs.

Acknowledgments

One of the author (Xu) thanks to Drs. Zhang Jingshang, Shen Qingbiao, Liu Tong and Su Zongdi for their very kind help and suggestions. This work was supported by CNDC.

References

[1] J. Benveniste et al., Phys. Rev. , 133, 27, (1964)
[2] Experimental Nuclear Data in EXFOR Master File.
[3] W. Bauhoff, Atomic Data and Nuclear Data Tables, 35, No.3, (1986)
[4] S. Sudar et al., Phys. Rev. ,C50, 2408, (1994)
[5] I. R. Williams et al., Phys. Rev. V162, 1055, (1967)
[6] Zhao Wenrong et al., Chin. J. Nucl. Phys., 15, 337,(1993)
[7] R. Michel et al., Nucl. Phys., A322, 40, (1979)
[8] R. Michel et al., J. Radio. Chem., 59, 467, (1980)
[9] Tao Zhenlan et al., Atom. Ener. Sci. and Tech. 5, 506, (1983)
[10] B. V. Zhuravlev et al., Sov. Nucl. Phys. 39, 264, (1984)
[11] A. E. Awtropov et al., 31th Annual Conf. on Nucl. Spect. and Nucl. Struc., Lengrd, 316, (1980)
[12] C. M. Lederer, Tables of Isotope (1978)
[13] Shen Qingbiao, Commu. Nucl. Data Progress 7, 41 (1992)
[14] Zhang Jingshang, Commu. Nucl. Data Progress 7, 14 (1992)
[15] Su Zongdi et al., Commu. Nucl. Data Progress 12, 83 (1994)
[16] P. D. Kunz, "Distorted Wave Code Dwuck4", University of Colorado.

III DATA EVALUATION

Energy Balance for Natural Elements

Zhang Jingshang

(China Nuclear Data Center, CIAE)

Introduction

In ENDF/B-6 format, The Q values for each reaction channels of natural element are defined[1] by

$$Q_{\mathrm{ENDF}} = \max \{Q_1, Q_2, \cdots, Q_f\} \tag{1}$$

where f is the number of isotopes in a natural element. For negative Q value, Q_{ENDF} gives the threshold energy of this threshold reaction channel. But this ill-defined values can not be relied on energy balance. As pointed in Ref.[2] the reasonable Q value of each reaction channel must be abundance and cross section dependent for natural element. So it is also incident energy dependent. It reads

$$Q = \frac{\sum_{i=1}^{f} \sigma_i(E_{\mathrm{in}}) A_i Q_i}{\sum_{i=1}^{f} \sigma_i(E_{\mathrm{in}}) A_i} \tag{2}$$

where A_i and $\sigma_i(E_{\mathrm{in}})$ refer to the abundance and cross section at incident energy E_{in} of the i-th isotope in this natural element, Q_i is the Q-value of the i-th isotope. It is easy to see that if only one isotope opens this reaction channel then $Q = Q_{\mathrm{ENDF}}$.

The kinetic energy released from this reaction channel is given by $E_{\mathrm{in}} + Q$. Thus the ill-defined Q_{ENDF} causes the "available" energy must be overestimated. In all cases the "taken" energies by outgoing particles and γ production should be small than the "available" energy. So the check program pointed out the energy "taken" smaller than "available " for natural element, it may not mean the problem for energy balance. From the ill-defined Q_{ENDF} the deviation percentage of energy balance can be obtained by

$$D = \frac{(E_{in} + Q_{ENDF}) - (E_{in} + Q)}{E_{in} + Q} = \frac{Q_{ENDF} - Q}{E_{in} + Q} \quad (3)$$

The D values of Eq.3 should be kept $D = 0$ from threshold to the energy point, at which the next isotope opens the reaction channel.

1 Calculation Example

Since the ill-defined Q_{ENDF} could not be relied for energy balance, but evaluators may want to know how much does the ill-defined Q_{ENDF} effect on the deviation percentage of energy balance. Therefore the calculations of the D values becomes to be attractive.

The NUNF code has the function to calculate the D values of the deviation percentage of energy balance for each reaction channels. NUNF code is the version of UNF program set[3] for fast neutron data calculation of natural elements. As a numerical example we performed the D value calculations of natural Ni. The isotopic mass numbers and abundances in natural Ni are shown in Table 1.

Table 1 The isotopic mass numbers and abundances in natural Ni.

mass number	58	60	61	62	64
abundance	0.6827	0.2610	0.0113	0.0359	0.0091

The calculated results of D values of Eq.3 of natural Ni are given in Tables 2 and 3 for each reaction channels.

Table 2 The D values of reaction channels (n,γ),(n,n'),(n,p),(n, α),(n,d),(n,t) for natural Ni

E_n/MeV	(n,γ)	(n,n')	(n,p)	(n, α)	(n,d)	(n,t)
5.000	0.122	0.277	0.003	0.106		
6.000	0.116	0.230	0.010	0.106		
7.000	0.108	0.198	0.017	0.100		
8.000	0.103	0.173	0.021	0.096		
9.000	0.098	0.153	0.023	0.092		
10.000	0.093	0.138	0.023	0.088	0.000	
12.000	0.086	0.115	0.026	0.080	0.018	
14.000	0.079	0.100	0.033	0.071	0.029	
14.500	0.078	0.096	0.035	0.069	0.030	
15.000	0.076	0.093	0.035	0.067	0.030	
16.000	0.074	0.088	0.035	0.063	0.030	
17.500	0.070	0.081	0.033	0.057	0.029	0.273
18.000	0.069	0.078	0.032	0.055	0.029	0.259
20.000	0.065	0.071	0.029	0.049	0.028	0.215

Table 3 The D values of reaction channels(n,2n),(n,np),(n,nα),(n,2p),(n,3n) for natural Ni

E_n/MeV	(n,2n)	(n,np)	(n,nα)	(n,2p)	(n,3n)
5.000					
6.000					
7.000					
8.000					
9.000	0.000				
10.000	0.029	0.000			
12.000	0.462	0.015	0.003		
14.000	0.483	0.022	0.006	0.000	
14.500	0.458	0.023	0.006	0.000	
15.000	0.433	0.024	0.007	0.000	
16.000	0.385	0.025	0.007	0.000	
17.500	0.330	0.026	0.007	0.000	0.911
18.000	0.315	0.026	0.006	0.000	0.871
20.000	0.268	0.025	0.006	0.001	0.724

2 Conclusion Remarks

From the results of D values of Eq.3 shown in Tables 2 and 3 we can see that the ill-defined Q_{ENDF} does not work on energy balance indeed. The deviation percentage of energy balance for some reaction channels are obvious. The large deviation percentage of energy balance could yield mainly in two ways. The first one is that if the Q_{ENDF} is just given by the isotope which has very small abundance or very small cross section, then the energy releasing different becomes very large (large numerator in Eq.3). On the other hand for high threshold reaction channels, for example (n,3n) channel, the energy releasing would be very little (little denominator in Eq.3) and it also yields the large deviation percentage of energy balance.

This numerical example indicates that without the calculation of D values of Eq.3 evaluators could not make any judgement on energy balance for a data file of natural element unless the "taken" energies are more than the "available" energy.

References

[1] P. F. Rose and C. L. Dunford, ENDF-102 (1992)

[2] Liu Tingjin Communication of Nuclear Data Progress 13. (1994)81.

[3] J. S. Zhang Nucl. Sci. Eng. 114, 55(1993).

Evaluation and Calculation of Activation Cross Sections for ^{169}Tm(n,2n), (n,3n), (n,γ) and (n,x) Reactions Below 20 MeV

Yu Baosheng
(China Nuclear Data Center, CIAE)

Tang Guoyou Shi Zhaomin
(Institute of heavy Ion Physics, Peking University)

Introduction

^{169}Tm is a rare-earth element. Its activation cross sections are a good indicator for nuclear science and technology applications. However, there are no evaluated data in several nuclear data libraries. The activation cross sections for ^{169}Tm(n,2n), (n,3n), (n,γ) and some emission charged particle (n,x) reactions below 20 MeV were evaluated and calculated on the basis of experimental and theoretical data.

1 Evaluation and Analysis of Experimental Data

1.1 ^{169}Tm(n,2n) Reactions

The previous evaluation[1] for ^{169}Tm(n,xn)^{166,167,168}Tm reactions were performed up to 100 MeV for adjusting model calculation parameters. At present evaluation, the emphasis is put on recommendation of accurate activation cross sections below 20 MeV. The new measured data[2~18] are listed in Table 1.

There are many differences and discrepancies among the existing cross section of (n,2n) reaction for ^{169}Tm. The half-lived, gamma branching ratio of ^{169}Tm and the standard cross section adopted by authors were first corrected and re-normalized using the newer data so as to eliminate the discrepancies. According to recent evaluation[19], the half-life of ^{168}Tm is 93.1 day and the characteristic gamma ray of 198.24 keV of product has a branching of ratio 53.8 ±1.25 %. After the data were corrected and re-normalized, some data are in agreement with recent measured data within errors. The evaluated value is 1946 ± 19 mb at 14.6 MeV. For the measured data using large Ge-loaded liquid scintillation between 10 ~ 13 MeV, the neutron flux with ^{238}U(n,f) cross sections were re-normalized with those of ENDF/B-VI. After these correction and re-normalization, evaluated experimental data below 20 MeV were obtained.

1.2 $^{169}Tm(n,3n)^{167}Tm$ Reaction

The data measured by B.P.Bayhurst[11], R.L.Veeser[12], Lu Hanlin[16] are consistent with each other within errors from threshold to 20 MeV. The data were used to adjust the model parameters in theoretical calculation.

1.3 $^{169}Tm(n, \gamma)^{170}Tm$ Reaction

For the $^{169}Tm(n,\gamma)^{170}Tm$ reaction, there are experimental data in thermal energy point and energy region from 0.19 keV to 3.0 MeV, the list of these experimental data[20-30] is shown in Table 2.

The earlier experimental data were measured by R.C.Block[21] in energy region of 0.19 ~ 7.8 keV and J.H.Gibbons[20] in energy region of 0.0095 ~ 0.7 MeV, the liquid scintillation tank were used to measure the prompt γ ray of capture events. The measured data in energy region of 0.52 ~ 3.0 MeV were carried out by S. Joly[25] with NaI(Tl) spectrometer.

With the improvement of nuclear science and technology, after the 1980s, R. L. Macklin[27] of Oak Ridge and Las Alamos laboratories commonly measured average cross sections in energy region of 0.003 ~ 2 MeV using electron linear accelerator and a non-hydrogenous liquid scintillator with 24 cm in thick and 10cm in diameter. The measured data indicate that the data measured by J.H.Gibbons[20] are systimatically higher than new one.

The neutron capture cross sections in energy region 0.158 ~ 1.47 MeV were measured by Jiang Songsheng[26] with activation method using T(p,n) and $^{7}Li(p,n)$ reaction source at 2.5 MV Van de Graaff accelerator of CIAE. The activity of the nuclide ^{170}Tm was measured by scintillation plastic anti-coincidence β-counter. Its efficiency was calibrated by so called imitation source method. The imitation source was a set of plates contained a known quantity of ^{170}Tm embedded uniformly in Tm_2O_3 with the form similar to the sample used in the irradiation at accelerator. The corrections of neutron multiple scattering in the target were calculated by the Monte Carlo method.

The standards cross sections for $^{197}Au(n,\gamma)^{198}Au$ reaction were taken from the data evaluated by himself. At present work, the cross sections have been corrected with the cross section of ENDF/B-6. The cross sections corrected should be dropped 2.7% and 5.4% at energy ports 0.45 and 0.55 MeV, respectively. Therefore, the cross sections measured by Jiang songsheng[26] are reliable, and lower than other ones.

Moreover Xu Haishan[29] of Sichuan University (SIU) measured the neutron capture cross sections at 1.01, 1.21 and 1.44 MeV. In order to reduce background due to neutron capture in the hydrogen of the liquid scintillation detector, only those pulses in coincidence between the two half sphere of the detector were counted. The data are consistent with ones of Jiang Songsheng[26]. The standard cross sections used were corrected with ENDF/B-6.

The measurements[30] in energy region of 10 ~100 keV were carried out at 2.5 MV Van de Grave accelerator of Sichuan University using two Moxon-Rae detectors by Xia Yijun[30].

The thermal cross section was measured by Luo Dexing[28], G.H.E.Sims,[23] respectively, using the same way as that of Jiang Sousheng[26]. Meanwhile, the cross sections from G.H.E.Sims[23] was deduced indirectly. The thermal cross sections are consistent among two laboratories within errors. The value measured by Luo Dexing[28] was adopted.

The capture cross section for $^{169}Tm(n,\gamma)^{170}Tm$ reaction measured by Luo Dexing[28], Xia Yijun[30] and Jiang Sonsheng[26] as well as S.Joly[25] were adopted, and Some earlier measured data were examined and corrected on the basis of the accurate data measured at CIAE, SIU. The evaluated data were obtained from 0.01 to 3.0 MeV.

1.4 $^{169}Tm(n, x)$ Reactions

There is an experiment value of 1.60±0.14 mb at 14.7 MeV for $^{169}Tm(n,\alpha)^{166}Ho$ reaction, which was measured by S.M.Qam[31]. Therefore, the cross sections of emission changed particle for $^{169}Tm(n,x)$ reactions must be calculated theoretically.

2 Theoretical Calculation and Recommendation

A set of neutron optical potential parameters for ^{169}Tm was taken from Ref.[31] based on the available total nonelastic cross sections and elastic scattering angular distributions. Adjusting this set of neutron optical potential parameters and the relevant level density and giant dipole resonance parameters, the cross sections of (n,2n), (n,3n),(n,γ) and (n,x) were calculated using NUNF Code[33], and the neutron radiation capture cross sections of ^{169}Tm were also calculated using other Code[34]. The comparison of experimental data with the theoretically calculated results were made. The calculated data can reproduce the measured data very well. The activation cross section ^{169}Tm (n,2n), (n,γ) reactions were recommended on the basis of evaluated and calculated results and shown Figs. 1 ~ 2. The cross sections for (n,γ) reaction in resonance energy region were taken from FENDL/A-2.

The calculated (n,α) cross section is in agreement with existing experimental data at 14.7 MeV. Then the cross sections of all (n,x) reactions were recommended on the basis of calculation and shown in Fig. 3.

Acknowledgments

The authors are indebted to IAEA (International Atomic Energy Agency), CNNC (China National Nuclear Corporation) and CIAE for their supports, and thank Drs. A. B. Pashchenko, T.Benson, O. Schwerer, Lu Hanlin and Zhao Wenrong for kind help and suggestions.

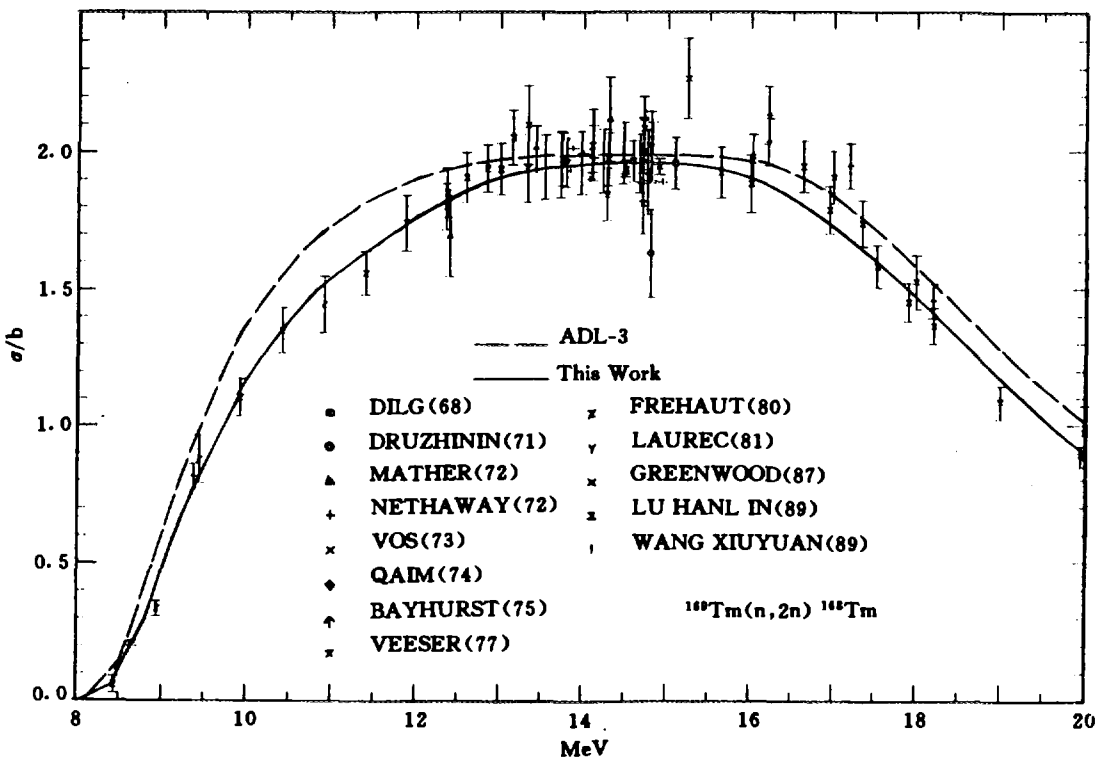

Fig.1 Comparison evaluated & measured data for $^{169}Tm(n,2n)^{168}Tm$

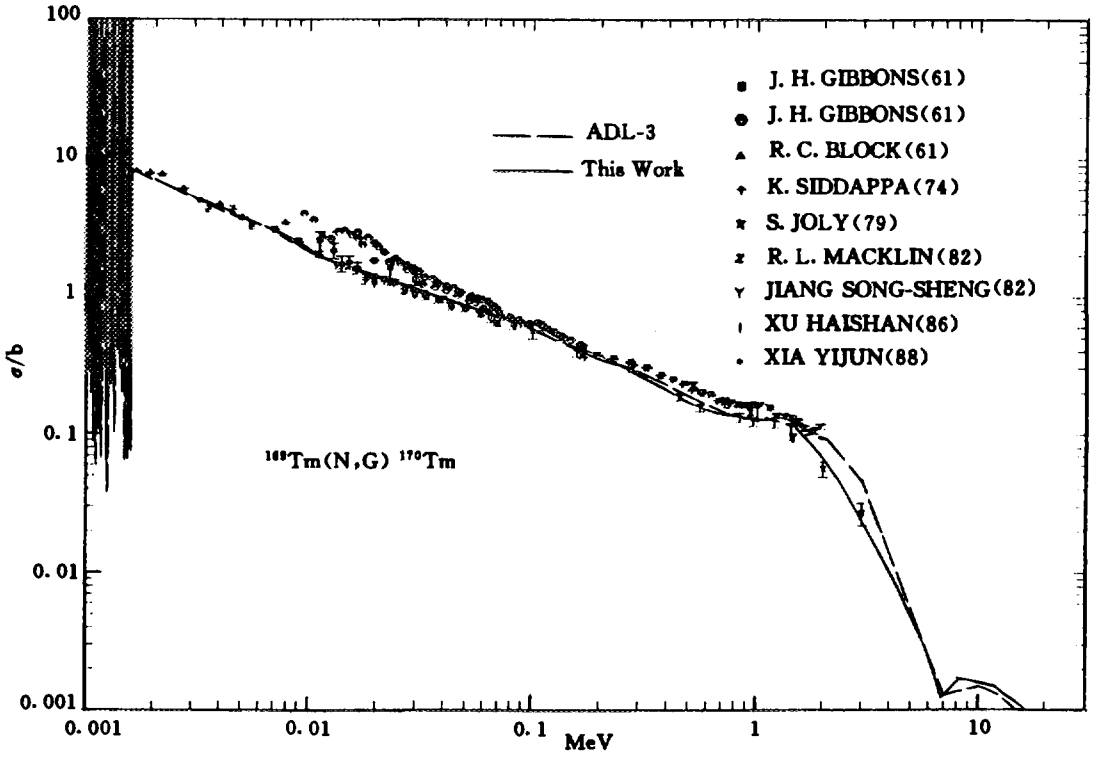

Fig-2. Comparison evaluated & measured data for $^{169}Tm(N,G)^{170}Tm$

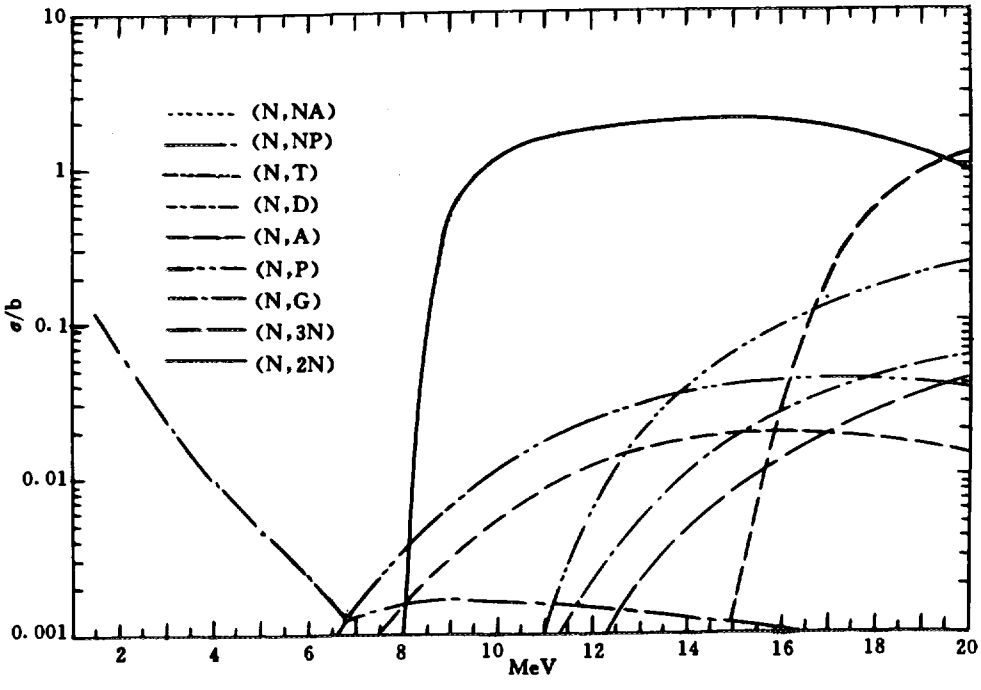

Fig-3. Evaluated Cross Sections for ^{169}Tm

Table 1 Collected data and relevant information for $^{169}Tm(n,2n)^{168}Tm$ reaction

Year	Author	E_n / MeV	$\sigma_0 \pm \delta\sigma$ / mb	n flux	R_1	R_2	R_3	R_4	σ
1960	H.A.Tewes	14.5	1032±412	H(n,n)	1.0000				1032±412
1966	D.G. Vallis	14.7	1022±116	^{27}Al (n,α)	1.0000	0.9500			971±116
1968	W. Dilg	14.8	2000±115	^{27}Al (n,α)	1.0000	1.0224			2044±115
1971	B.Bari	14.8	1443±129	^{27}Al (n,α)	1.0000	1.0224	1.0000	1.1407	2044±115
1971	A.A.Druzhinin	14.8	1630±160	Absolute	1.0000				1630±160
1972	D.R.Nethaway	14.78	1920	^{27}Al (n,α)	1.0000		1.0000	0.9665	1855±160
1972	D.S. Mather	14.3	2118±153	^{238}U(n,f)	1.0000				2120±170
1973	R. Vos	14.7	2084±117	^{27}Al (n,α)	1.0000				2084±117
1974	S.M.Qaim	14.7	1971±152	^{27}Al (n,α)	1.0000				1971±152
1975	B.P.Bayhurst	14.1	2010±85	^{27}Al (n,α)	1.0028	0.9738			1960±111
1977	L.R.Veeser	14.7	1811±111	H(n,n)	1.0000		1.0000	1.0000	1811±111
1980	J.Frehaut	14,76	1926±155	^{238}U(n,f)	1.0000			0.9740	1868±115
1981	J. Laurec	14.8	2016±130	^{27}Al (n,α)	1.0000	1.0179	0.9738	1.0000	1998±130
1987	L.R.Greenwood	14.5	1939±30	^{27}Al (n,α)	1.0000	0.9891	1.0701	0.9915	2034±30
1989	Lu Hanlin	14.59	1966±75	^{27}Al (n,α)	1.0000	1.0000	1.0000	0.9384	1845±75
1989	Wang Xiuyan	14.67	1957±107	^{27}Al (n,α)	1.0000	0.9905	1.0000	0.9701	1880±30
1990	K. Ikeda	14.66	2060± 160	^{27}Al (n,α)	1.0000	1.0000	1.0000	0.9328	1921±160

R_1: Adjusted factor for neutron energy

R_2: Adjusted factor for relevant cross section

R_3: Adjusted factor for half-life

R_4: Adjusted factor for gamma branching ratio

σ_0: Original cross sections

σ : Adjusted cross sections

Table 2 Collected Data and Relevant Information for $^{169}Tm(n, \gamma)$ Reaction

Year	Author	E_n	Detector	n flux	comment
1961	J.H.Gibbons	9.5 ~ 170 keV	STANK	In(n, γ)	
1961	R.C.Block	0.19 ~ 7.8 keV	STANK		
1967	R.L.Zimmerman	0.0253 eV		Absolute	Deriv
1970	G.H.E.Sims	0.0253 eV	STANK	$^{59}Co(n, \gamma)^{60}Co$	
1974	K. Siddappa	23 keV	NaI(Tl)	$^{127}I(n,\gamma)^{128}I$	
1979	S. Joly	0.52 ~ 3.0 MeV	NaI	Long counting	
1982	Jiang Songsheng	0.16 ~ 1.47 MeV	β-spectrometer	$^{197}Au(n,\gamma)$	Anti-coincidence plastic scientillator
1982	R. L. Macklin	3 keV ~ 2.0 MeV	C_6F_6	$^{6}Li(n,t)^{4}H$ $^{235}U(n,f)$	Average cross sections
1984	Luo Dexing	0.0253 eV	β-spectrometer	$^{197}Au(n,\gamma)$	Anti-coincidence plastic scientillator
1986	Xu Haishan	1.0 ~ 1.4 MeV	STANK	$^{197}Au(n,\gamma)$	
1988	Xia Yijun	11 ~ 100 keV	Moxon-Rae	$^{197}Au(n,\gamma)$	

STANK (Liquid scientillator Tank) To measure the prompt gamma-ray

References

[1] Yu Baosheng et al., CNDP, 16, 68(1996)
[2] H.D.Tewes et al., UCRL-6028-T(1966)
[3] D.G.Vallis et al., AWRE-O-76(1966)
[4] W.Dilg et al., NP/A, 118, 9(1968)
[5] B.Bari et al., EXFOR DATA No. 10431059(1971)
[6] A.A.Druzhinin et al., EXFOR DATA N0. 40171002(1971)
[7] D.R.Nethaway et al., Nuclear Physic/A, 190, 635(1972)
[8] D.M.Mather., AWRE-O-72(1972)
[9] R.Vor et al., BAP, 18, 775(1973)
[10] S.M.Qaim et al., N P/A, 224, 319(1974)
[11] B.P.Bayhurst et al., PR/C, 12, 451(1975)
[12] L.R.Veeser et al., PR/C, 16, 1792(1977)
[13] J.Frehaut et al., EXFOR DATA N0. 20416014(1980)
[14] J.Laurec et al., CEA-R-5109(1981)
[15] L.R.Greenwood et al., ASTM-STP-956, 743(1987)
[16] Lu Hunlin et al., INDC(CPR)-16(1989)
[17] Wang Xiuyuan et al., EXFOR DATA N0. 30935004
[18] Y.Ikeda et al., NEANDC-1989 (1990)
[19] Zhou Chunmei et al., Private communication (1996)
[20] J.H.Gibbons et al., PR,122,182(1961)
[21] R.C.Block et al., Inter. Conf. on Nuclear Data for Science and Technology p203 Saclay(1961)
[22] R..L.Zimmerman et al., NP/A, 95, 683(1967)
[23] G.H.E.Sims et al., JIN, 32, 2839(1970)

[24] K.Siddappa et al., AP, 83, 3 55(1974)
[25] S.Joly et al., NSE, 70, 53(1979)
[26] Jiang Songsheng et al., CNP, 4, 136(1982)
[27] R.L.Macklin et al., NSE, 82, 143(1982)
[28] Luo Dexing et al., CNP, 6, 84(1984)
[29] Xu Haishan et al., NTC, 9, 5(1986)
[30] Xia Yijun et al., CNP,10,102(1988)
[31] She Qinbaio et al., CNDP, 16(1996)
[32] S.M.Qaim et al., EXFOR Data N0. 21997012 (1984)
[33] Zhang Jingshang , INDC(CPR)-027/L, 14(1992)
[34] Tang Guoyou and Liu Jianfeng , Private Communication(1996)

CN9702243

Evaluation of Activation Cross Sections for (n,2n) Reactions on $^{58, 60, 61, 62, 64, Nat}$Ni

Ma Gonggui Wang Shiming

(Institute of Nuclear Science and Technology, Sichuan University, Chengdu)

Introduction

Nickel is a very important structure material in nuclear fusion engineering. The neutron activation cross section are very useful in fusion research and other applications such as radiation safety, environmental, material damage and neutron dosimetry. More efforts are required to identify and resolve the discrepancies in the existing activation cross sections from different laboratories.

The natural nickel consists of five stable isotopes. Their abundaces and threshold energies are shown in Table 1.

Table 1 Isotopic abundaces and their reaction threshold energies of natural nickel

isotope	58	60	61	62	64
abun./ %	68.27	26.1	1.13	3.59	0.91
thresh./ MeV	12.408	11.581	7.9498	10.771	9.8094

The cross sections of $^{58, 60, 61, 62, 64}$Ni(n,2n)$^{57, 59, 60, 61, 63}$Ni are recommended based on the recent experimental measured data and theoretically calculated results[1] from threshold up to 20 MeV. The evaluated cross sections are given in Figs. 1~4 with experimental data and compared with other evaluated data.

1 ^{58}Ni(n,2n)^{57}Ni Reaction

The experimental data were measured by Yuan Junqian(92), Molla(91), Viennot (91), Kimura(90), Ikeda(88), Zhou Muyao(87), Greenwood(87), Pavlik(85), Lu Hanlin(82), Adamski(80), Zhao Wenrong(89), Kobayashi(88), Rama(86), Harper(82) and Hudson(78)[1~15] in the energy range from 12.79 MeV to 19.57 MeV, respectively.

The evaluated data were obtained by fitting experimental data from threshold energy to 20.0 MeV. The recommended data above 15.0 MeV mainly were determined based on measured data by Pavlik .

2 $^{60}Ni(n,2n)^{59}Ni$ Reaction

The experimental data were measured by Weselka(1991) and Greenwood (1989)[17,18] at 14.7 MeV energy point, respectively. There are large discrepancy among these measured data. The recommended data were taken from calculated result[19], and normalized to the evaluated data of 324 mb at 14.1 MeV by Zhou(1991)[16] from threshold energy to 20.0 MeV. The comparison of experimental data with evaluated ones is shown in Fig. 2.

3 $^{61,62,64}Ni(n,2n)^{60,61,63}Ni$ Reaction

Due to no experimental data for $^{61,62,64}Ni$, the cross sections were theoretically calculated with code UNF[19]. At 14.7 MeV energy point, the evaluated data 570, 1000, 1000 mb by Zhou (91)[16] were used to refer to corresponding model calculated results, respectively (see Figs. 3 ~ 5).

4 The (n,2n) Reaction for Natural Nickel

For natural Ni, the experimental data was measured by Veeser(77)[20] in the energy range from 14.7 to 20.0 MeV and Ashby(58)[21] at 14.1 MeV energy point. The (n,2n) cross sections of natural Ni were obtained from summing the isotopic data weighted by the abundance . The comparison of experimental data with evaluated ones is shown in Fig.6. It is found that the present evaluation is in agreement with the experimental data.

Acknowledgement

The authors would like to thank Dr. Yu Baosheng for helpful discussion and suggestions.

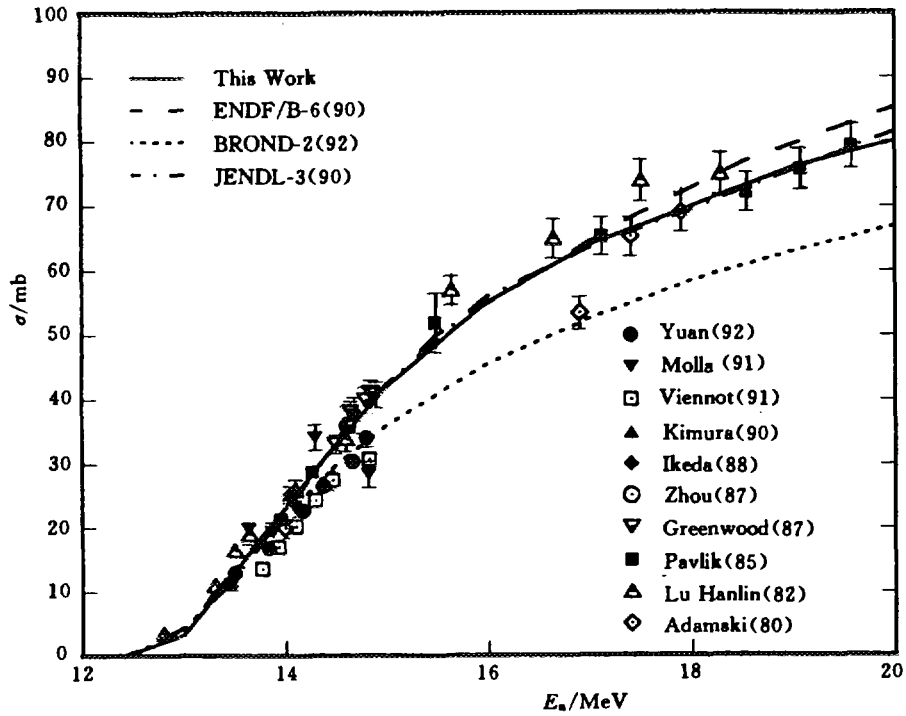

Fig.1 (n,2n) Cross Section for ^{58}Ni

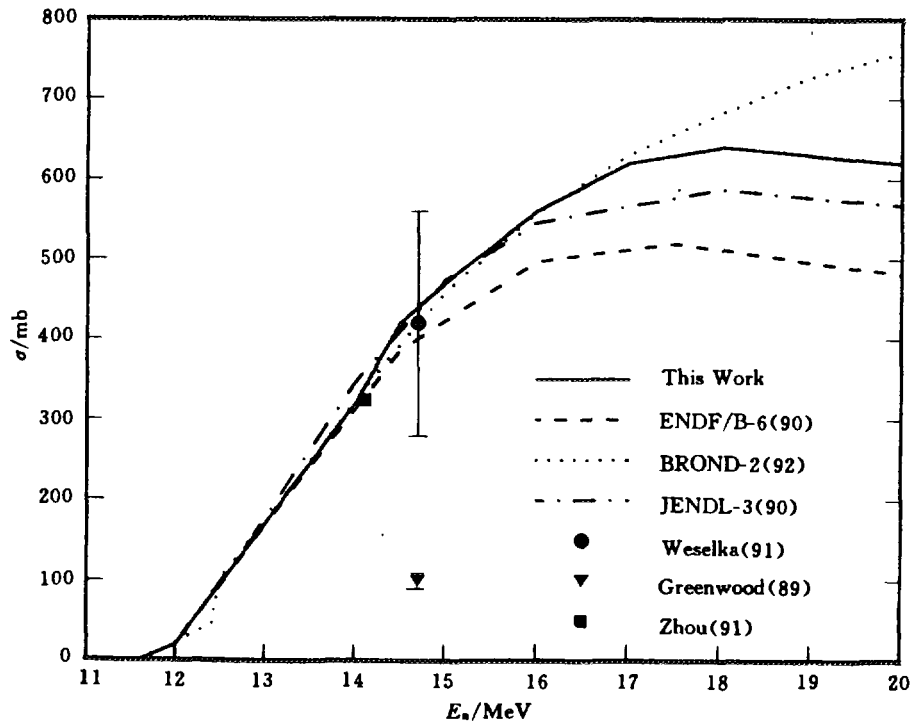

Fig.2 (n,2n) Cross Section for ^{60}Ni

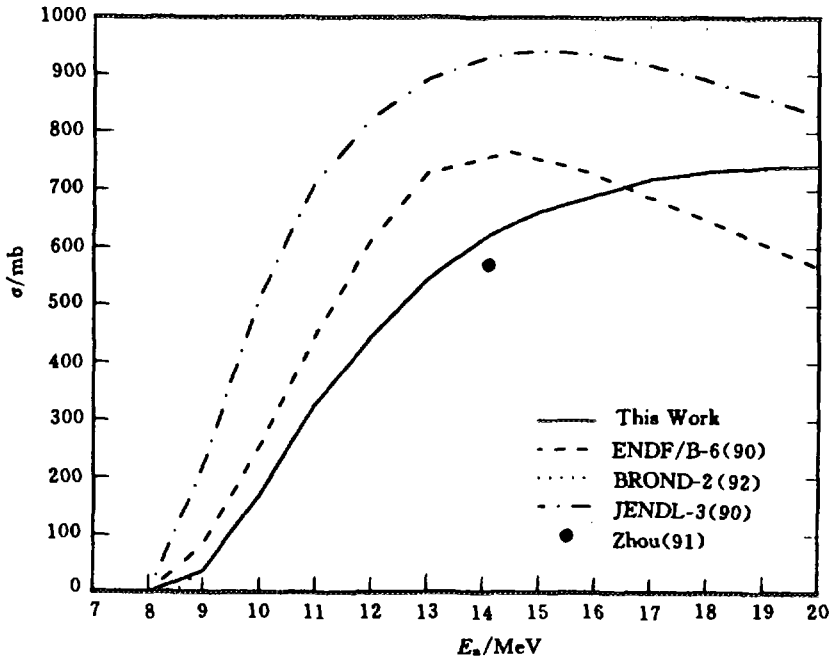

Fig.3 (n,2n) Cross Section for ^{61}Ni

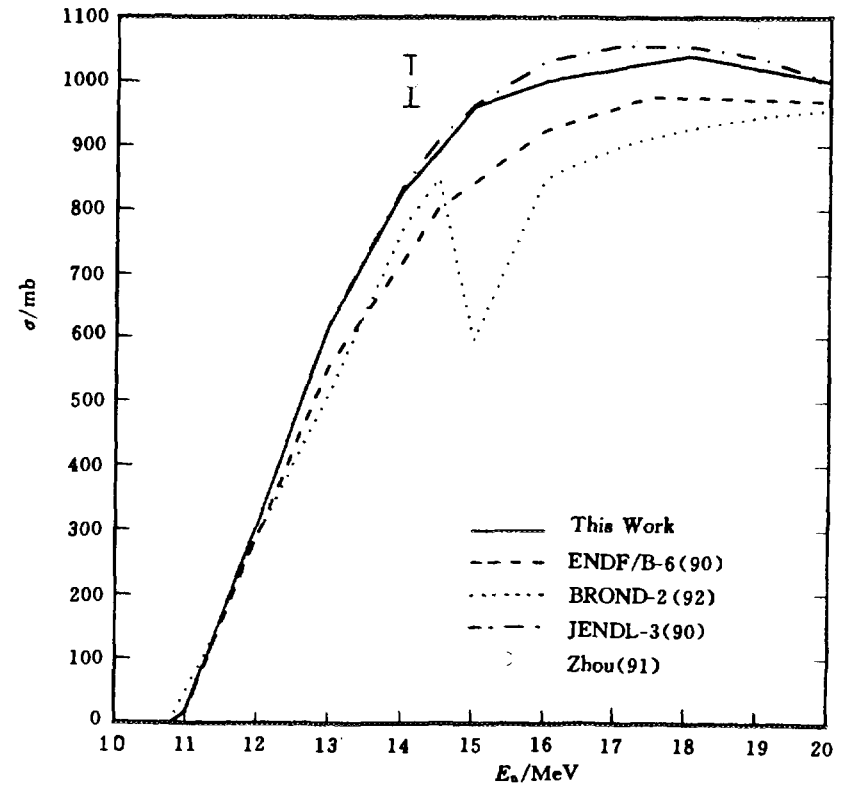

Fig.4 (n,2n) Cross Section for ^{62}Ni

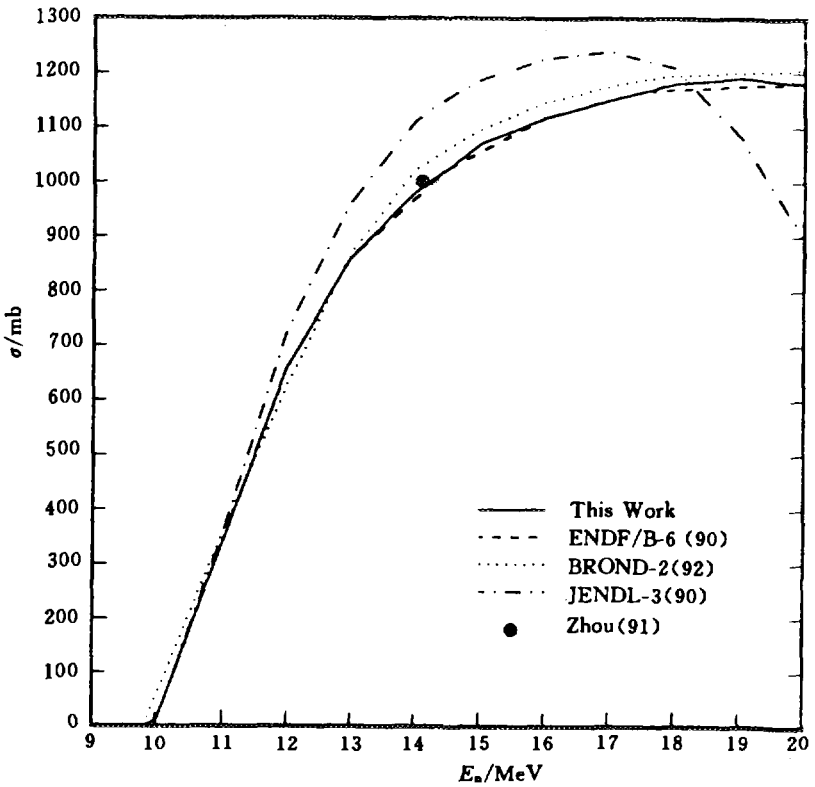

Fig.5 (n,2n) Cross Section for ^{64}Ni

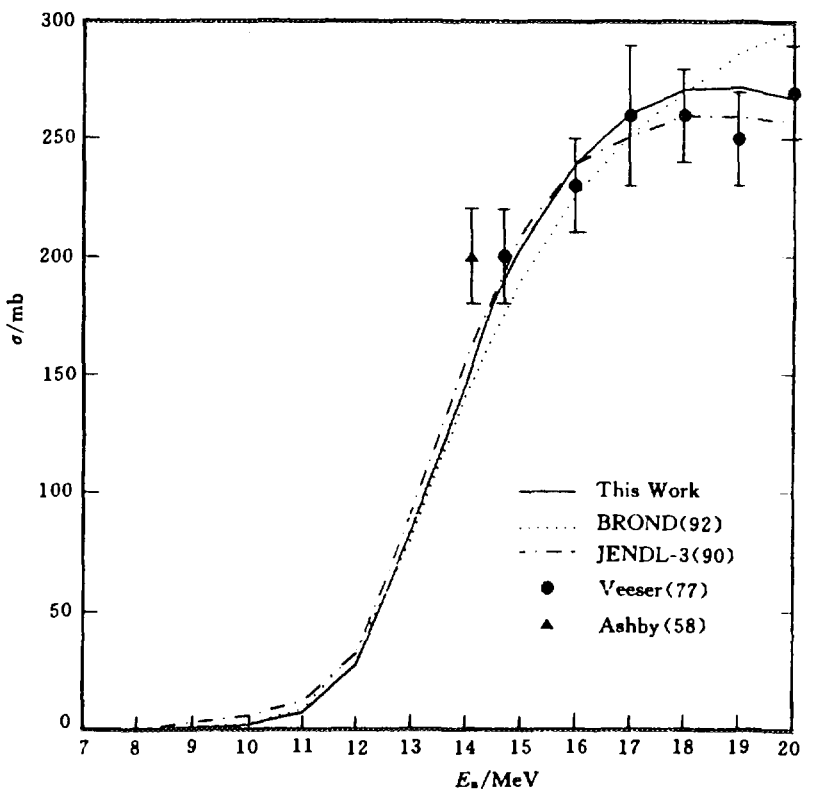

Fig.6 (n,2n) Cross Section for ^{nat}Ni

References

[1] Yuan Junqian et al., High Energy Physics and Nuclear Physics, 16(1), 57(1992)

[2] N. I. Molla et al., Proc. of Conf. on Nucl. Data for Science and Technology, Julich, 355 (1991)

[3] M.Viennot et al., Nucl. Sci. Eng., 108, 289(1991)

[4] Kimura et al., Nucl. Sci. Eng., 106, 332(1990)

[5] Y.Ikeda et al., Report JAERI-1312, Japan Atomic Energy Research Inst., Tokai-mura (1988)

[6] Zhou Muyao et al., Chinese J. Nuclear Physics, 9, 34(1987)

[7] L. R. Greenwood et al., ASTM-STP-956, 743(1987)

[8] A. Pavlik et al., Nucl. Sci. Eng., 90,186(1985)

[9] Lu Hanlin et al., IAEA-NDS-306379(1982)

[10] Adamski et al., Annual Nuclear Energy, 7, 397(1980)

[11] Zhao Wenrong et al., INDC(CPR)-16(1989)

[12] K. Kobayashi et al., Proc. of Conf. on Nucl. Data for Science and Technology, Mito, 261(1988)

[13] J. Rama et al., Nucl. Instrum. Methods, B17, 368(1986)

[14] R. C. Harper et al., J. Phys. G8, 153 (1982) ; EXFOR 1273004

[15] C. G. Hudson et al., Annual of Nuclear Energy 5, 589(1978)

[16] Zhou Delin et al., A Progress Report to FENDL Meeting(1991)

[17] L. R. Greenwood et al., ASTM-STP-1001, 1(1989)

[18] D. Weselka et al., Proc. of Conf. on Nucl. Data for Science and Technology, Julich, 559 (1991)

[19] Zhang Jingshang. Nucl. Sci. Eng., 114, 55(1993)

[20] L. R. Veeser et al., 77BNL, 231; EXFOR 12936008(1977)

[21] V. J. Ashby et al., 58GENEVA 15, 3, 2494(1958)

Progress on the Evaluation of Total Cross Section for Some Fission Product Nuclides

Su Weining Zhao Jingwu

(Department of physics, Nanjing University, Nanjing)

The total cross section for some fission product nuclides or their substitutes, ^{139}La, ^{133}Cs, ^{103}Rh, ^{120}Sn, ^{127}I, ^{140}Ce, ^{nat}Sb, ^{nat}Cd, ^{nat}Ag, ^{nat}Ce, ^{nat}Pd, ^{nat}La, ^{nat}Te, ^{nat}Xe and ^{nat}Ba, have been evaluated on the basis of the experimental data.

The experimental data were collected from EXFOR library and recent publications, the recommended data were obtained by fitting the experimental data and compared with those of ENDF/B-6, JENDL-3, BROND-2 and EFF-2.

Nuclear Data Sheets for A=51

Zhou Chunmei

(China Nuclear Data Center, CIAE)

The 1991 version of Nuclear Data Sheets Update for A=51 (NUCLEAR DATA SHEETS, Vol. 63, 229(1991)) has been revised. The detailed level and decay schemes are presented for the nuclei of the A=51 mass chain. The level and γ-ray properties obtained from reaction and decay experiments are shown in drawing, or tables. The data sets of high-spin levels and γ-rays for ^{51}V, ^{51}Cr, and ^{51}Mn are added too. The experiment methods, references, and comments are given in text.

The evaluated data have been put into Evaluated Nuclear Structure Data File, and be published in "NUCLEAR DATA SHEETS ".

Recent Evaluation of Some Dosimetry Data for Reactor Application

Yu Baosheng

(Chinese Nuclear Data Center, CIAE)

Knowledge of dosimetry data is very useful in reactor research and application. For reactor dosimetry, radiation safety, environmental and material damage in fission and fusion engineering, more accurate data are required and it is necessary to identify and correct several differences and discrepancies in the existing dosimetry cross sections from different laboratories.

The evaluated dosimetry data are recommended in this work on the basis of the recent experimental data, especially the new measured results at CIAE, and compared with other evaluated data.

The main characteristics of evaluated dosimetry data are as follows.

1 The cross sections in the so-called 'gap' energy region from 5 to12 MeV are being researched using the activation method with quasi-monoenergetic neutron produced by $H(^{11}B,n)^{11}C$ reaction and D(d,n) reaction using D-D gas target at several laboratories. A programme of dosimetry and activation cross section measurements and evaluation has been under-way at CIAE for a long time. Some accurate cross sections were measured by Lu[1] in the energy region of 6~12 MeV at CIAE in 1996. These newly measured data could supplement the scarce data in this energy region so as to modify the previous evaluation.

2 In order to eliminate the discrepancies in the existing cross sections, the background neutron yield depend on both the "gas-out" effect and D-D breakup neutron are needed to accurate determination and subtraction. It is worthy of note that both effects increase with the neutron energy and strongly depend on the threshold of the specific reaction. Therefore, recently the accurate experimental data have been obtained in many laboratories.

3 In present work, the available experimental data were evaluated so as to guide the theory calculation for scarce data energy region. The parameters for the theoretical calculation were adjusted referring to the measured data. The calculated

various nuclear data, such as (n,2n), (n,d), (n,p) and (n,α) cross sections are in good agreement with the existing experimental data.

The new evaluations are as follows.

(1) The Cross Section for $^{46}Ti(n,p)^{46}Sc$ Reaction

As we known, the excitation function of $^{nat}Ti(n,x)^{46}Sc$ reaction varies quite slowly with neutron energy above 12 MeV due to the effect of (n,np)+(n,pn)+(n,d) reactions for ^{47}Ti in natural sample. The new value measured by N. I. Molla[2] is 226.2 ± 22.4 mb at 14.8 MeV, using an enriched ^{46}Ti sample, superseded their earlier data , which was measured by S. M. Qaim and N.I. Molla[3]. The new value at 14.6 MeV measured by N.I. Molla[2] is 236.28 ± 24 mb and is well consistent with 236 ± 13 mb value at 14.6 MeV measured by Y. Ikeda[4] using an enriched ^{46}Ti sample. In this work, the recommended value is 236 ± 11.5 mb at 14.6 MeV.

Above 12 MeV, the present evaluation work took account of the result of 14.6 MeV measurement and the data measured by Lu[5,6] in energy region 13 to 18 MeV, in which the contribution of $^{47}Ti(n,np+pn+d)^{47}Sc$ was subtracted from other measured data.

Below 12 MeV, the effect of (n,np)+(n,pn)+(n,d) reactions for ^{47}Ti could be negligible due to very small ^{46}Sc product. Therefore, those measured data below 10 MeV were adopted in present evaluation with the exception of a few early data having large scattering and uncertainty. Meanwhile, the new data measured by Lu[1] in energy region 6 to 12 MeV have superseded and supplemented the scarce data in the energy region, and modified the previous evaluated data[7]. The recommended data were compared with other evaluated data from IRDF-90 and ADL-3I. and shown in Fig. 1.

The average reaction cross section in the ^{252}Cf fission neutron spectrum were calculated using the evaluated data from IRDF-90. It was shown that the calculated value is 12.31 and lower than the experimental value 14.20 ± 0.24[8]. At present evaluation, the evaluated data are higher than the IRDF-90 and in agreement with the trend of the experimental data.

(2) The Cross Section for $^{54}Fe(n,p)^{54}Mn$ Reaction

Lot of experimental data for $^{54}Fe(n,p)^{54}Mn$ reaction exist from threshold to 20 MeV. The new and accurate measurements were done by Lu[1] in the energy region 6 to 12 MeV where the measured data are very scarce, because the threshold value and shape of standards cross section were carefully selected so as to counteract the

effects of neutron back-ground from "gas-out " and backup neutron from D(d,np) reactions. The data measured by S.K.Saraf[9] around 8.0 MeV are consistent with the new data measured by Lu[1]. Based on these data measured, the evaluated data in the energy region 6 to 12 MeV become more reliable. The data were compared with experimental and other evaluated data from JENDL-3.2/A, ENDF/B-VI AND ADL-3I, and shown in Fig. 2.

(3) The Cross Section for $^{59}Co(n,p)^{59}Fe$ Reaction

The cross sections for $^{59}Co(n,p)^{59}Fe$ reaction were evaluated in some early works[5,7] from threshold to 20 MeV at CIAE. In order to subtract neutron back-ground produced from the gas cell structure and breakup neutron from D(n,np) reaction, a "gas-out" measuring data accompanied with each measured data were carried out. The measured data of W. Mannhart[11] are higher than those evaluated data previously. Recently, the new data measured by Lu[1] were performed in the energy region 6 to 12 MeV. The problems of neutron background were careful considered and corrected, because the threshold value and its shape of standards cross section were selected carefully so as to reduce the background effects from " gas-out " and backup neutron from D(d,np) reactions. The measured data by Lu[1] and W. Mannhart[11] are in good agreement with each other within errors. Therefore, based on these new data, present evaluation has improved the previous evaluated results below 14 MeV. The comparison with other evaluations from JENDL-3, ENDF/B-VI AND ADL-3I, are shown in Fig.3.

(4) The Cross Section for $^{60}Ni(n,p)^{60}Co$ Reaction

For the cross section for $^{60}Ni(n,p)^{60}Co$ reaction , the discrepancies exist in the energy region from threshold to 12 MeV. But the new data measured by Lu[1] at CIAE in 1996 and M Wagner[12] at both LAS, U.S.A. and IRK, Austria are in good agreement with each other within errors. The data measured by M.Wagner[12] superseded their earlier data by H. Vonach and M.Wagner[13] in 1989.

These data and other latest data can provide a complete shape of curve for the $^{60}Ni(n,p)^{60}Co$ reaction. Meanwhile, the half-life of residual nuclei ^{60}Co are known very well (5.271 a), the characteristic gamma ray 1173.2 keV and 1332.5 keV and their branching ratio 0.9989 and 0.9998 respectively were adopted in the world after 1978. The corrections for the characters of gamma ray of ^{60}Co are negligible.

Present evaluation is based on these new measured data, and compared with other evaluated data from ENDF/B-6, JENDL-3, BROND-2, shown Fig.4.

(5) The Cross Section for $^{181}Ta(n,2n)^{180m}$ Reaction

The cross sections for $^{181}Ta(n,2n)^{180m}$reaction were measured by Y. Ikeda[4] and Lu[5] in energy region 13 to 15 MeV and 12 to 18 MeV, respectively. Their measured data are in good agreement within errors..

The new data could supplement scarce data below 12 MeV. At present evaluation, the recommended cross sections are based on them, especially the new measured data from threshold to 12 MeV at CIAE in 1996, and shown in Fig. 5.

Acknowledgments

The author is indebted to IAEA (International Atomic Energy Agency), CNNC (China National Nuclear Corporation) and CIAE for their supports, and thank Drs. A. B. Pashchenko, T. Benson, O. Schwerer, Lu Hanlin and Zhao Wenrong for kind help and suggestions.

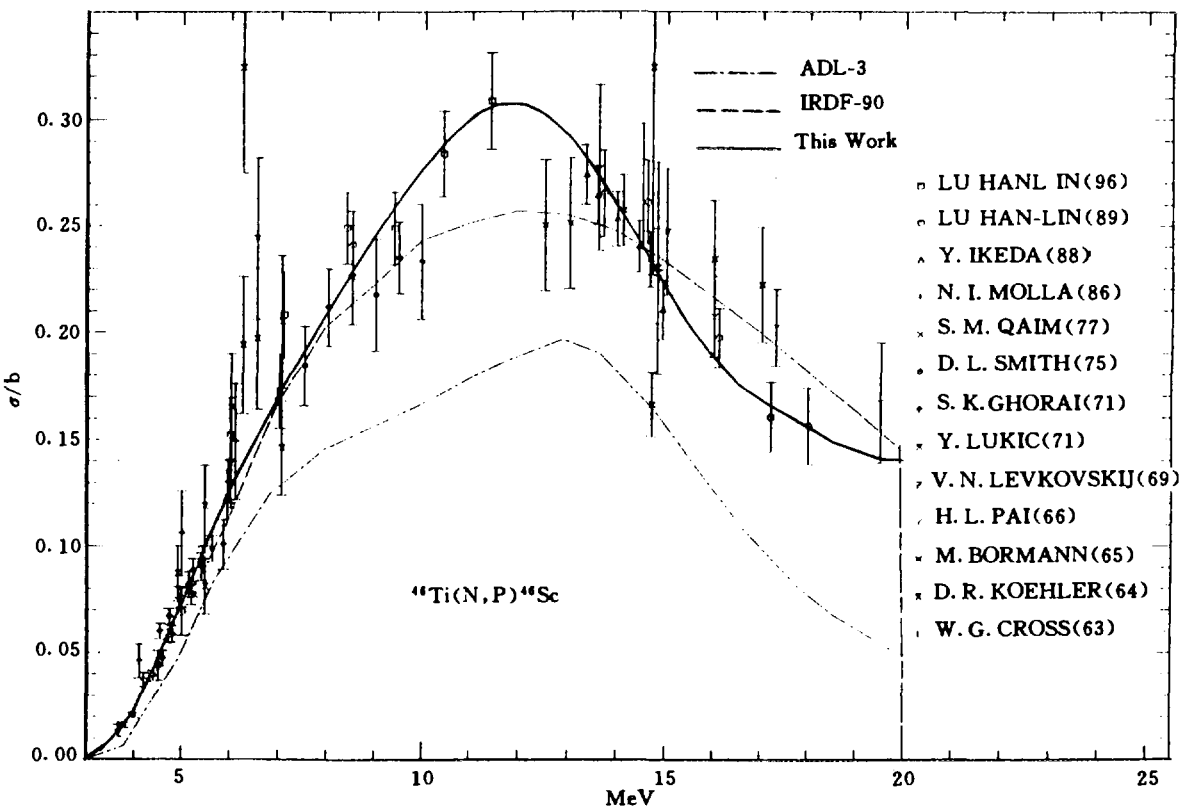

Fig.1 Comparison evaluated & measured data for $^{46}Ti(n,p)^{46}Sc$

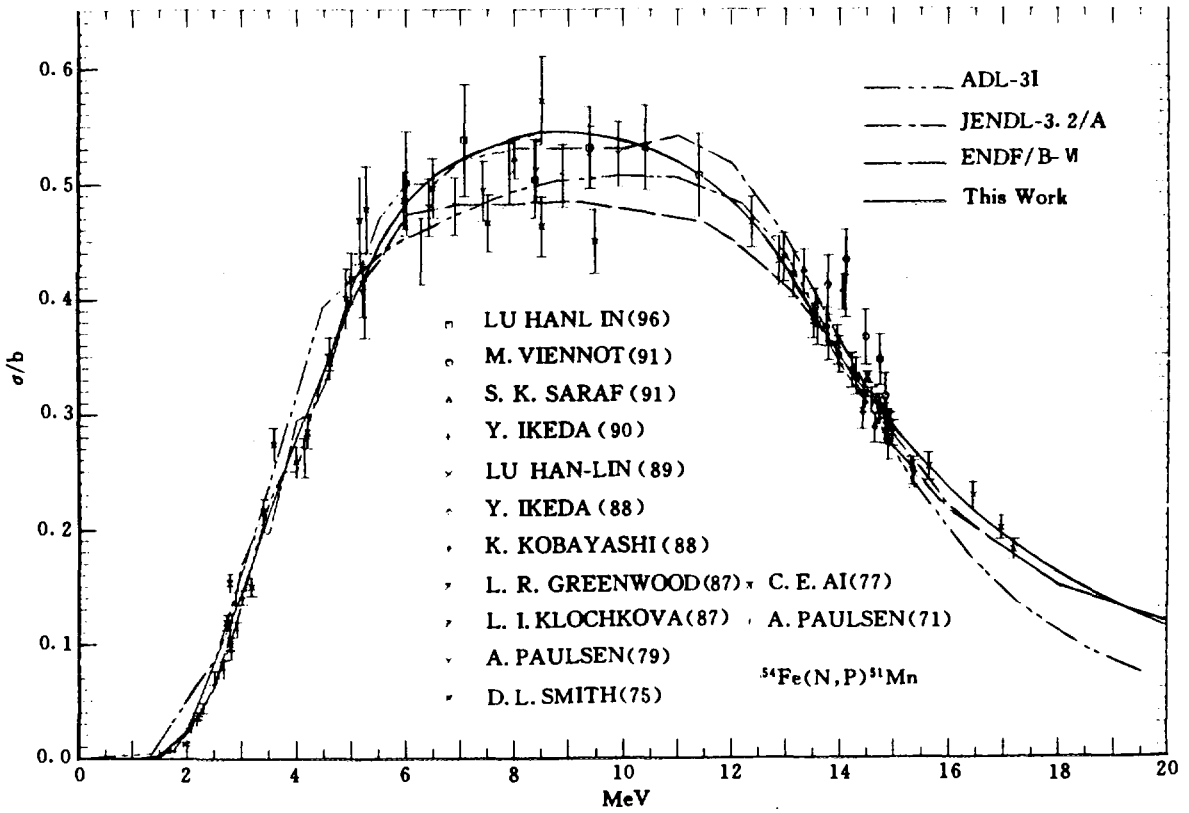

Fig.2 Comparison evaluated & measured data

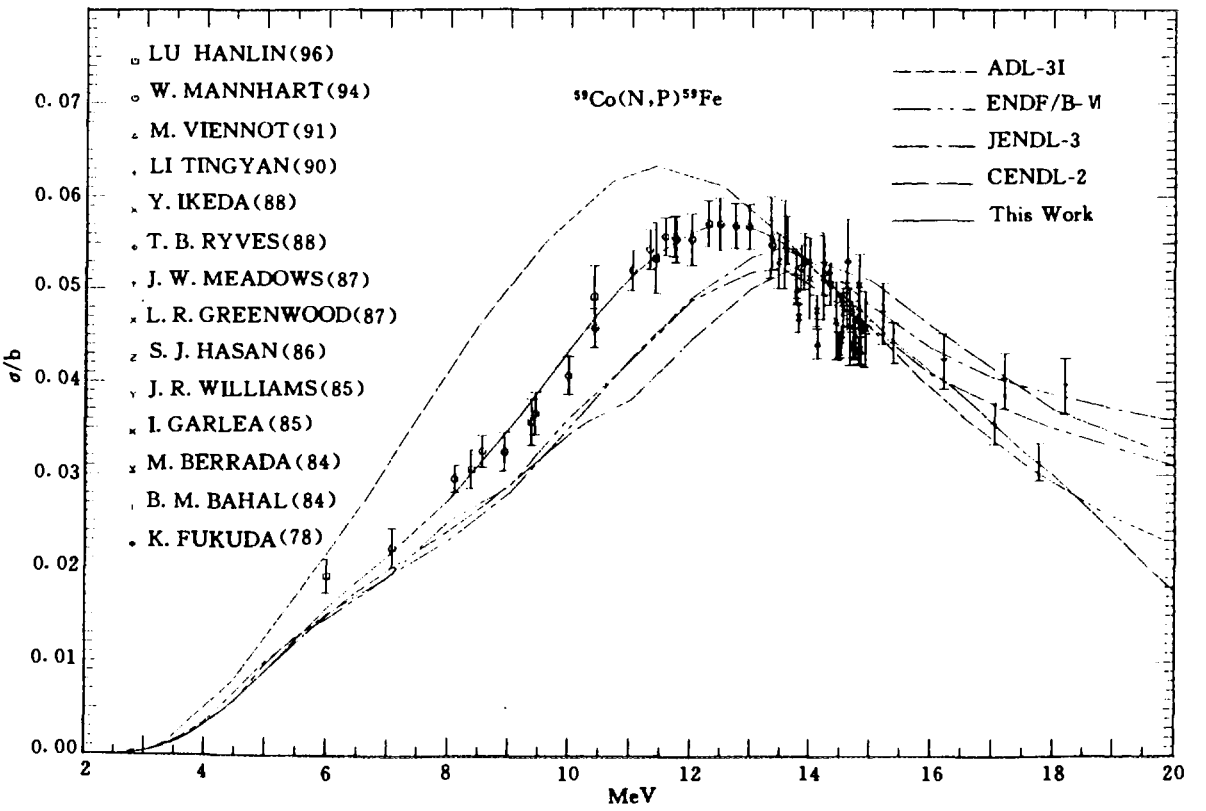

Fig.3 Comparison evaluated & measured data for $^{59}Co(n,p)$ reaction

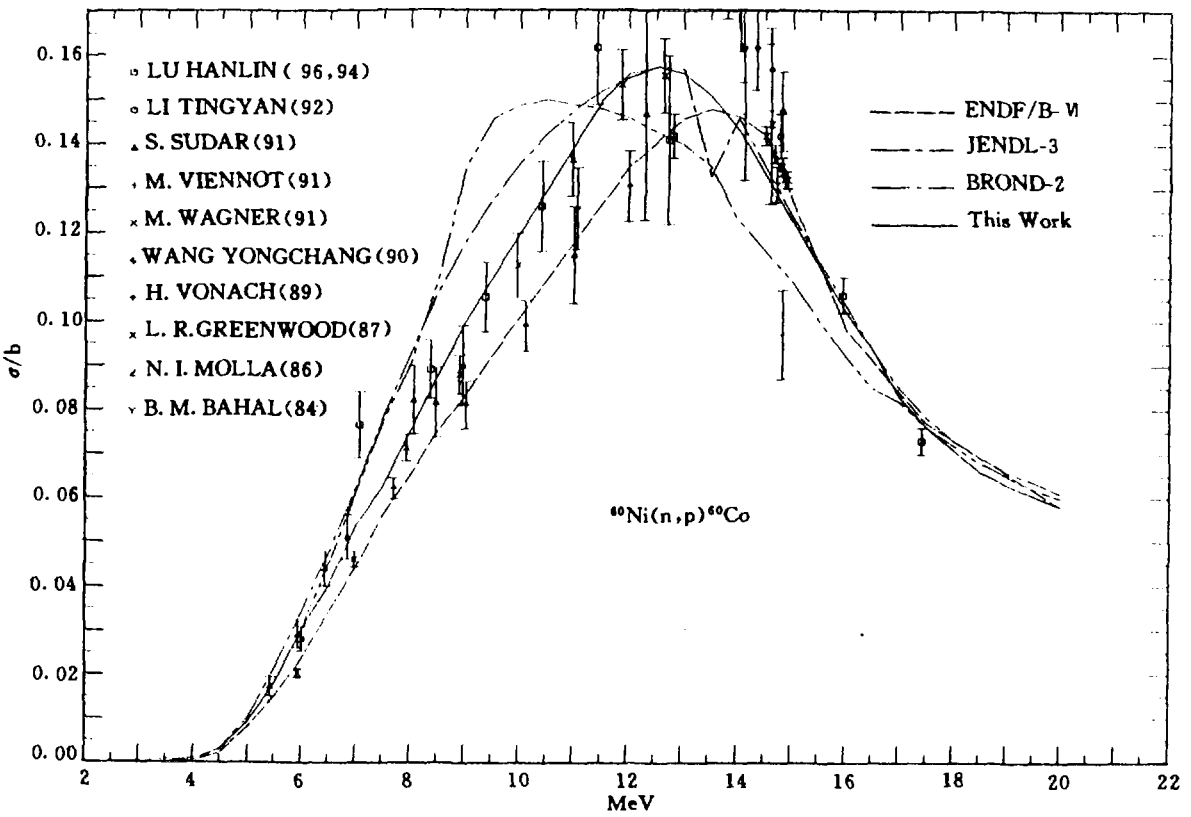

Fig.4 Comparison evaluated & measured data

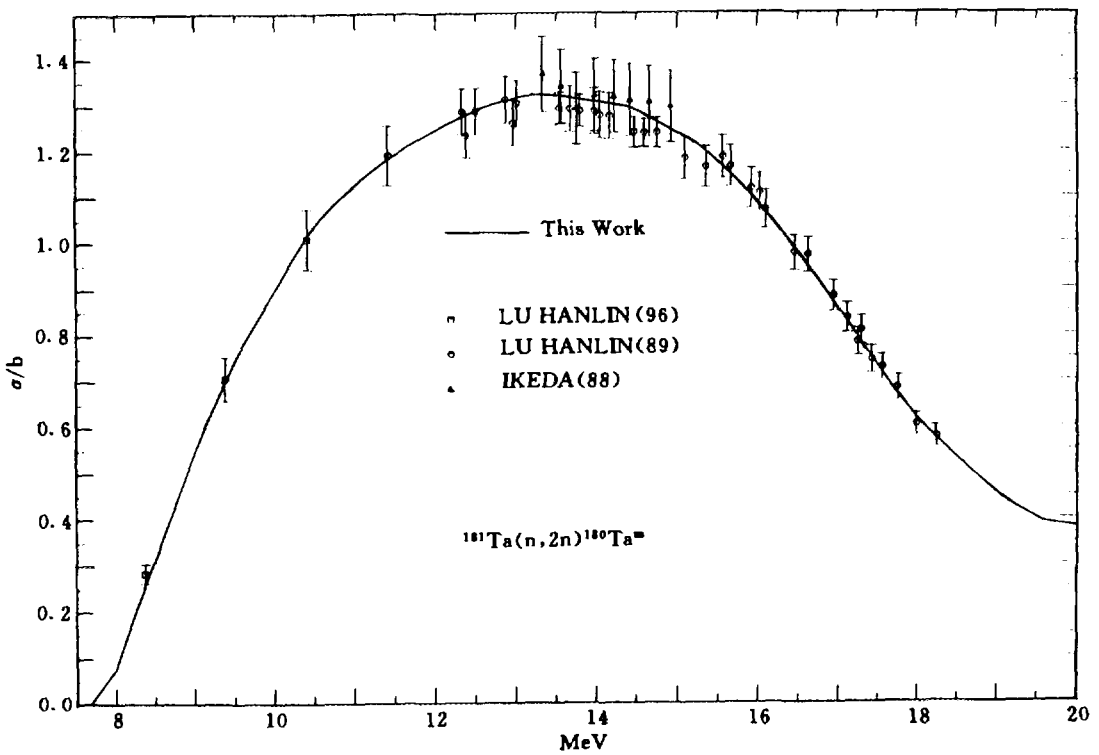

Fig.5 Comparison evaluated & measured data

References

[1] Lu Hanlin et al., Private Communication(1996)
[2] N.I.Molla et al., INDC(BAN)-003(1986)
[3] S.M.Qaim, N.I. Molla et al., Nucl. Phys. /A, 283,269(1977)
[4] Y.Ikeda et al., JAERI-1312(1988)
[5] Lu Hanlin et al., INDC(CRP)-16(1989)
[6] Lu Hanlin et al., J. China Atomic Scie. and Tech.,9,113(1975)
[7] Yu Baosheng et al., INDC(CPR)-024(1991)
[8] S. A. Badikov et al., Nucl. Data for Scie. and Tech., p.617, (1994) Gatlinburg, U. S. A.
[9] S.K.Saraf et al., Nucl. Sci. and Eng., 107,365(1991)
[10] Lu Hanlin et al., J. China Nucl. Phys., 7,242(1985)
[11] W.Mannhart et al., Conf. on Nucl. data for scie. and Tech., P.258(1994) Gatlinburg, U.S.A.
[12] M.Wagner, H. Vonach et al., Conf. on Nucl. data for Scie. and Tech., P.258(1994), Juelic.
[13] H. Vonach, M. Wagner et al., NEANDC-259,165(1989)
[14] Li Tingyan et al., High Energy Phys. and Nucl. Phys., 16,151(1992)

IV BENCHMARK TESTING

A New Method to Correct ^{238}U Fission Rate Measured Using Uranium Foils

Zhong Wenfa

(Institute of Nuclear Energy Technology, Tsinghua University, Beijing, 100084)

Abstract

A new method to correct measured data from highly depleted uranium foils is presented in this paper. It is used for correcting ^{238}U fission rate distribution measured with uranium foils. The corrected ^{238}U fission rate data compare with the measured data (only fission rate of ^{238}U) using miniature fission chambers with Cd-covered. The results of corrected ^{238}U fission rates are satisfied.

Introduction

High temperature gas-cooled reactors inherent safety characteristics, due to unique features such as multiple fission product barriers up to very high temperatures and high heat capacity in the core, make them especially suitable for sites close to densely-populated areas[1].

A series of new critical experiments need to be done in the design of high temperature reactor. The experiments are aimed at reducing the design and licensing uncertainties for small- and medium-sized, helium-cooled reactors using low-enriched uranium and graphite, high temperature fuel[2]. The main experiments are: critical loading, the measurements of reactivity worths and reaction rates. The highly depleted uranium foils were used for the measurement of ^{238}U fission rates, which have to be corrected for the ^{235}U fission contribution in reaction rate measurement. These measured data need to be processed.

A new method to correct measured data from highly depleted metallic uranium foils is presented. It is used for correcting measured ^{238}U fission rate distribution with uranium foils. Because there are ^{235}U atoms in highly depleted metallic uranium foil. The measured counting in the foils is a sum of ^{235}U atom fission and ^{238}U atom

fission. In order to get real ^{238}U fission rate, we should subtract the ^{235}U fission rate from measured fission rate using the uranium foils. We will state the correcting method in the following.

1 Measured Methods

The vertical channels in the core are availabe, which allow the insertion of fission chambers or activation foils for the mapping of axial and radial reaction rate distribution.

There are two methods of reaction rate measurement used in a reactor:

(1) Miniature fission chamber;

(2) Foil activation.

Uranium/Aluminum foils (20% U, ^{235}U enrichment 93%) and highly depleted metallic uranium foils (^{235}U content 0.0378%) were used for foil activation. The foils were placed on Al-strips.

Axial reaction rate distribution were measured in some radial positions. The axial distribution includes bottom reflector, core, cavity and top reflector.

2 Correcting Method

Since the metallic uranium used for foil activation contains ^{235}U of 0.0378 %, the fission rate measured with these uranium foils contains ^{238}U fission rate and ^{235}U fission rate. That is

$$\begin{aligned} F_{8m} &= \int_0^{\infty} (N_8 + N_5)\sigma_f(E)\phi(E)dE \\ &= \int_0^{E_T} N_5\sigma_f^5(E)\phi(E)dE + \int_{E_T}^{\infty} N_5\sigma_f^5(E)\phi(E)dE \\ &\quad + \int_0^{E_T} N_8\sigma_f^8(E)\phi(E)dE + \int_{E_T}^{\infty} N_8\sigma_f^8(E)\phi(E)dE \\ &= N_5\sigma_{fT}^5\phi_T + N_5\sigma_{fF}^5\phi_F + N_8\sigma_{fF}^8\phi_F \end{aligned} \qquad (1)$$

were F_{8m} is the fission rate measured using the metallic uranium foil,

N_5, N_8 is atomic number of ^{235}U and ^{238}U in the foil, respectively,

σ_{fT}^5,σ_{fF}^5 is microscopic fission cross section of thermal group and fast group of ^{235}U, respectively,

σ_{fF}^8 is microscopic fission cross section of fast group of ^{238}U,

ϕ_F,ϕ_T is fast neutron flux and thermal neutron flux, respectively.

E_T is upper limit of energy of thermal group.

From Eq.(1) we can see that fission rate measured using uranium foil relative to the ratio between fast neutron flux and thermal neutron flux. In fact

$$F_{8m} = \phi_F [N_5 \sigma_{5f} \frac{\phi_T}{\phi_F} + (N_5 \sigma_{5f} + N_8 \sigma_{8f})] , \tag{2}$$

$$\phi_F = \frac{F_{8m}}{N_5 \sigma_{5f} \frac{\phi_T}{\phi_F} + N_5 \sigma_{5f} + N_8 \sigma_{8f}} , \tag{3}$$

$$F_8 = N_8 \sigma_{8f} \phi_F = \frac{F_{8m}}{\frac{\sigma_{5f}}{\sigma_{8f}} \frac{N_5}{N_8} \frac{\phi_T}{\phi_F} + \frac{\sigma_{5f}}{\sigma_{8f}} \frac{N_5}{N_8} + 1} . \tag{4}$$

Let

$$f(Z) = \frac{N_8 \sigma_{8f} \phi_F}{N_5 \sigma_{5f} \phi_T} = \frac{F_{8,Cd}}{F_5} , \tag{5}$$

were F_5 and $F_{8,Cd}$ is ^{238}U fission rate and ^{238}U fission rate measured using miniature fission chamber with Cd, respectively and then $f(z)$ is normalized at certain point.

However, the ratio of ^{238}U fission rate to ^{238}U fission rate is previously known by some measurements for giving reactor. The reaction rates of the core with a hexagonal close-packed pebble bed lattice with a void fraction of 0.26 are measured using miniature fission chamber (see Fig.1)[3]. The fast fission rate distribution $F_{8,Cd}$ displays asymmetry in the core region caused by the lower reflector and the cavity above the core. For the thermal fission rate distribution F_5 the asymmetry is much more pronounced. The thermal fission rate distribution F_5 in the adjacent lower reflector is considerably higher than at the core centre, while it is nearly constant in the cavity and peaks only slightly in the upper reflector. If the results are measured, the function $f(z)$ values will be obtained.

$$F_8 = \frac{F_{8m}}{1 + \frac{N_5 \sigma_{5f}}{N_8 \sigma_{8f}} + \frac{1}{f(z)}} . \tag{6}$$

We will correct fission rate measured using uranium foils by Eq.(6).

3 Results and Discussion

An example is made by the method descried above for the fission rate measured with uranium foils. If measured fission rate data F_{8m} are not corrected, the error of relative measured $F_{8,Cd}$ with Cd is too large (see Fig.2). The biggest relative error is

4746.15%, namely, the F_{8m} is about 47 times of the $F_{8,Cd}$. The results of correcting fission rates measured using these uranium foils are obtained by Eq.(6). They show that the biggest relative error is 26.43% after correcting. The relative error in the core is about 9%.

The fission rate distribution F_{8m} measured using metallic uranium foils (not corrected) and the results F_8 corrected to it by Eq.(6) are shown in Fig.2. The corrected F_8 compare with the measured data (only fission rate of ^{238}U) using miniature fission chambers with cadmium (Cd). The results of corrected F_8 are satisfied.

The analysis above shows that the measured with uranium foils the ratio of ^{238}U fission rate relative to ^{238}U fission rate in the reactor.

Acknowledgements

Thanks are due to Dr. R. Seiler, Mr. P. Bourquin and Mr. O. Koberl for many discussions and their invaluable help.

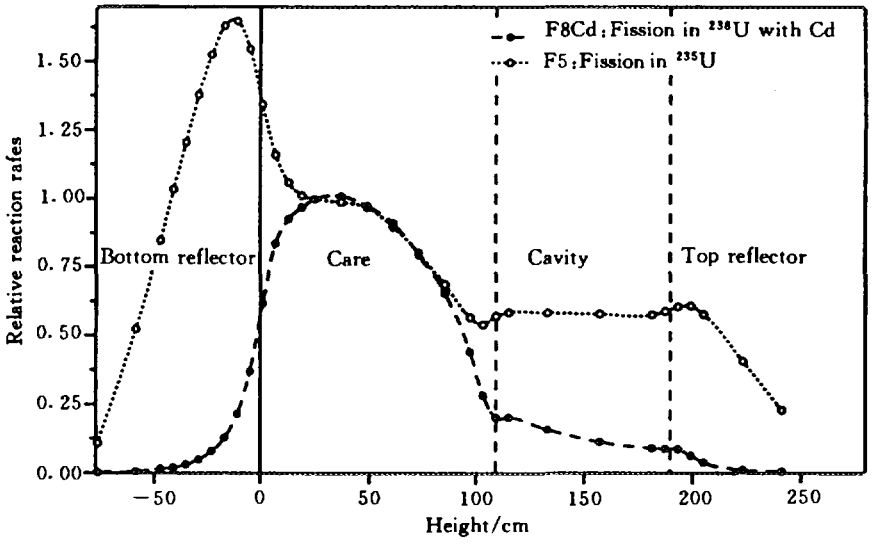

Fig.1 Axial fission rate distribution

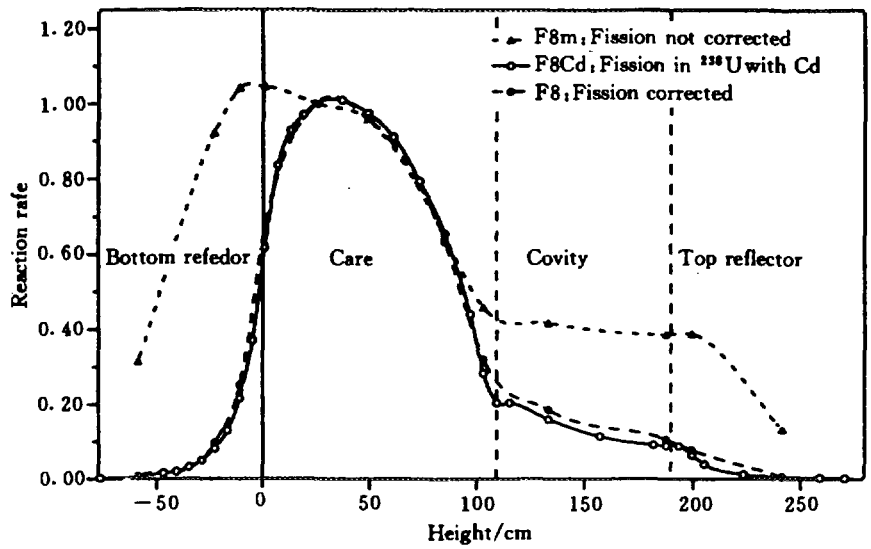

Fig.2 Axial fission rate distribution

References

[1] D. Mathews et al., PSI Nuclear Energy Research Progress Report, Annex IV, Annual Report (1990) p. 25.

[2] D. Mathews et al., Proceedings of an IAEA Specialists Meeting, Villigen, Switzerland, 9-11 May 1990, IWGGCR/24, IAEA, Vienna (1991).

[3] O. Koberl et al., Proceedings Jahrestagung Kerntechnik '94, May 17-19, 1994, Stuttgart.

The Integral Test of the Reactor Dosimetry Data

Rong Jian Liu Guisheng

(China Nuclear Data Center , CIAE)

Abstract

The spectrum averaged cross sections for several reactions based on four Evaluated Nuclear Data Libraries have been calculated. For the comparisons the calculational results for four evaluated nuclear data libraries and the experimental results are tabulated. From these calculations some useful information can be gotten .

Introduction

Nowaday, the mainly spectral reactor dosimetry flies in the world are the JENDL Dosimetry File[1], the International Reactor Dosimetry File Version 90(IRDF -90[2]) and the ENDF/B-5 Dosimetry File. A dosimetry file is a data set of neutron reaction cross sections that are basically used for determinations of neutron flux and energy spectrum in specific neutron fields. The data in those libraries are given in ENDF/B-6 format. The data of the JENDL Dosimetry File are based on the Japanese Evaluated Nuclear Data Library Version 3 (JENDL-3), and the data of the IRDF-90 are mainly based on the ENDF/B-6 and ENDF/B-5.

The reactor dosimetry data are very important for nuclear engineering, safety, shielding, and so on. Thus, higher accuracy and reliability are required for cross sections for the dosimetry data. Moreover, various applications need appropriate cross section sensitive to the specific neutron energy spectra depending on the field characteristics. So two neutron fields are used in this work: the spectrum of the Coupled Fast Reactivity Measurement Facility (CFRMF[3]) and the BIG-10[4].

In this work, 36 nuclear reactions' spectrum averaged cross sections which are based on CENDL-2, ENDF/B-6, JEF-2.2 and JENDL-3.2 evaluated nuclear data libraries have been calculated respectively. In order to confirm these data, the calculated results are compared with the experimental data[5] in the CFRMF and the BIG-10 two standard neutron fields. And the calculated results for four libraries are compared each other too.

1 Integral Test Calculations

The integral testing consists of calculating the spectrum averaged cross sections for each section in different library and different energy spectra.

The spectrum averaged cross section calculation takes this form:

$$\bar{\sigma} = \int_{E_L}^{E_U} \frac{\sigma(E)\phi(E)\,dE}{\phi(E)\,dE} \tag{1}$$

where $\sigma(E)$ and $\phi(E)$ are the group cross section and the energy spectrum, respectively. The lower E_L and the upper E_U are defined by the limits of the energy spectrum. Different lower (E_L) and upper (E_U) energies can be selected for defining a dosimeter sensor's response range in a given spectrum. A different response range can be required. In this work, the definitions of E_L and E_U are different for the two experimental facilities: E_L = 0.41 eV, E_U = 16.49 MeV for the CFRMF and E_L =10.9 eV, E_U = 20 MeV for the BIG-10. By those ranges the entire spectra can be included in the calculations, respectively .

These is a 71 group spectra of the CFRMF in the Ref.[3]. A spline interpolation code has been used to generate the 620 group spectra used for the integral test computations. The 70 group spectra of the BIG-10 is calculated by using the transport calculation code system SCALE-3. The same spline scheme can also be used to generate the 620 group spectra. The comparison of the broad-group fluxes and the fine-group fluxes for the two facilities are showed in figure[1] and figure[2], respectively. The 620 group cross sections are generated with NJOY-91.91 and the two 620 group energy spectra are used as inputed weighting spectrum. Using the group cross sections and the fluxes, we can easily get the spectrum averaged cross sections by the formula (1).

2 Results and Comparisons

In Table 1, our calculational results for the four libraries are obtained using the energy spectrum of the CFRMF as compared with the experimental data extracted from the APPENDIX A in Ref. [5]. The calculational data for the ENDF/B-6 are also extracted from the Ref. [5]. In the same form , the results of the energy spectrum of the BIG-10 are listed in Table 2 .

Discrepancies between the calculational results and experimental data are $C/E \geq$ 10%. And the discrepancies are different for the two neutron energy spectra.

The calculational results for the exoergic reactions are better than the results for the threshold reactions. The discrepancies for the threshold reactions are probably caused by the high threshold energies, i.e. in the region of the "high energy tail" of

the spectrum, which part of the spectrum need to be well defined[5].

For the $^{27}Al(n,p)$, $^{238}U(n,\gamma)$ and $^{235}U(n,f)$, the calculational results are almost identical for the four libraries but those exist discrepancies with the experimental data. Perhaps the experimental data for these reactions need to be checked.

For the $^{47}Ti(n,p)$, $^{58}Fe(n,\gamma)$ and $^{115}In(n,\gamma)$, the calculational results among these libraries are very different and their calculational results are also different to the experimental data. Perhaps it indicate the need for re-analysis or reevaluation of the energy dependent cross section.

Though the number of nuclides in CENDL-2 is not very much , from the testing calculation we can draw a conclusion that the evaluated cross section in CENDL-2 are better. In general the IRDF-90 is better than the JENDL DOSIMETRY FILE for those reactions .

Acknowledgements

The authors would like to thank Dr. Zhang Baocheng and Dr. Liu Ping (CNDC) for their kindly help .

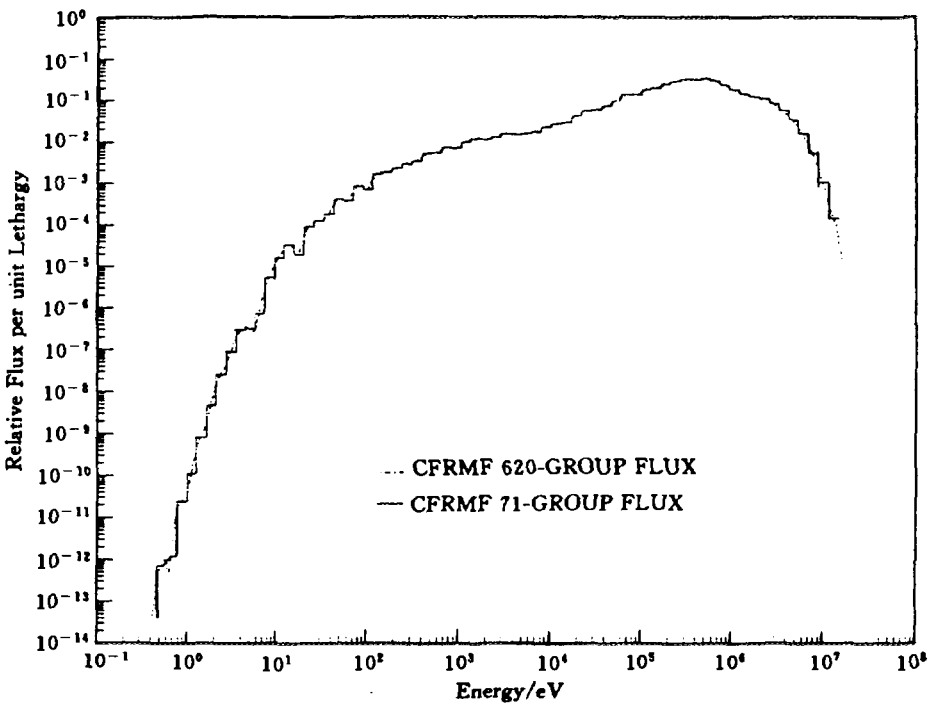

Fig.1 Comparison of 620-group and 71-group fluxes for CFRMF spectrum

Table 1⁺ Spectrum Averaged Cross Section (mb) of CFRMF

Nuclide	Reaction	B6	C2	JEF2.2	J3.2	B5	EXP.
^{27}Al	(n,p)	0.791	0.795		0.795	0.939	0.863±0.030
^{27}Al	(n,α)	0.143	0.137		0.137	0.158	0.160±0.005
^{55}Mn	(n,2n)	0.056	0.056	0.064	0.056	0.044	
^{59}Co	(n,2n)	0.047	0.057	0.047	0.049	0.040	
^{59}Co	(n, α)	0.030	0.031	0.030	0.032	0.033	
^{59}Co	(n,γ)	92.3	90.0	90.1	92.1	85.01	90.4±3.3
^{232}Th	(n,f)	18.7		17.7	19.7	19.14	19.6±1.0
^{232}Th	(n,γ)	282		301	262	252.00	290±11
^{238}U	(n,f)	77.5	77.6	77.5	78.5	79.59	75.1±2.5
^{238}U	(n,γ)	222	221	222	221	216.80	217±8
^{46}Ti	(n,p)	2.48			2.55	2.46	2.58±0.09
^{47}Ti	(n,np)	0.002			0.002	0.002	
^{47}Ti	(n,p)	4.58			5.00	5.30	4.12±0.20
^{48}Ti	(n,np)	0.0004			0.0005	0.0003	
^{48}Ti	(n,p)	0.070			0.062	0.062	0.068±0.002
^{54}Fe	(n,p)	17.9	17.7	18.8	17.8	18.42	17.2±0.5
^{56}Fe	(n,p)	0.197	0.200	0.264	0.203	0.228	
^{58}Fe	(n,γ)	8.77	10.13	7.28	7.00	6.61	6.04±0.19
^{58}Ni	(n,2n)	0.001		0.001	0.001	0.0006	
^{58}Ni	(n,p)	24.2		24.2	24.2	24.22	23.8±0.7
^{60}Ni	(n,p)	0.456		0.456	0.614	0.574	
^{63}Cu	(n, α)	0.123	0.130		0.130	0.123	
^{63}Cu	(n,γ)	43.3	38.5		45.0	44.22	43.3±2.7
^{65}Cu	(n,2n)	0.079	0.081		0.081	0.067	
^{115}In	(n,intl)	49.9				51.42	50.6±2.0
^{115}In	(n,γ)	302		260	345	273.40	269±10
^{127}I	(n,2n)	0.246		0.410	0.328	0.266	
^{32}S	(n,p)	14.58		15.43	15.43	16.08	
^{23}Na	(n,γ)	1.56	1.39	1.40	1.40	1.40	
^{235}U	(n,f)	1568	1568	1568	1567	1552	1538±48
^{237}Np	(n,f)	533	530	530	546	606.10	548±18
^{239}Pu	(n,f)	1775	1790	1783	1772	1773	1792±39
^{6}Li	(n,tot He)		941.6			890.50	942.1±27.3
^{10}B	(n,tot He)					1599	1850±67
^{45}Sc	(n,γ)	24.4			24.8	23.36	23.2±0.8
^{197}Au	(n,γ)	419	419	416		379.50	419±12

Table 2[+] Spectrum Averaged Cross Section (mb) of BIG-10

Nuclide	Reaction	B6	C2	JEF2.2	J3.2	B5	EXP.
^{27}Al	(n,p)	0.683	0.687		0.687	0.644	
^{27}Al	(n,α)	0.096	0.092		0.092	0.107	0.106±0.004
^{55}Mn	(n,2n)	0.038	0.038	0.044	0.038	0.029	
^{59}Co	(n,2n)	0.031	0.038	0.031	0.033	0.026	
^{59}Co	(n, α)	0.020	0.021	0.020	0.022	0.022	
^{59}Co	(n,γ)	12.74	11.56	11.60	13.66	12.36	12.81±0.40
^{232}Th	(n,f)	12.27		11.62	12.87	13.02	
^{232}Th	(n,γ)	198		220	186	181.10	
^{238}U	(n,f)	50.4	50.4	50.4	50.4	54.26	50.9±1.1
^{238}U	(n,γ)	160.4	160.1	160.6	160.1	149.80	149.5±4.5
^{46}Ti	(n,p)	1.79			1.84	1.69	1.76±0.06
^{47}Ti	(n,np)	0.002			0.002	0.001	
^{47}Ti	(n,p)	3.15			3.49	3.62	2.91±0.14
^{48}Ti	(n,np)	0.0003			0.0005	0.0002	
^{48}Ti	(n,p)	0.048			0.037	0.042	0.048±0.002
^{54}Fe	(n,p)	12.72	12.69	15.24	12.68	12.63	12.23±0.53
^{56}Fe	(n,p)	0.134	0.136	0.180	0.138	0.155	
^{58}Fe	(n,γ)	6.91	8.34	5.67	5.14	3.44	4.14±0.16
^{58}Ni	(n,2n)	0.0007		0.0007	0.0007	0.0004	
^{58}Ni	(n,p)	16.95		16.95	16.97	16.59	16.65±0.57
^{60}Ni	(n,p)	0.320		0.320	0.430	0.391	
^{63}Cu	(n, α)	0.086	0.091		0.091	0.083	
^{63}Cu	(n,γ)	26.1	19.5		28.5	21.77	22.1±1.5
^{65}Cu	(n,2n)	0.054	0.055		0.055	0.044	
^{115}In	(n,intl)	32.6				35.98	36.6±1.3
^{115}In	(n,γ)	303		256	336	217.40	
^{127}I	(n,2n)	0.168		0.279	0.224	0.176	
^{32}S	(n,p)	10.3		10.9	10.9	11.00	
^{23}Na	(n,γ)	0.750	0.611	0.622	0.622	0.641	
^{235}U	(n,f)	1398	1398	1399	1400	1361	1361±18
^{237}Np	(n,f)	399.98	399.45	397.30	411.00	486.40	433.55±11
^{239}Pu	(n,f)	1594	1609	1601	1590	1623	1632±33
^{6}Li	(n,tot He)		942			866.70	959±4
^{10}B	(n,tot He)					1172	1373±4
^{45}Sc	(n,γ)	22.11			22.32	18.50	17.87±0.60
^{197}Au	(n,γ)	239	239	236		209.30	225±7

+ : The symbols, B6, C2, J3.2 and B5 in the Table, ENDF/B-6, CENDL-2, JENDL-3.2 and ENDF/B-5,

respectively. The blanks in the Table mean these nuclear reactions are not involved in the library, or there are no experimental data for these nuclear reactions.

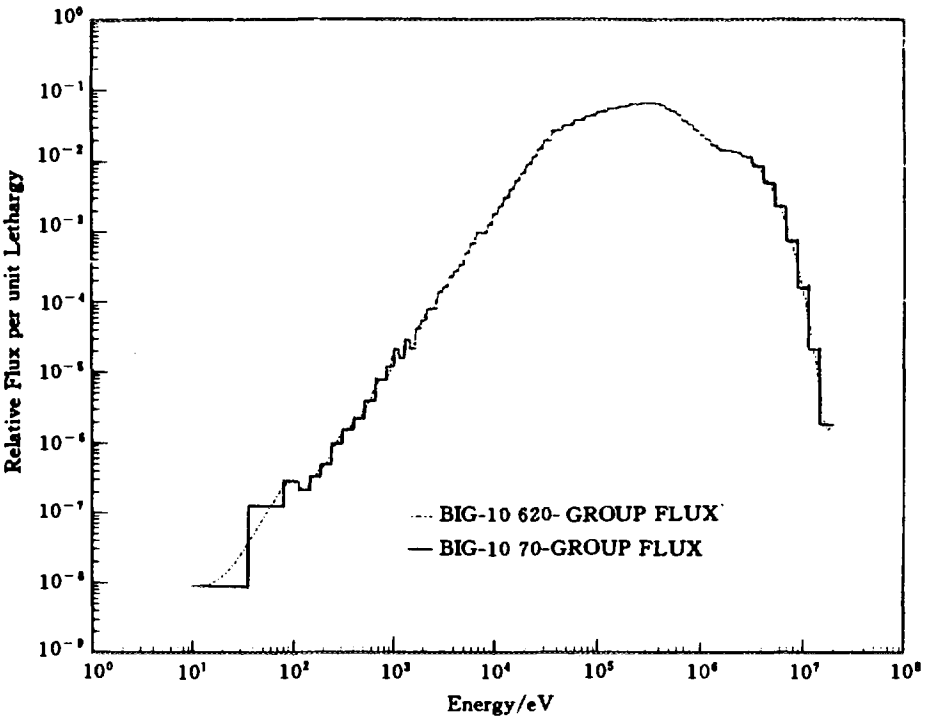

Fig.2 Comparison of 620-group and 70-group fluxes for BIG-10 spectrum

References

[1] K.Kobayashi et al., JENDL Dosimetry file. Reactor Dosimetry. ASTM 04-012280-35 (1993).

[2] H.J.Nolthenius et al., Testing of the IRDF-90 Cross Section Library in Benchmark Neutron Spectra. Reactor Dosimetry. ASTM 04-012280-35(1993) .

[3] JW.Roqers et al., The Coupled Fast Reactivity Measurement Facility. IAEA-208(1978) .

[4] ENDF-202. Cross Section Evaluation Working Group Benchmark Specifications. November 1974 .

[5] ENDF-311. Benchmark Data Testing of ENDF/B- γ (part 6). August 1982 .

V SYSTEMATICS RESEARCH

Calculation for Cross Section of (p,n) Reaction on Sixteen Targets in Energy Region up to 100 MeV

Fan Sheng Zhao Zhixiang

(China Nuclear Data Center, CIAE)

Abstract

A semiempirical method based on the evaporation and exciton models is developed to calculate the cross section of the (p,n) reaction, in the mass number region $30 \leq A \leq 140$, and incident proton energy $E_P \leq 100$ MeV, and the systematics of two parameters obtained. Using the formulas, the calculation for sixteen targets has been performed, the results of the calculation are in agreement with the measured data.

Introduction

A large amount of nuclear reaction data at medium energies is required for different important applications, such as medical and biomedical needs, and the research of cosmic-ray effects on spaceships and astronauts.

Recently, the authors developed a semiempirical method[1,2], based on the evaporation and exciton models. The systematics study for the two parameters, i.e. the formation cross section σ_c of the compound system and R connecting with the Coulmn barriers, were performed, good results of the two parameters were obtained.

1 Semiempirical Formulas

Within the incident proton energy $E_P \leq 100$ MeV, the reaction channels (p,n),(p, p′),(p,α),(p,2n),(p,n+p),(p,n+α) and (p,3n) are considered, where (p,n+q) denote the reaction of (p,nq) and (p,qn) (q=p,α). Based on evaporation and exciton model the cross section of (p,n) reaction can be written as

$$\sigma(p,n) = \sigma_{pn}^{eq} + \sigma_{pn}^{pre} \quad (1)$$

In Eq.(1), the equilibrium cross section σ_{pn}^{eq} can be calculated by the evaporation model, and the preequilibrium cross section σ_{pn}^{pre} by the exciton model.

$$\sigma_{pn}^{eq} = \sigma_c \frac{\lambda_{+2}}{L+\lambda_{+2}} \frac{\Gamma_n}{\Gamma} \tag{2}$$

$$\sigma_{pn}^{pre} = \sigma_c \frac{L}{L+\lambda_{+2}} \frac{L_n}{L} \tag{3}$$

where σ_c is the formation cross section of compound nucleus system, which is assumed to be independent of proton energy, in this work, it is a adjusted parameter, λ_2 is the average internal transition rate, $\Gamma = \Gamma_n + \Gamma_p + \Gamma_\alpha$ and Γ_q are the total and q particle decay width of compound nucleus respectively, $L = L_n + L_p + L_\alpha$ and L_q are total and q particle emission rate at the preequilibrium state of $N = 3$, respectively, $\lambda_{+2}/(L+\lambda_{+2})$ and $L/(L+\lambda_{+2})$ are probability of compound nucleus formation and preequilibrium emission, respectively.

For (p,n) reaction, the second and third particle emission must be considered, we assumed that the second and third particle preequilibrium emission can be neglected .

In order to simplify the calculation , the constant temperature density level is adopted

$$\rho(A, E_A) \propto \exp(E_A / T) \tag{4}$$

where E_A is exciton energy, T is nuclear temperature[3,4]

$$T = \frac{13}{\sqrt{A}} \tag{5}$$

The Coulumn barrier adopted the formulas of the following[5]

$$E_c^q = R \frac{(Z - Z_q) Z_q}{(A+1-A_q)^{1/3} + A_q^{1/3}} [1.0 - \frac{1.13}{(A+1-A_q)^{1/3}}] \tag{6}$$

Where R is a adjust parameter, A and Z are target mass number and atomic number respectively, A_q, and Z_q are outgoing particle mass number and atomic number.

2 Systematics of the Two Parameters

Using the semiempirical formulas, the calculation for 16 targets including ^{65}Cu, ^{63}Cu, ^{56}Fe, ^{51}V, ^{89}Y, ^{90}Zr, ^{69}Ga, ^{59}Co, ^{79}Br, ^{75}As, ^{107}Ag, ^{93}Nb, ^{45}Sc, ^{103}Rh, ^{55}Mn, ^{48}Ti were performed, the parameters R and σ_c were adjusted to fit the measured cross section for these nuclei. In this work , we find $R = 1.03$ is in agreement with all the nucleus, and the systematics of another parameter σ_c is obtained,

$$\bar{\sigma}_c = (1 + A^{1/3})^{-2} \exp(11.16 - 0.96\frac{N-Z}{A} - 92.06A^{-2/3}) \qquad (18)$$

In Eq.(18), N is the neutron number of target.

3 Discussions

Within the incident proton energy $E_P \leq 20$ MeV, the contribution of the equilibrium emission is important, and that of preequilibrium emission is very evident within the energy up to 100 MeV, see Fig. 1.

Acknowledgments

Fan Sheng, one of the authors, would like to thank Drs. Youxiang Zhuang, Tong Liu and Caiwan Shen for fruitful discussions during this work.

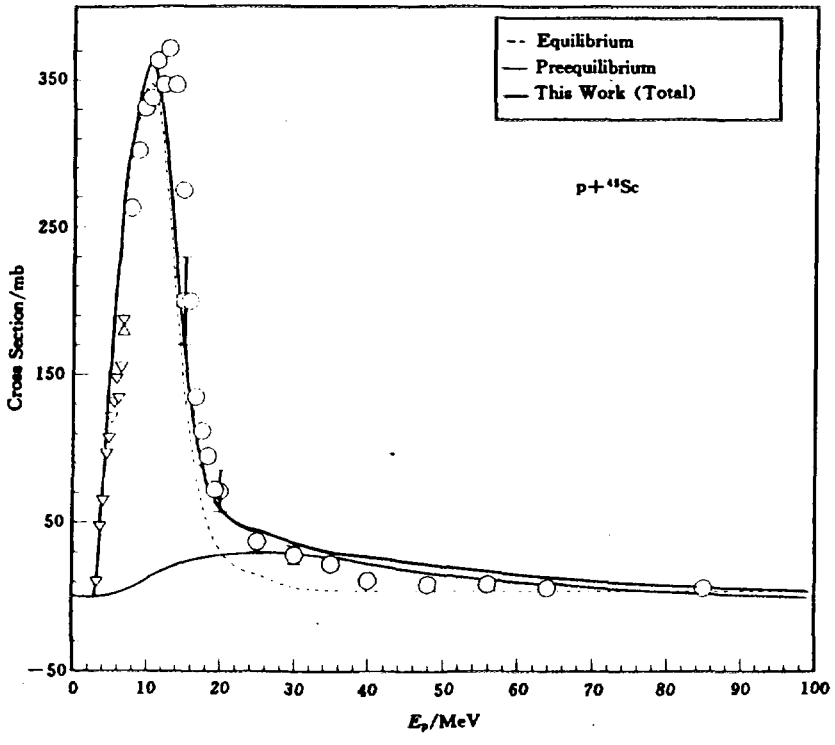

Fig.1 The cross section of ^{45}Sc(p,n) reaction

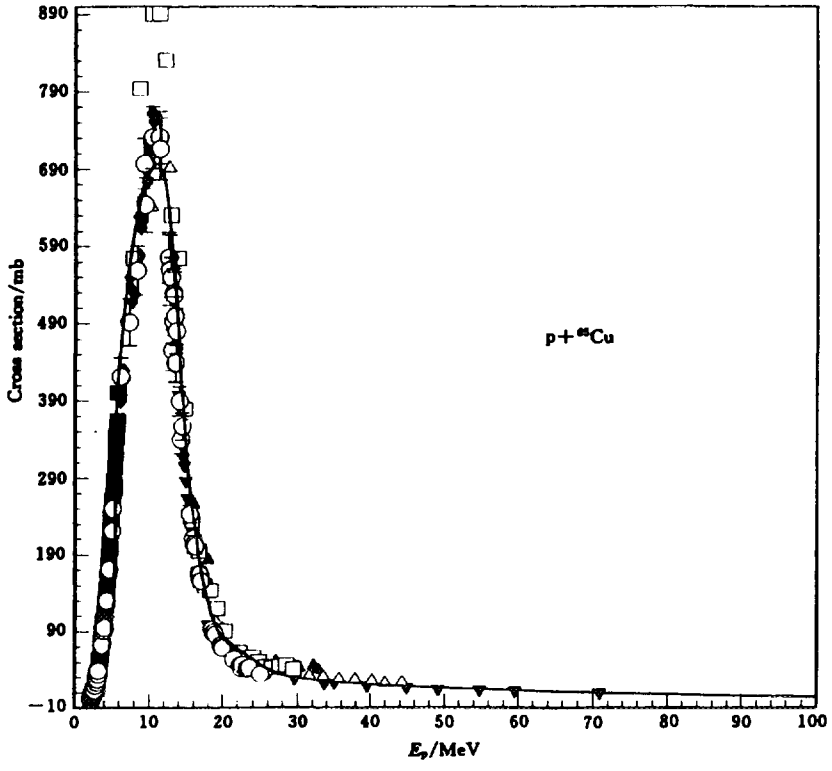

Fig.2 The cross section of ^{65}Cu(p,n)

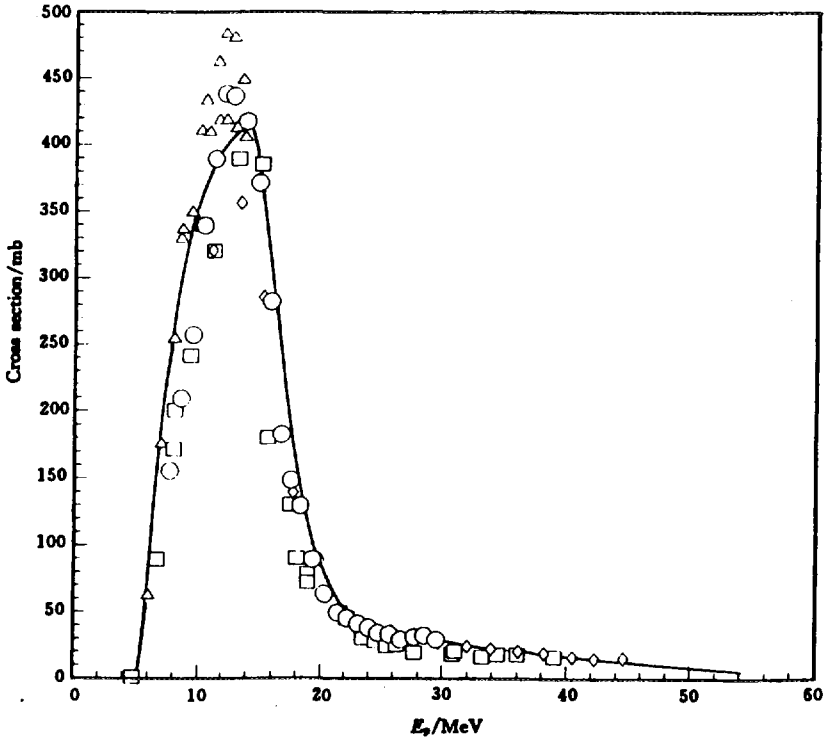

Fig.3 The cross section of ^{56}Fe(p,n) reaction

Table.1 The reference of the expermental data

Nuclide	Author	Energy/ MeV	Ref.
^{45}Sc	L.W.Mitchell	2.9 ~ 4.0	Nucl.Phys. A380,318,(1982)
	V.N.Levkovskij	7.7 ~ 19	B,LEVKOVSKIJ,(1991)
	H.G.Blosser	12	Phys.Rev.,100,1340,(1955)
	T.Mcgee	10 ~ 85	Nucl.Phys.,A150,11,(1970)
	R.M.Humes	6.7 ~ 6.8	Phys.Rev.,130,1522,(1963)
	G.F.Dell	3.3 ~ 6.8	Nucl. Phys.,64,513,(1965)
	R.G.Thomas	7.8~ 14	Nucl.Phys.,A106,323,(1968)
^{56}Fe	T.Asano	12	Phys.Rev.,C28,1840,(1983)
	B.V.Zhuravlev	22	Fad.Fiz.,39,264,(1984)
	V.N.Levkovskij	7.7 ~ 30	B,LEVKOVSKIJ,(1991)
	E.Gadioli	11 ~ 45	Nuovo Cimento,A22,547,(1974)
	I.L.JenKins	4.8 ~ 39	J.Inorg.Nucl.Chem.,32,1419,(1970)
	S.Tanaka	6 ~ 14	J.Phys.Soc.Jap.,14,1269,(1959)
	A.E.Antropov	6.2	*
	Zhao Wenrong	16 ~ 19	J.China Phys.Nucl.,15(4),337,(1993)
^{65}Cu	A.E.Antropov	6.1	*
	M.E.Sevior	2.2 ~ 3.2	Astr.J.Phys.,36,463,(1983)
	P.Kopecky	4.4 ~ 32	Int.J.Appl.Radiat.Isotop.,36(8),657,(1985)
	V.N.Levkovskij	7.7 ~ 30	B,LEVKOVSKIJ,(1991)
	E.Gadioli	11 ~ 44	11-44/Nuovo Cimento,A22,547,(1974)
	C.H.Johnson	2.2 ~ 5.5	Phys.Rev.,109,1243,(1958)
	J.P.Blaser	2.8 ~ 6.3	Helv.Phys.Acta.,24,3,(1951)
	R.Colle	2.9 ~ 25	Phys.Rev.,C9,1819,(1974)
	H.A.Howe	6.4 ~ 11	Phys.Rev.,109,2083,(1958)
	G.A.Jones	9.8 ~ 9.9	TID-12696
	G.F.Dell	6.7 ~ 6.8	Nucl.Phys.,64,513,(1965)
	J.Wing	4.5 ~ 11	Phys.Rev.,128,280,(1962)
	L.F.Hansen	5.0 ~ 11	Phys.Rev.,128,291,(1962)
	B.W.Shore	7.5	Phy.Rev.,123,276,(1961)
	C.H.Johnson	2.2 ~ 5.8	ORNL-2910,25
	K.F.Chackett	9.3	Proc.Phys.Soc.,80,738,(1962)
	I.R.Williams	14 ~ 32	Phys.Rev.,162,1055,(1967)
	M.W.Greene	16 ~ 33	Int.J.Appl.Radiat.Isotop.,23,342,(1972)
	T.Pulfer	14 ~ 71	Thesis of T.Pulfer

*: 30.Annual Conf. on Nucl.Spectroscopy and Nucl.Structure, Leningrad,18 ~ 21 Match 1980

References

[1] S. Fan, Q. B. Shen, Z.X.Zhao and D.Z.Ding , to be published.

[2] S. Fan, Q. B. Shen, Z.X.Zhao and D.Z.Ding , to be published.

[3] D.L.Livesey, Can. J.Phys.,33,391,(1955).

[4] G. Eder, G. Winkler, P. Hille, Z. Phys., 253,335,(1972).

[5] I.Dostrovsky, Z.Fraenkel, Phys. Rev., 116,683,(1959).

VI DATA AND PARAMETER LIBRARIES

Progress on Chinese Evaluated Nuclear Parameter Library (CENPL) (VI)

Su Zongdi Huang Zhongfu Dong Liaoyuan
Liu Jianfeng Sun Zhengjun Zuo Yixin Zhang Limin
Ge Zhigang Chen Zhenpeng Yu Ziqiang Zhang Xiaocheng
Wang Baijin Ma Gonggui

The project supported in part by the International Atomic Energy Agency and the National Natural Science Foundation of China(19445005, 19475067).

The objective of the improved and updated Chinese Evaluated Nuclear Parameter Library CENPL-2(The Second Version) is to develop the nuclear model parameters further, to update and expand the data files of the CENPL, and to improve and perfect its management-retrieval codes for wider application. The project of CENPL-2 was commenced in 1996, the main progress in the past year was as follows.

1 Average Neutron Resonance Parameters, Cumulative Number of Low Lying Levels and Data File Relative to Level Density(LRD)

The average level spacing D_0 of s-wave neutron at the neutron separation energy B_n and the cumulative number N_0 of low lying levels are the most basic data in the researches of the nuclear level density. It is necessary and important to estimate the reliable D_0 and N_0 values in order to get and recommend the accurate level density parameters. The D_0, as well as the neutron strength function S_0, radiative capture width $G\Gamma_0$ etc. for s-wave neutron at B_n are major parameters describing the mean properties in the resonance region. In the past two years, the resolved resonance parameters from BNL-325, ENDF/B-6, JEF-2, and JENDL-3 were collected and analysed, a set of the resolved resonance parameters were reevaluated, and the data of nuclear discrete levels were further supplemented and corrected according to the new data published in "Nuclear Data Sheets" up to 1993. In addition, Estimating method of the D_0 which contains the moment method, maximum likelihood method, Bayesian approach and so on, as well as corresponding program AVRPES[1] were further improved and perfected, A new set of average

neutron resonance parameters D_0 and S_0 for more than 300 nuclides have been reestimated on the basis of the work mentioned above. The N_0 values were also evaluated by means of the histogram for more than 300 nuclides.

A new data file with the data relative to level density, LRD-2 (The Second Version) was completed and recommended in 1996. These updated D_0, S_0, N_0 values and their deviations dD_0, dS_0 of 309 nuclides ranging from ^{15}N to ^{254}Es were compiled in the LRD-2 file. It contains the other D_0 values of 35 nuclides and the GW_0 of 208 ones ranging from ^{32}S to ^{250}Bk, which were taken from BNL-325[2] and other Refs.[3~5].

2 Level Density Parameters

The nuclear level density is crucial ingredient in the statistical model of nuclear reaction and nuclear model calculations. Many kinds of level density formulae have been accumulated in the past, and they, especially three kinds of popular level formulae, i.e. the composite formula of the constant temperature-Fermi gas(Gilbert-Cameron(GC) formula)[6], the back-shifted Fermi gas model(BS)[5] and generalized superfluid model(GSM))[7], are still being used widely today, and the requirements of accuracy and reliability for nuclear level density are even higher in the practical application. Therefore, it is very necessary and important to reestimate level density parameters by using the new experimental data.

In the past year, our optimum program to fit the D_0 and N_0 values and calculate the GSM level density parameters were further examined and compared with the Ignatyuk's one. The optimum program including GC, BS and GSM formulae was further refined. Three sets of level density parameters for the GC, BS and GSM formulae have been re-estimated by fitting the D_0 and N_0 values mentioned above in both Beijing and Guangxi, respectively. The new sets of level density parameters of GC and BS formulae for more than 300 nuclides ranging from ^{15}N to ^{254}Es, and the new set of GSM ones for 249 nuclides ranging from ^{15}Ca to ^{254}Cf will be recommended after they are further checked in physics. And the comparison between the new level density parameters with old ones and an intercomparison of three kinds of popular level density formulae are being done.

3 Giant Dipole Resonance Parameters of γ-Ray Strength Function

The giant dipole resonance parameters(GDRP) of γ-ray strength function characterize the average electromagnetic properties of excited nucleus. Besides their fundamental importance for nuclear structure, γ-ray strength function is an indispensable component for nuclear reaction model calculations. The GDRP are necessary and

important in the calculations of average radiation widths, radiation capture cross sections, γ-ray production cross sections and γ-ray spectra. But there are only the GDRP of 102 nuclides ranging from ^{51}V to ^{239}Pu up to now, which were extracted from the data on the photoneutron cross sections[8]. It can not satisfy the needs in practical application. There are no reliable theoretical method by which the GDRP can be calculated precisely so far. The GDRP are estimated by using some semiempirical systematics formulae in the sub-library of giant dipole resonance parameters (GDP-1, The First Version)[9] of the CENPL. Among them, only the peak energy formula of the GDRP for the spherical nuclei can give better results[10]. There are no systematics formulae to calculate the double peaks GDRP up to now. For supplementing the GDRP required in nuclear model calculations and developing the systematics approaches of the GDRP, the experimental data of the photonuclear reaction were collected and analysed, the GDRP of some nuclides with $A < 50$ were extracted with the Lorentz curve to fit the data of the photonuclear reaction cross sections, their integrated cross sections and first and second moments. The data file of the GDP sub-library were expanded. The semiempirical formulae for the peak energy calculations of the double peak giant dipole resonances of the photonuclear reaction in the large deformation nuclear regions have be derived in view of the formula to calculate the peak energy of the single peak giant dipole resonance in spherical regions presented by Zheng Jinyan and Yang Fujia[10], and by leading the deformation parameter in formula reasonably. The peak energies in the nuclear mass region $50 < A < 250$ have been calculated by using Zheng-Yang's and our formulae. The calculated results are better coincident with the experimental data available. Thus, the calculation formulae of the peak energies for single peak(for spherical nuclei and nuclides located in the transition regions i.e. nuclides with the spherical equilibrium shape) and double peaks (for large deformation regions) of the giant dipole resonances have been recommended.

4 The Other Sub-Libraries

An improved second version of sub-library of atomic masses and characteristic constants for nuclear ground states(MCC-2) is being set up, in which the masses for nuclides between the proton and neutron drip lines and superheavy nuclides up to A=339, and ground state deformations will be included. All data are from the evaluated experimental[11] or calculated ones[12] published in 1995.

The levels and corresponding gamma-rays measured by Chinese scientists were collected and evaluated, and the data of ^{120}Cs, ^{129}La, ^{130}La, ^{135}Gd, ^{153}Ho, ^{157}Tm and ^{209}Rn obtained with electron capture and β^+ decay method were compiled to correct and supplement the data file of the sub-library of discrete level schemes and

branching ratios of gamma decay(DLS).

The optical model parameter sub-library(OMP) and fission barrier parameter sub-library(FBP), are further being expanded. The dispersion optical model parameters of ^{40}Ca, ^{90}Zr, ^{208}Pb, ^{209}Bi and so on, are being collected and analysed.

The management-retrieval codes of the six sub-libraries of the CENPL are being improved and perfected for wider application. Retrieving data by window-menu will be carried out.

5 A New Developing Project

A new project "Development of Nuclear Reaction Model Computation System (NRMCS) for Nuclear Model Calculations" was proposed in 1996. The NRMCS contains the following three parts:

(1) Nuclear Reaction Model Code Library(MCL),

(2) Nuclear Parameter Databases(NPD),

(3) Analyses-Selection-Calculation-Analyses(ASCA) System.

The various popular programs of the nuclear reaction model will be collected and integrated in the MCL. These programs deal with the optical model, statistical theory of the compound nucleus reaction, preequilibrium emission model, direct reaction theory and so on, and can calculate the various cross sections of neutron, proton, deuteron, triton, ^3He, α and photon- induced reactions.

The NPD contains the atomic masses and related data, discrete level schemes and branching ratios of γ decay, nuclear level density parameters, average neutron resonance parameters, giant resonance parameters of γ-ray strength functions, fission barrier parameters, optical model parameters and so on. These data sets have been compiled in the CENPL.

The MCL and NPD will be connected and combined by the ASCA system. There are the following functions in the ASCA system.

(1) Analysing the input information on target nucleus, incident particle and energies, and computational functions required,

(2) Selecting the suitable theoretical model programs from the MCL, retrieving the input parameters from the NPD and generating of input files required for the selected programs,

(3) Nuclear model calculations for required nuclear reaction data.

(4) Analysing calculated results and comparing ones with the input experimental data. There is also function of re-optimization of the model parameters.

Finally, the calculated results and used model parameters will be written respectively.

Acknowledgements

The authors would like to thank NDS/IAEA and NNDC/BNL for providing us the data on mass excesses, ENSDF and so on.

The project supported in part by the International Atomic Energy Agency and the National Natural Science Foundation of China(19445005, 19475067).

References

[1] Huang Zhongfu, J. Chinese Atomic Sci. & Tec., 22, 3(1988).

[2] S. F. Mughabghab et al., "Neutron Cross Section", Part A(1981) and Part B(1984).

[3] J. Kopecky et al., INDC(NDS)-238(1990).

[4] J. A. Harver et al., Phys. Rev., C28, 24(1983).

[5] W. Dilg et al., Nucl. Phys., A217, 269(1973).

[6] A. Gilbert and A. G. Cameron, Can. J. Phys., 43, 1446(1965).

[7] A. V. Ignatyuk et al., Sov. Nucl. Phys., 29, 450(1979).

[8] S. S. Dietrich and B. L. Berman, Atomic Data and Nuclear Data Tables, 38, 199 (1988).

[9] Zuo Yixin, Liu Jianfeng, Su Zongdi et al., Commu. Nucl. Data Progress, 14, 95(1994).

[10] Zheng Jinyan and Yang Fujia, Chin. J. Nucl. Phys., 3,245(1980).

[11] G. Audi and A. H. Wapstra, Nucl. Phys., A595, 409(1995).

[12] P. Moller, J. R. Nix, et al., Atomic Data and Nuclear Data Tables, 59, 185(1988).

VII NUCLEAR DATA NEWS

Activities and Cooperation on Nuclear Data in China During 1996

Zhuang Youxiang

(China Nuclear Data Center, CIAE)

1 The Activities and Meeting in Nuclear Data Field in 1996

(1) " The Meeting on Macroscopic Data Working Group ",May 6 ~ 10, Taian City, Shandong Province. Communicated and Summarized the achievements and experiences of multigroup constant generating and benchmark testing, worked out the work plan for 1996-2000.

(2) " The Working Meeting on Fission Yield, Decay Data and Activation Cross Section Evaluations ", Nov.5 ~ 8, China Institute of Atomic Energy, Beijing. Reviewed the progress on fission yield, decay data and activation cross section evaluations, discussed some technical problem and arranged the future work.

2 The International Meetings and workshops in Nuclear Data Field Attended by Staff Members of CNDC in 1996

(1) " The 2nd Research Co-ordination Meeting on an International Reference Data Library of Nuclear Activation Cross Sections ", May 13 ~ 17, Madrid, Spain;

(2) " The 2nd International Conference on Accelerator Driven Transmutation Technology and Application ", June 3 ~ 6, Karlmar, Sweden;

(3) " The Advisory Group Meeting on the Co-ordination of the Nuclear Reaction Data Centres ", June 3 ~ 7, Brookhaven, USA;

(4) " The NEA Working Party on International Cooperation Evaluation and Measurement ", June 10 ~ 14, ANL, USA;

(5) " The Workshop on Nuclear Reaction Data and Nuclear Reactors—Physics, Design and Safety ", Apr.15 ~ May 17, Trieste, Italy;

(6) " The Research Co-ordination Meeting on Compilation and Evaluation of Fission Yield Nuclear Data ", Oct.14 ~ 16, Vienna, Austria;

(7) " The Advisory Group Meeting on the Co-ordination of the Nuclear Structure and Decay Data Evaluators Network ", Oct.14 ~ 18, Budapest, Hungary;

(8) " The 1996 Japan Symposium of Nuclear Data ", Nov.16 ~ 24, JAERI, Tokai, Japan.

3 The Foreign Scientists in Nuclear Data Field Visited CNDC/CIAE in 1996

Dr. Y. Kikuchi, NDC/JAERI, Japan, March 16 ~ 29;
Dr. K. Shibata and Mr. T. Narita, NDC/JAERI, Japan, Oct.6 ~ 19;
Dr. Edward T. Cheng, USA, Oct.21.

4 A staff member of CNDC as visit scientist worked at Hiroshima University, Japan, for four months.

CINDA INDEX

Nuclide	Quantity	Energy/ eV		Lab	Type	Documentation				Author, Comments
		Min	Max			Ref	Vol	Page	Data	
^{6}Li	(d,x)	Thrsh	3.0+7	AEP	Theo	Jour CNDP	17	27	Jun 97	Han Yinlu+, MDL CALC, CFD, CRV
^{7}Li	(d,x)	Thrsh	3.0+7	AEP	Theo	Jour CNDP	17	45	Jun 97	Han Yinlu+, MDL CALC, CFD, CRV
^{7}Be	(d,x)	Thrsh	3.0+7	AEP	Theo	Jour CNDP	17	27	Jun 97	Han Yinlu+, MDL CALC, CFD, CRV
^{45}Sc	(p,n)	Thrsh	1.0+8	AEP	ExTh	Jour CNDP	17	99	Jun 97	Fan Sheng+, SIG, SYSTEMATICS
^{46}Ti	(n,p)	Thrsh	2.0+7	AEP	Eval	Jour CNDP	17	81	Jun 97	Yu Baosheng, SIG, CFD, CRV
^{47}Ti	(n,p)	Thrsh	2.0+7	AEP	Eval	Jour CNDP	17	81	Jun 97	Yu Baosheng, SIG, CFD, CRV
^{51}V	(d,x)	Thrsh	3.0+7	AEP	Theo	Jour CNDP	17	36	Jun 97	Xu Xiaoping+, MDL CALS, CFD, CRV
^{52}Cr	(d,x)	Thrsh	3.0+7	AEP	Theo	Jour CNDP	17	36	Jun 97	Xu Xiaoping+, MDL CALS, CFD, CRV
^{54}Fe	(n,α)	6.0+6	7.0+6	BJG	Expt	Jour CNDP	17	1	Jun 97	Tang Guoyou+, SIG, ANGDIS, CRV
^{56}Fe	(p,x)	Thrsh	3.0+7	AEP	Theo	Jour CNDP	17	53	Jun 97	Xu Xiaoping+, MDL CALC, CFD, CRV
	(d,x)	Thrsh	3.0+7	AEP	Theo	Jour CNDP	17	36	Jun 97	Xu Xiaoping+, MDL CALS, CFD, CRV
	(p,n)	Thrsh	1.0+8	AEP	ExTh	Jour CNDP	17	99	Jun 97	Fan Sheng+, SIG, SYSTEMATICS
^{57}Fe	(p,x)	Thrsh	1.0+8	AEP	Theo	Jour CNDP	17	53	Jun 97	Xu Xiaoping+, MDL CALS, CFD, CRV
	(d,x)	Thrsh	1.0+8	AEP	Theo	Jour CNDP	17	36	Jun 97	Xu Xiaoping+, MDL CALS, CFD, CRV
^{59}Co	(n,p)	Thrsh	2.0+7	AEP	Eval	Jour CNDP	17	81	Jun 97	Yu Baosheng, SIG, CFD, CRV
^{58}Ni	(n,α)	6.0+6	7.0+6	BJG	Expt	Jour CNDP	17	1	Jun 97	Tang Guoyou+, SIG, ANGDIS, CRV
	(n,2n)	Thrsh	2.0+7	SIU	Eval	Jour CNDP	17	74	Jun 97	Ma Gonggui+, SIG, CFD, CRV
^{60}Ni	(n,2n)	Thrsh	2.0+7	SIU	Eval	Jour CNDP	17	74	Jun 97	Ma Gonggui+, SIG, CFD, CRV
	(n,p)	Thrsh	2.0+7	AEP	Eval	Jour CNDP	17	81	Jun 97	Yu Baosheng, SIG, CFD, CRV
^{61}Ni	(n,2n)	Thrsh	2.0+7	SIU	Eval	Jour CNDP	17	74	Jun 97	Ma Gonggui+, SIG, CFD, CRV

Nuclide	Quantity	Energy/ eV		Lab	Type	Documentation				Author, Comments
		Min	Max			Ref	Vol	Page	Data	
^{62}Ni	(n,2n)	Thrsh	2.0+7	SIU	Eval	Jour CNDP	17	74	Jun 97	Ma Gonggui+, SIG, CFD, CRV
^{64}Ni	(n,2n)	Thrsh	2.0+7	SIU	Eval	Jour CNDP	17	74	Jun 97	Ma Gonggui+, SIG, CFD, CRV
^{Nat}Ni	(n,2n)	Thrsh	2.0+7	SIU	Eval	Jour CNDP	17	74	Jun 97	Ma Gonggui+, SIG, CFD, CRV
^{65}Cu	(p,n)	Thrsh	1.0+8	AEP	ExTh	Jour CNDP	17	99	Jun 97	Fan Sheng+, SIG, SYSTEMATICS
^{169}Tm	(n,x)	Thrsh	2.0+7	AEP	Theo	Jour CNDP	17	66	Jun 97	Yu Baosheng+, MDL CALC, CRV
	(n,2n)	Thrsh	2.0+7	AEP	Eval	Jour CNDP	17	66	Jun 97	Yu Baosheng+, SIG, CFD, CRV
	(n,3n)	Thrsh	2.0+7	AEP	Eval	Jour CNDP	17	66	Jun 97	Yu Baosheng+, SIG, CFD, CRV
	(n,γ)	Thrsh	2.0+7	AEP	Eval	Jour CNDP	17	66	Jun 97	Yu Baosheng+, SIG, CFD, CRV
	(n,x)	Thrsh	2.0+7	AEP	Eval	Jour CNDP	17	66	Jun 97	Yu Baosheng+, SIG, CFD, CRV
^{181}Ta	(n,2n)	Thrsh	2.0+7	AEP	Eval	Jour CNDP	17	66	Jun 97	Yu Baosheng+, SIG, CFD, CRV
^{182}W	(n,2n)	1.4+7		LNZ	Expt	Jour CNDP	17	9	Jun 97	Kong Xiangzhong+, SIG, TBL, SCTIV
	(n,n'α)	1.4+7		LNZ	Expt	Jour CNDP	17	9	Jun 97	Kong Xiangzhong+, SIG, TBL, SCTIV
	(n,p)	1.4+7		LNZ	Expt	Jour CNDP	17	9	Jun 97	Kong Xiangzhong+, SIG, TBL, SCTIV
^{184}W	(n,2n)	1.4+7		LNZ	Expt	Jour CNDP	17	9	Jun 97	Kong Xiangzhong+, SIG, TBL, SCTIV
	(n,p)	1.4+7		LNZ	Expt	Jour CNDP	17	9	Jun 97	Kong Xiangzhong+, SIG, TBL, SCTIV
^{186}W	(n,2n)	1.4+7		LNZ	Expt	Jour CNDP	17	9	Jun 97	Kong Xiangzhong+, SIG, TBL, SCTIV
	(n, α)	1.4+7		LNZ	Expt	Jour CNDP	17	9	Jun 97	Kong Xiangzhong+, SIG, TBL, SCTIV
^{180}Hf	(n,γ)	5.2+5	1.6+6	BJG	Expt	Jour CNDP	17	13	Jun 97	Chen Jinxiang+, SIG, TBL, ACTIV

(京)新登字 077 号

图书在版编目(CIP)数据

中国核科技报告: CNIC-01170，CNDC-0020: 核数据进展通讯: 英文/刘廷进等著. -北京: 原子能出版社，1997.6
ISBN 7-5022-1680-4

Ⅰ. 中… Ⅱ. 刘… Ⅲ. 核技术-研究报告-中国-1997-英文 Ⅳ. TL-2

中国版本图书馆 CIP 数据核字（97）第 05438 号

原子能出版社出版发行
责任编辑: 李曼莉
社址: 北京市海淀区阜成路 43 号 邮政编码: 100037
中国核科技报告编辑部排版
核科学技术情报研究所印刷
开本: 787 × 1092 1/16 · 印张 7 · 字数 116 千字
1997 年 6 月北京第一版 · 1997 年 6 月北京第一次印刷

CHINA NUCLEAR SCIENCE & TECHNOLOGY REPORT

ISBN 7-5022-1680-4

9 787502 216801 >